COPPER VAPOR GENERATOR

T. W. Karras, et al

General Electric Company

Prepared for:

Air Force Weapons Laboratory
Advanced Research Projects Agency

November 1973

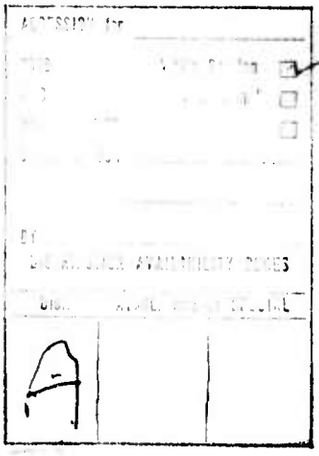

AIR FORCE WEAPONS LABORATORY
Air Force Systems Command
Kirtland Air Force Base
New Mexico 87117

AFWL-TR-73-133

COPPER VAPOR GENERATOR

T. W. Karras
R. S. Anderson
B. G. Bricks
T. E. Buczacki
L. S. Springer

Space Sciences Laboratory
General Electric Company
Philadelpnia, PA 19101

Final Report for Period April 1972 through March 1973

Approved for public release; distribution unlimited.

FOREWORD

This report was prepared by the General Electric Space Sciences Division, P. O. Box 8555 Philadelphia, PA, 19101, under Contract F29601-72-C-0079 during the period from April 1972 to March 1973. The research was performed under Program Element 62301D, Project 0870301, and was funded by the Advance Research Projects Agency, under ARPA Order 870, Amendment 14.

Inclusive dates of research were April 1972 through March 1973. The report was submitted 25 October 1973 by the Air Force Weapons Laboratory Project Officer, Captain George W. Rhodes (LRT).

The authors wish to thank Earl Feingold for his help with materials characterization and analysis, Gene Austin for his aid with switching circuitry, and Cordell Anderson who helped in many stages of test assembly and operation. The participation of Carl Anderson in all stages of this program from its inception is also gratefully acknowledged.

This technical report has been reviewed and is approved.

GEORGE W. RHODES
Captain, USAF
Project Officer

JOHN C. RICCI
Lt Col, USAF
Advanced Technology Branch

RUSSELL K. PARSONS
Colonel, USAF
Laser Division

UNCLASSIFIED
Security Classification

AD771803

DOCUMENT CONTROL DATA - R & D

(Security classification of title, body of abstract and indexing annotation must be entered when the overall report is classified)

1 ORIGINATING ACTIVITY (Corporate author)	2a. REPORT SECURITY CLASSIFICATION
General Electric Company Space Sciences Laboratory Philadelphia, PA 19101	UNCLASSIFIED 2b. GROUP

3 REPORT TITLE

COPPER VAPOR GENERATOR

4. DESCRIPTIVE NOTES (Type of report and inclusive dates)

April 1972 through March 1973

5. AUTHOR(S) (First name, middle initial, last name)

T. W. Karras, T. E. Buczacki, R. S. Anderson, L. S. Springer, B. G. Bricks

6. REPORT DATE	7a. TOTAL NO. OF PAGES	7b. NO. OF REFS
November 1973	124	36

8a. CONTRACT OR GRANT NO.	9a. ORIGINATOR'S REPORT NUMBER(S)
F29601-72-C-0079 b. PROJECT NO. 0870301 c. d.	AFWL-TR-73-133 9b. OTHER REPORT NO(S) (Any other numbers that may be assigned this report)

10 DISTRIBUTION STATEMENT

Approved for public release; distribution unlimited.

11. SUPPLEMENTARY NOTES	12. SPONSORING MILITARY ACTIVITY
	AFWL (LRT) Kirtland AFB, NM 87117

13. ABSTRACT

(Distribution Limitation Statement A)

The development of an efficient high flow velocity copper vapor generator, as a source for a copper vapor laser, is described. Generator operating times of several hours and copper densities within the laser cavity of the order of 10^{17} atoms/cc are also reported. Copper vapor lasers have been operated with this source using both longitudinal and transverse discharges. Almost 0.1 j/l of laser excitation has been obtained at vapor densities of only 4×10^{14} copper atoms/cc. This represents lasing more than 33 percent of the available copper atoms. Super-radiant emission at 5105 Å and operation at 5782 Å have been observed.

DD FORM 1 NOV 65 1473

UNCLASSIFIED
Security Classification

14. KEY WORDS	LINK A		LINK B		LINK C	
	ROLE	WT	ROLE	WT	ROLE	WT
Copper Vapor Generator						
Copper Vapor Laser						
Electronic Laser						
Metal Vapor Laser						

ABSTRACT

(Distribution Limitation Statement A)

The development of an efficient high flow velocity copper vapor generator, as a source for a copper vapor laser , is described. Generator operating times of several hours and copper densities within the laser cavity of the order of 10^{17} atoms/cc are also reported. Copper vapor lasers have been operated with this source using both longitudinal and transverse discharges. Almost .1 j/l of laser excitation has been obtained at vapor densities of only 4×10^{14} copper atoms/cc. This represents lasing more than 33 percent of the available copper atoms. Superradiant emission at 5105 $\mathring{A}$ and operation at 5782 $\mathring{A}$ have been observed.

TABLE OF CONTENTS

TABLE OF CONTENTS (Cont'd.)

TABLE OF CONTENTS (Cont'd.)

LIST OF ILLUSTRATIONS

LIST OF ILLUSTRATIONS (Cont'd.)

LIST OF ILLUSTRATIONS (Cont'd.)

LIST OF TABLES

SECTION I
INTRODUCTION

The development of a supersonic flow, copper vapor laser is potentially an extremely significant advance in laser technology. Projections of the power efficiency of this device show that it compares well with similar projections of other lasers but with a substantial reduction in the mass flow rates required for a given output power. Additionally, it will provide a beam of smaller divergence with the same size optics and use an optical cavity of smaller dimensions.

The very high power efficiency results from the high quantum efficiency of the copper atom laser transition (64 percent of the excitation energy is carried off by the laser photon). The rest of this potential derives primarily from the fact that the wavelength emitted by the copper vapor laser lies in the green (5106 $\mathring{A}$) part of the visible spectrum. Each emitted photon possesses 6 to 20 times the energy of the photons emitted by efficient infrared lasers. As a result, at least a 6 to 20 times greater gas mass efficiency is obtained, since the mass of the molecules of copper and the gases of the other lasers is comparable. Furthermore, for equivalent power output at equal mass flow rates, the optical cavity will be more than 6 to 20 times smaller. Optical components of the same diameter will produce 6 to 20 times smaller beam divergence because the diffraction limit associated with optical apertures is wavelength dependent. The remarkably high transmissivity of this laser through the atmosphere, window materials, plasma, and even sea water, of particular significance for many applications, is also a result of wavelength.

The operation of a copper vapor laser had previously been demonstrated in an equilibrium vapor during 1966[1]. The advantages of a supersonic flow were not discussed, however, until 1971[2, 3]. Lasing has been reported in a supersonic copper vapor flow only recently[4].

The subject of this report is "the development of an efficient technique for producing the necessary quantities of copper vapor for use in high power copper vapor

lasers." This technique rests upon use of a supersonic flow. The copper vapor generator requirements that were sought were:

1. Copper vapor densities of 10^{17} atoms/cc
2. Vapor temperatures below 1800 ^{o}K
3. Vapor density variations of one percent
4. High flow velocity
5. Vapor purity compatible with laser operation
6. Run times of at least one minute

"The development of an efficient excitation technique for producing optical gains" was not the principal subject of this program. Substantiation of the usefulness of the generator as a laser source was to be demonstrated, however, by operation of a copper vapor laser at kilohertz rates with ten percent efficiency and producing .25 joules per liter of laser cavity volume.

SECTION II

BACKGROUND

The copper vapor, electrical discharge laser falls into a class of lasers first described by Walter, Solimene, Piltch and Gould[1]. Its operation follows a cyclic pattern in which excitation and lower laser state relaxation occurs sequentially. The upper laser state is a resonance level strongly connected to the ground state (see Figure 1), so that its cross section for excitation by electron collision is very high. Transitions from the lower laser state to the ground state are forbidden by quantum mechanical rules and it is, therefore, metastable and only weakly excited by electron collisions. Excitation functions for these transitions have been computed[5]. Their integration over a Maxwellian electron velocity distribution shows that a transient inversion should exist for electron temperatures over about 2 ev.

Such temperatures can be reached easily in an electrical discharge. It is only necessary that the current density and the consequent excitation rate be high enough. For instance, experiments[1, 5] have shown lasing to occur when the discharge current density reached the order of 10 amps/cm^2. This is just the current density level which, when used with computed excitation rates[5], will produce a greater number of atoms in the upper laser state than were in the lower laser state through thermal excitation.

This inversion leads to extremely high gain lasing at 5105.4 Å and 5782 Å. Table 1 lists a comparison of wavelength dependent characteristics with those of the carbon dioxide laser. It is immediately apparent that the copper vapor laser characteristics are entirely competitive.

A summary of other copper vapor laser characteristics as described in references 1 and 5 is listed in Table 2. Many of these are quite interesting, even without further improvement. A proposal has been made to operate at 10^4 pulses per second in a 10^3 cc system at up to 10^{-4} joules/cc to obtain average powers of up to a kilowatt[5]. Such a device, considering its high efficiency and wavelength, would have a wide variety of applications. The practicality of the proposal is, however, uncertain.

Table 1. Fundamental Laser Characteristics

Characteristic		Copper Vapor Laser	Carbon Dioxide Laser
Dominant Wavelength	(μm)	.5106	10.6
Photon Energy	(ev)	2.43	.117
Spot Size	(meters)	.75	15
diffraction limited 10^3 km range 1 m mirror			
Atmospheric Interaction			
Absorption constant	(km^{-1})	$<10^{-6}$	3.28×10^{-1}
mid-latitude, summer sea level			
Aerosol Scattering	(km^{-1})	1.68×10^{-1}	7.78×10^{-4}
clear day			
Window Absorption		$<10^{-3}$ (glass) anti-reflection coating	$<10^{-2}$ (salt)
Detectors		Efficient, room temperature operation	Low efficiency, cryogenic operation

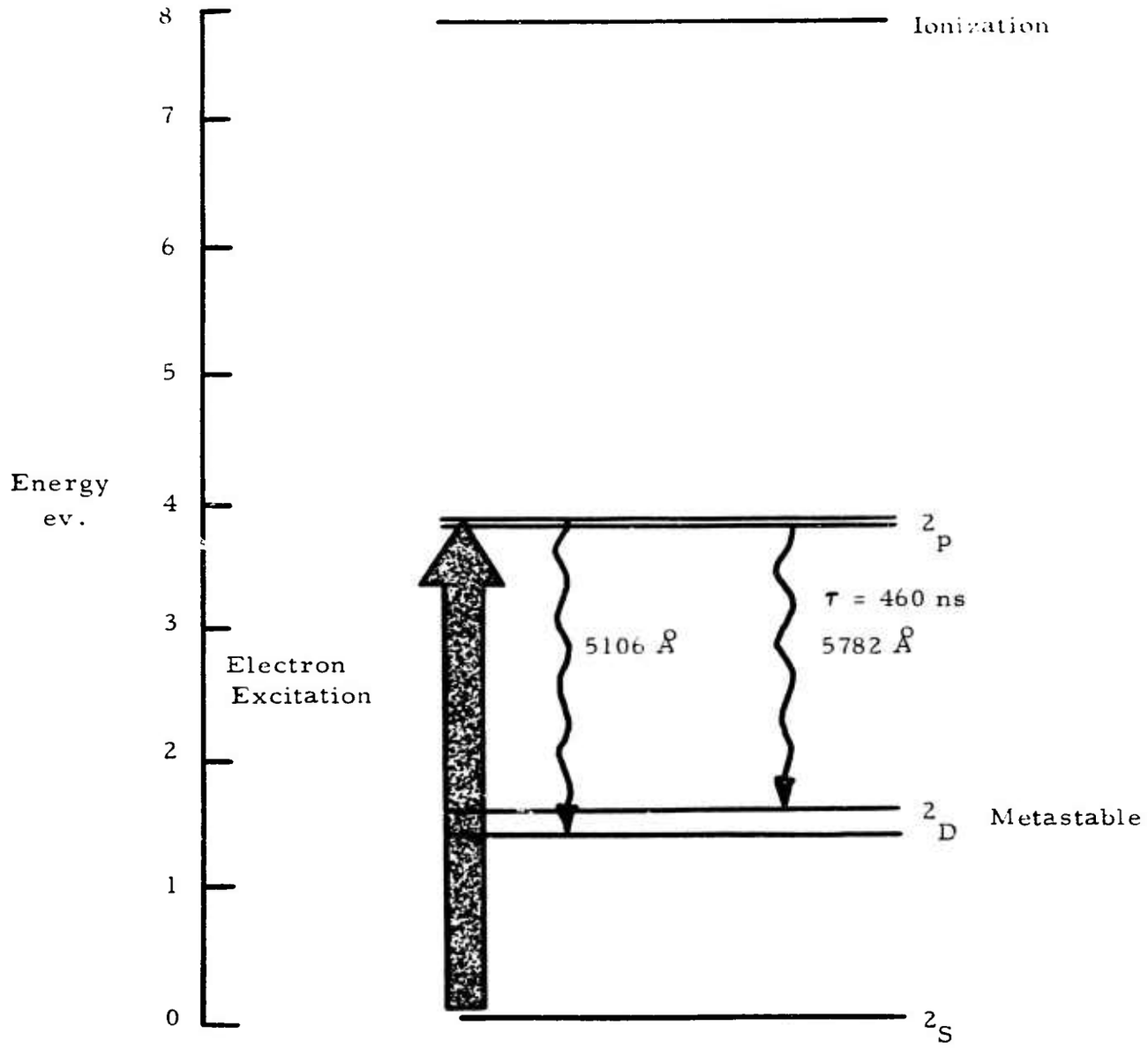

Figure 1. Copper Energy Levels

Table 2. Copper Vapor Laser Status

Parameter	Value
Oven power required for vapor production	5-20 kw
Vapor Density	5×10^{15} atoms/cc
Flow Rate	1.3×10^{3} cm/sec
Current Pulse Width	100 nanoseconds
Laser Pulse Width	15×10^{-9} sec
Gain	400 db per meter
Electrical Energy Efficiency	1%
Laser Energy per Unit Laser Volume	8 micro-joules/cm^3
Peak Power per Unit Laser Volume	650 w/cc

Efficiencies of up to 23 percent may be possible in a low flow velocity system, in large part because of the 63 percent quantum efficiency[1]. In practice, however, only about 1 percent has been demonstrated[1, 5]. A large fraction of the energy has been wasted in an electrical discharge whose ringdown time far exceeded the period of the laser pulse. This discharge length also limited the peak current densities so that only one or two percent of the available atoms could be excited. Reduced circuit inductance was needed. However, it was difficult to reduce the inductance of the discharge circuit because of the techniques used for production of the copper vapor.

Hot walls and associated problems forced temperature sensitive components, such as discharge capacitors, to be placed remotely. As a result the discharge pulses used for metal vapor lasers in this country invariably exceeded 100 nanoseconds[1, 4, 5, 6]. Only work reported by Isaev[7] and Petrash[8] in the Soviet Union indicated faster currents. Unfortunately experimental detail was not given in those papers.

SECTION III

IDENTIFICATION OF THE COPPER VAPOR GENERATOR REQUIREMENTS

The development of a new type of copper vapor source could improve laser characteristics substantially. The requirements for such a device follow from an elementary consideration of laser system goals.

A. Waste heat and metastable copper atom rejection from a stationary vapor cloud must depend upon diffusion. This mechanism requires milliseconds, limiting repetition rates to kilohertz. To overcome this limitation, a flowing vapor source is required instead of an oven. Furthermore, in a flowing system only the source need be hot, allowing walls to be cool and heat sensitive components close to the discharge for minimum inductance.

B. To maximize laser power as rapid a means as possible is desired for waste removal. Flow velocities of the order of 10^5 cm/sec will give each atom roughly as much kinetic energy as the photon has electromagnetic energy. Much higher velocities will require more energy in the flow than is in the lasing, dramatically lowering laser system efficiency. Consequently, a flow velocity of about 10^5 cm/sec is optimum.

C. Copper vapor is wasted if it is directed in any direction but into the electrode gap. In addition, copper deposits on windows and insulator surfaces can be harmful. The flow must then be well directed.

D. The threshold current for lasing is minimized if the thermal population of the lower laser state is small. There is also no benefit derived from energy invested into the random thermal motion of the vapor. Thus, for ease of operation and optimum efficiency the vapor within the laser cavity should be kept as cool as possible, e.g., less than $1800\ ^{o}K$.

E. Current understanding indicates that the laser output power will be maximized if the copper atom density within the laser cavity is as large as possible. At a given flow velocity this is equivalent to a maximum in flow density.

Clearly, to maximize the output power the copper atom density in the flow must be as high as possible.

F. Laser beam quality can suffer from non-uniformities in the vapor density through diffraction effects and non-uniform light generation. Consequently, a relatively homogeneous vapor flow is needed.

G. The efficiency of the laser will be highest if there are no atoms other than copper present to absorb energy from the discharge. Consequently, the copper vapor generator should inject no vapors that can be excited during operation. Obviously a generator that provides only copper would be most desirable.

H. Losses through radiation and conduction should be kept as small as possible. In addition, the start up and shut down time of the generator should be short. To satisfy these the hot area of the device and its thermal inertia should be minimized by making the hot parts of the devices as small as possible

I. Efficient laser operation requires that as little energy as possible be spent on copper vapor production. The generator should then be very power efficient.

J. Long device life and a minimum failure rate are correlated with device simplicity, the wearing of moving parts and availability of working fluid. The copper vapor generator should then be as simple as possible, have no moving parts, and be easily refilled.

K. The usefulness of the generator will be greatest if it can be used almost anywhere in any orientation. Thus, the generator should be insensitive to vibrations and to gravity orientation.

L. Maximum efficiency will result if both the working fluid and some substantial fraction of its heat content are recirculated.

SECTION IV
GENERATOR DESIGN CONSIDERATION

The copper vapor generator requirements discussed in the previous section, when taken together, dictate certain design characteristics for the device.

For instance, the source of the vapor flow must be a hot liquid copper surface. The energy used to produce the phase change can then be converted into a 10^5 cm/sec flow velocity in an expansion which also cools the flow making the total energy costs of the process a minimum. Any technique that injects the copper at lower temperature would have to provide the high velocity through some other technique at a net cost in energy equal to what is required by the whole vapor production--acceleration process off of a hot surface. This satisfies requirements A, B, D, G, and J.

One technique with this failing involves the use of a copper bearing compound with a vapor pressure lower than that of liquid copper. In principle, lower temperatures could then be used to produce a given flow of copper. A simple expansion would not provide as high velocity as pure copper vapor, however, even at the same temperature, since the molecule weight would be higher than that of copper. More serious, the energy required to disassociate the molecule once it entered the laser cavity (so that copper atoms could be available for lasing) is the order of an ev. or more. In addition, if losses involved in accelerating the gas and exciting the non-copper atoms in the discharge are considered, even if the vapor production costs are zero (i.e., the compound is a gas at room temperature), the power efficiency of the technique will be lower than that of a hot copper expansion.

Vaporization off a hot liquid copper surface, besides being efficient and providing a high velocity flow of pure copper, will also satisfy the requirement that the vapor be well defined or a jet. An expansion will reduce the velocities perpendicular to the jet axis and increase those parallel to that axis, contributing to jet confinement. A high pressure ratio will enhance this process. Therefore, a

low pressure or vacuum background is desirable. The ideal generator would then be a liquid copper surface emitting a supersonic jet into a low pressure or a vacuum.

The vapor jet can come directly from a liquid surface or it can come from a set of nozzles fed by a high pressure plenum. The requirements that the source be small, have low thermal inertia, and be immune to environmental variations weigh against the high pressure plenum concept. A plenum volume and conventional small nozzles added over the liquid surface would certainly raise the size, the thermal inertia, and time response of the device. In addition, the high flow density requirement also dictates that a large fraction of the generator surface facing into the flow direction must be emitting vapor. The emitting parts of the surface have to produce enough flow to compensate for those that do not emit, thereby reducing the effective flow density from the generator. If most of the vapor generator area is taken up by nozzles a substantial sacrifice in the flow density downstream will result.

On the other hand, the use of vapor flow directly from the surface of a small mass of liquid would minimize the size and thermal inertia of the device and maximize the fraction of the generator providing flow. A particularly simple design could use a small open trough. The trough could be a small channel of graphite or tungsten (e.g. 1 mm wide, and .2mm deep), thereby, having a thermal inertia small enough to allow millisecond cooling and heating. This design would also have long life, allow the highest temperatures and flow rates that might be needed, and provide the largest possible area of exposed liquid surface. Unfortunately, the free liquid surface presents certain limitations. It must be properly oriented with respect to gravity and vibrations must be kept to a minimum. Furthermore, no significant positive feed pressure can be tolerated, otherwise the liquid will overflow its trough. Some pressure would be needed to replenish the copper lost to vaporization and so a modification is indicated.

The solution to this shortcoming is to place a cover on the channel, made of a material that is not wet by the copper, and perforated by many small holes. The liquid could fill the channel up to the cover and then be restrained by surface tension from flowing out the holes. In this way, as indicated in requirements K and J, the device could be immune to moderate vibrations and the orientation of gravity, and could support a moderate pressure driving liquid into the channel without forcing liquid out. Since the vapor flow would leave through the small holes, a well directed vapor flow would also result[9, 10] satisfying requirement C. If the holes are sufficient in number and size over 50 percent of the liquid surface would be exposed, providing the high flow densities needed when surface temperatures are the order of 2500 ^{o}K and meeting condition E. Furthermore, if the holes are the order of a mean free path mixing of the individual jets should occur rapidly, leading to a highly uniform flow[2] and supporting requirement F. The size of the device and the materials of its construction would remain small, as described for the open channel, keeping the thermal inertia small as specified in requirement H. Of course, the characteristics of a supersonic jet expanding into a low pressure or vacuum would typify the flow[9].

While the volume and mass of copper involved must be small, a long, thin region must be filled with vapor for the laser application. Thus, the length and width of the hole array and the liquid copper surface are determined by the laser cavity. Only the thickness of the volume of copper can be varied to control the mass of metal or to fit the heating mechanism chosen.

Heat supplied by any thermal source outside of the liquid copper strip would of necessity increase the thermal inertia of the system. Furthermore, losses will be increased above those from a thin strip (i.e., radiation from the surfaces and conduction from its ends) if there is an added thermal source of higher temperature.

Electrical heating of the thin strip would remove the need for any other heat source. This technique has been used successfully by Karras et al for vaporizing very small volumes of mercury[11, 12] and copper[12]. The hottest element is then the copper itself and thermal losses can be kept to a minimum.

The low thermal mass of the copper indicates that dc electrical heating be used since a steady flow of vapor is desired here. Pulsed flows and pulsed heating are considered elsewhere[13].

Efficiency considerations indicate that the liquid copper resistance be larger than any other elements of the circuit. Internal resistances of power supplies and lead cable cannot be reduced much below the order of .001 ohm. Consequently, resistance of .010 ohm or higher should be designed.

The requirement dictates a copper strip thickness of about .005 inch (e.g., a strip length 10 cm and width of 1 cm). The high surface tension of copper, which is useful in preventing the liquid from flowing through the holes filling one surface of its enclosure, will now prevent the liquid from flowing into that enclosure. Any pressure adequate to drive liquid copper into the .005 inch thick spacing would require much smaller holes in the wall of the enclosure, a severe manufacturing problem. Furthermore, pressures on the order of an atmosphere would be required, leading to substantial convection cooling at the liquid surface in the reservoir supplying the copper.

A high resistivity metal, such as bismuth, would offer no such problem. The thickness of the strip needed can be so large a small head of the liquid itself can provide sufficient pressure. This has been successfully demonstrated[14].

Low resistivity metals, such as copper, require other methods to drive them into the cavity. The simplest solution discovered thus far is to line the inner surface of the enclosure with a film that is wet by the liquid copper. Effective pressures of an atmosphere then pull the liquid into the enclosure from the reservoir. This satisfies requirement I, while still meeting requirement J.

The only requirement not met by this concept is that of recirculation, L. There is every reason to believe that modifications will allow this to be done also but the added complexity involved has caused its postponement.

A copper vapor generator based upon the principals just discussed has been built. The following sections describe it in more detail.

SECTION V

AN ALL GRAPHITE COPPER VAPOR GENERATOR FOR FILLING LASER CAVITIES

A. MATERIALS

The copper vapor generator design following from the considerations just given requires materials with very special characteristics. The basic generator material must be:

1. insoluble in liquid copper,
2. not wet by liquid copper,
3. easily machinable so that many small holes can be placed in a thin wall,
4. highly refractory so that little material loss will occur at the highest temperatures encountered, and
5. electrically conducting so that current can be carried before copper enters.

Fine grain graphite was found to have all these characteristics. Solubility in liquid copper is exceedingly small[15]. Wetting, as measured by contact angle, is negligible[16, 17]. Its machinability, electrical conductivity, and refractory qualities are well known.

Uncertainty in the solubility and wetting references, however, indicated that tests should be conducted to verify these measurements with the materials used in the copper vapor generator. Such graphite walls left in contact with liquid copper have not shown a measurable decrease in thickness even after tens of hours of contact. Consequently, solubility and other questions of compatibility are satisfied. Similarly, sessile drop measurements of the contact angle between copper and a lightly polished plaque of the graphite gave values of about 154° ($\cos\theta = .906$) for temperatures between 1080°-1680° C (see Figure 2). This value corresponds to even less wetting than had been found for other forms of graphite[16].

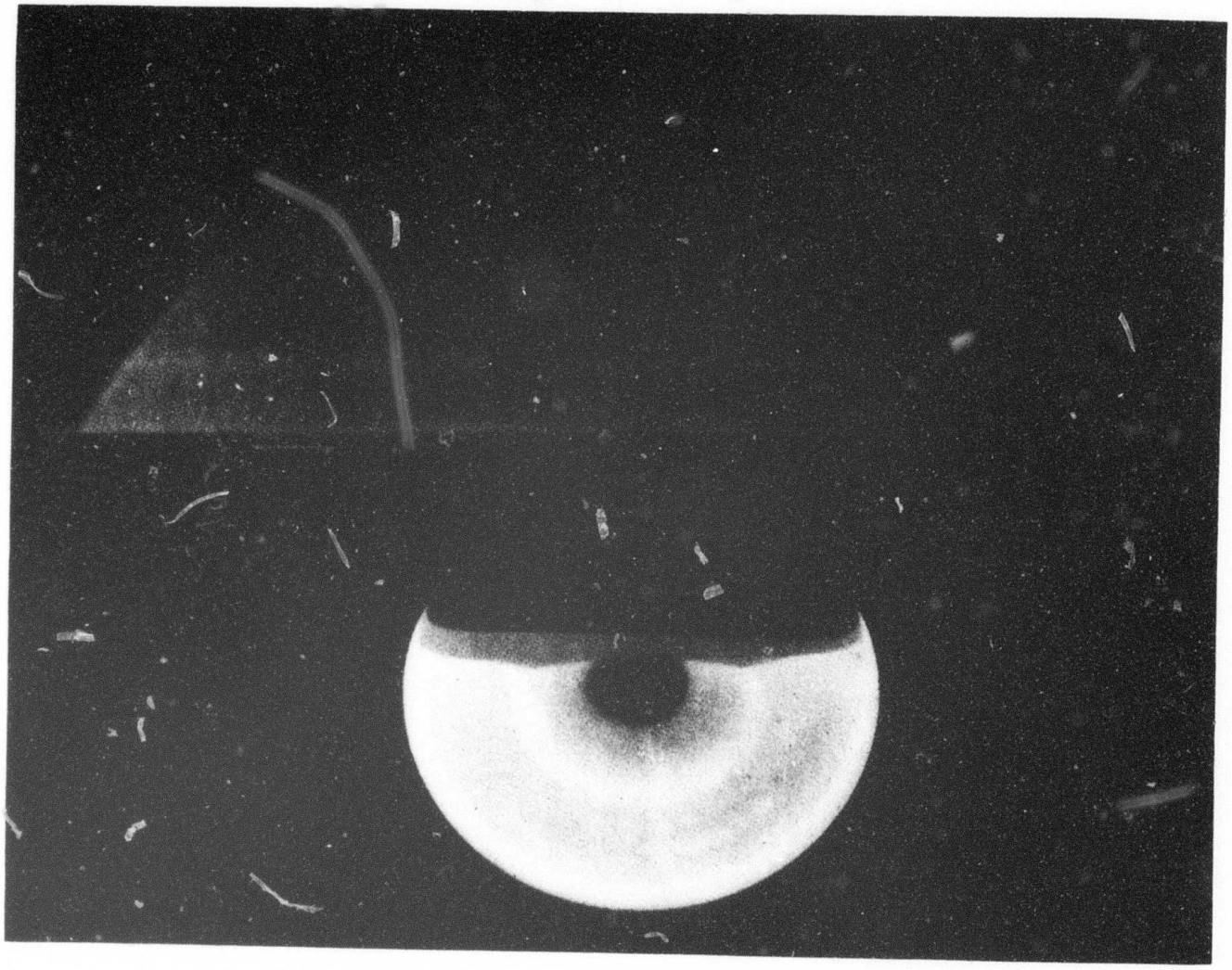

Figure 2. Sessile Drop Test of Copper on Fine Grain HPD Graphite, 1680 °C

Clearly, the fine grain graphite was adequate for containing the copper in all components of the system. As a result ultimately both reservoirs and the enclosure with holes containing the thin copper strip (the injector) were made of this graphite. Appendix I discusses several early designs.

A thin film that will be wet by liquid copper must line the interior of the injector as pointed out in Section IV. Other characteristics needed are:

1. Insolubility in copper,
2. high temperature compability with the graphite substrate which will not change its characteristics with time,
3. good mechanical bonding to the graphite substrate,
4. very high temperature capability,
5. easy deposit on the graphite substrate.

A mixture of tantalum and tungsten carbide has proven to be most advantageous for this function. Indications that the primary wetting requirement would be met by the carbides was obtained from measurements made in bulk material[16, 17, 18]. Sessile drop tests were then conducted with one micron films on graphite substrates to verify these indications (see Appendix II). Tungsten carbide was found to be wet well immediately upon melting. The sessile plaque was totally covered so that a quantitative measure of contact angle could not be obtained. This is entirely consistent with the literature[17, 18]. Tantalum carbide-copper sessile drop measurements, however, led to quantitative values because of the larger contact angles at the melting point of copper (see Figure 3). Figure 4 gives values of the contact angle measured in this way as a function of temperature and shows rough agreement with bulk material experiments. It can be seen that wetting is marginal at the melting point of copper and only becomes very good above 1200 ^{o}C.

The tungsten carbide film was also found to adhere better to the graphite substrate than the tantalum carbide film. Appendix III discusses the experiments that led to that conclusion.

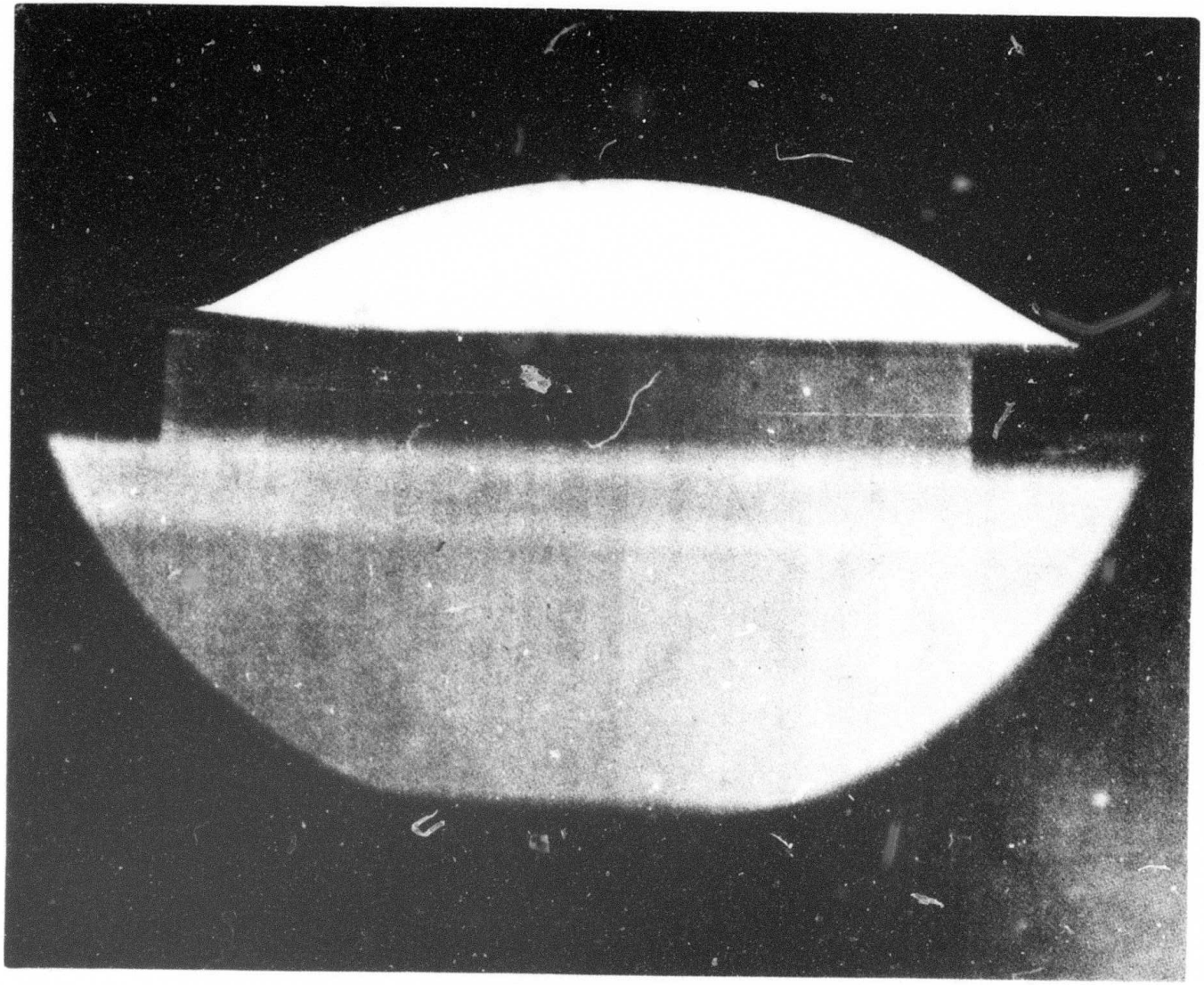

Figure 3. Sessile Drop Test of Copper on Tantalum Carbide Film on Graphite Substrate

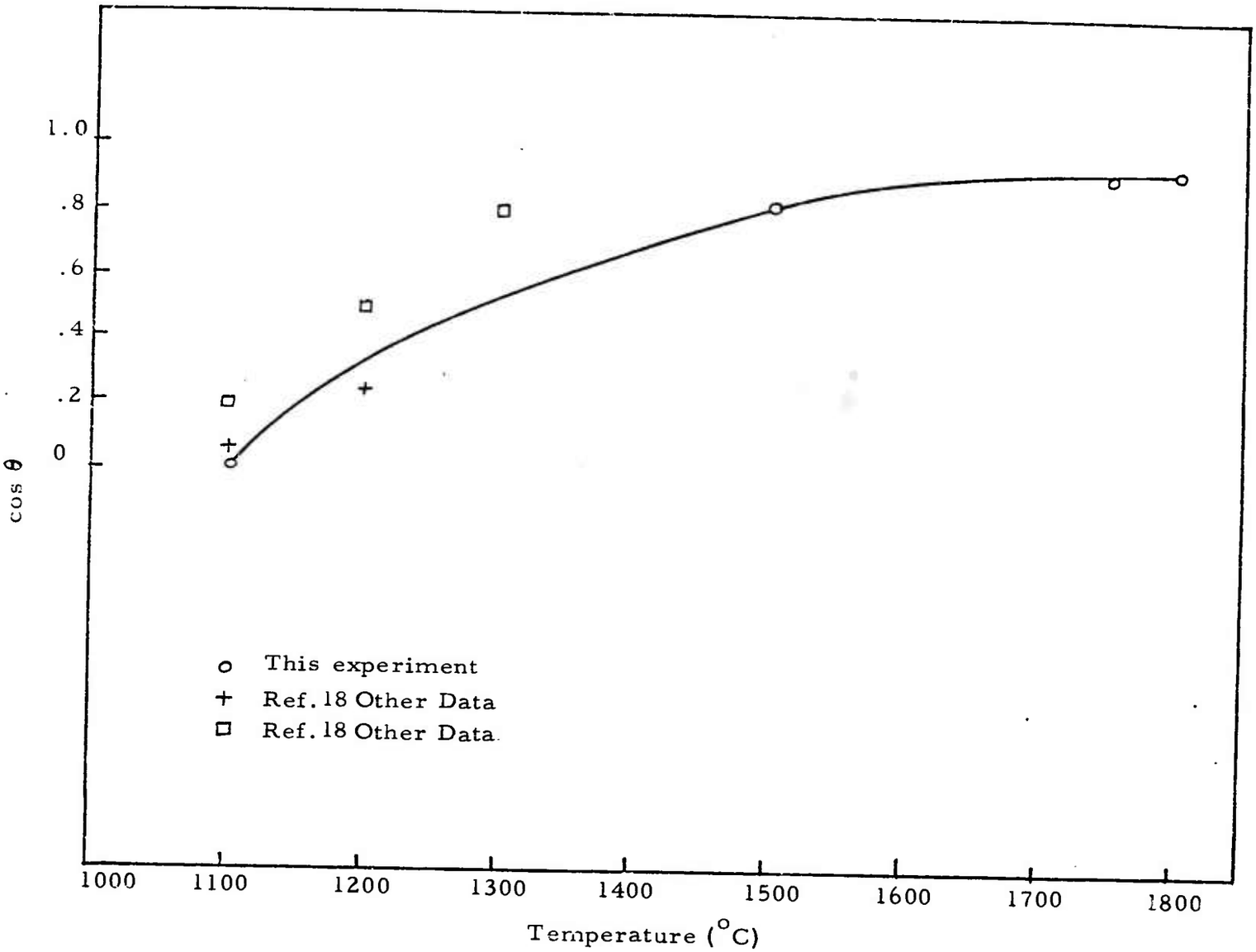

Figure 4. Contact Angle of Copper on Tantalum Carbide vs. Temperature

The superiority of pure tungsten carbide films for wetting as well as adherence indicated that such a film should be used. However, greater reliability was found by using it in combination with tantalum carbide. Furthermore, the use of tantalum carbide is an advantage at high temperature where it wets as well as tungsten carbide and is substantially more refractory[15].

Reliable information regarding the compatibility of such a film in the long term presence of very hot (i.e., above 2,000 ^{o}K) copper was not available in the literature. Even slight solubility would quickly destroy such a small quantity of material. The strong wetting forces would also tend to lift the film from its graphite substrate unless very strong bonding was present as indicated in Appendix III.

Tests conducted with sputtered tungsten-tantalum carbide films at temperatures above 2400 ^{o}C have proven successful. The film remains bound to its substrate and wet by copper. Long term tests of many hours at lower temperatures achieved similar results.

B. DESIGN

The most important component of the copper vapor generator is, of course, the injector. This element confines the liquid copper while it is emitting vapor. The only other components necessary to the design developed are the reservoirs and their support structure. The copper is melted within the reservoirs and is held there until drawn into the injector by the wetting forces.

The copper reservoirs have also been made of graphite (see Appendix I). This solves any compatibility problems and allows the injector heating current to be carried directly through their walls. Furthermore, since the injector is also made of graphite each end of it may be inserted into each reservoir through a close fitting slot. During heating the injector can then expand into the reservoirs, since the graphite surfaces will slide easily, without bowing and distorting the surface from which vapor is being emitted. If the fit between the outer injector surfaces and the walls of the reservoir slot are sufficiently close, surface tension forces will prevent copper leakage.

For convenience each reservoir was made in the shape of a hollow tube with one end closed. The injector slots were placed just above the closed end. Figure 5, an assembly drawing of the whole copper vapor generator, shows these reservoirs at each end of the injector.

The copper vapor injector itself consists of a base, spacer and lid held together by several types of clips. Figure 6 is a photograph of the basic pieces. Figure 7 shows how they are assembled. Table 3 gives the dimensions of the injectors used most frequently (Appendix I discusses others). The side clips can be held in place with graphite cement or by a separate set of C-clips as shown in Figure 7.

Figure 8 is a photograph of an injector inserted into the appropriate reservoir slots forming a copper vapor generator.

Table 3. Injector Dimensions

	Injector A	Injector B	Injector C
Length of hole array	10 cm	10 cm	10 cm
Width of hole array	.380 inch	.165 inch	.065 inch
Width of injector cavity	.395 inch	.180 inch	.180 inch
Height of injector cavity	.005 inch	.005 inch	.005 inch

Note: Hole arrays were composed of .015 inch holes drilled on .020 inch centers, staggered so that adjacent holes are the vertices of equilateral triangles. The surface of the hole array is thus 51 percent open area.

Figure 5 shows more details of this assembly. Mechanical support and electrical connections are made with molybdenum tubing that slips over the reservoirs. That tubing is held in place by pins passed through holes that are located at the tops of the reservoirs. Radiation shields were also placed around the reservoirs to reduce thermal losses (see Appendix IV).

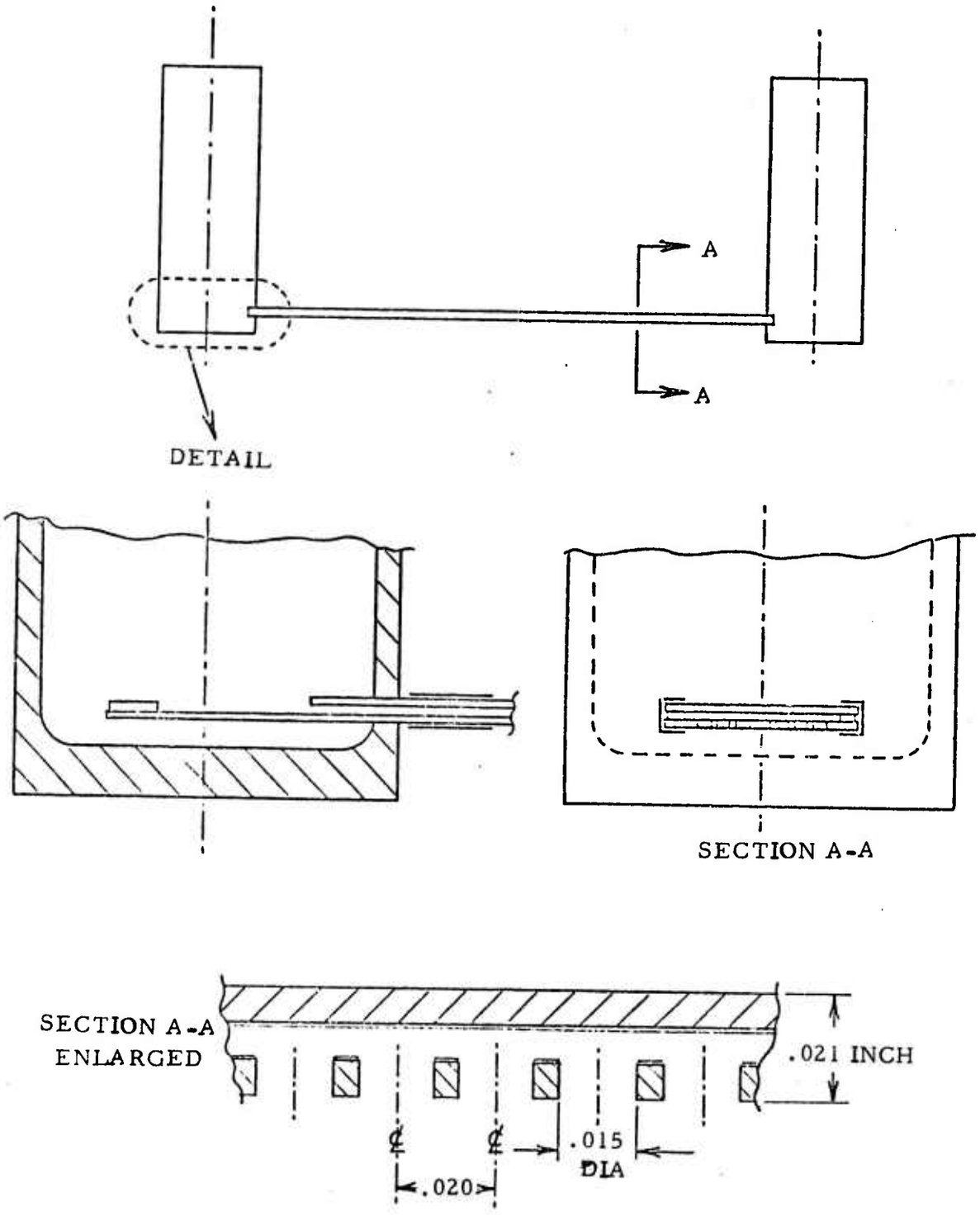

Figure 5. Assembly Drawing of Copper Vapor Generator

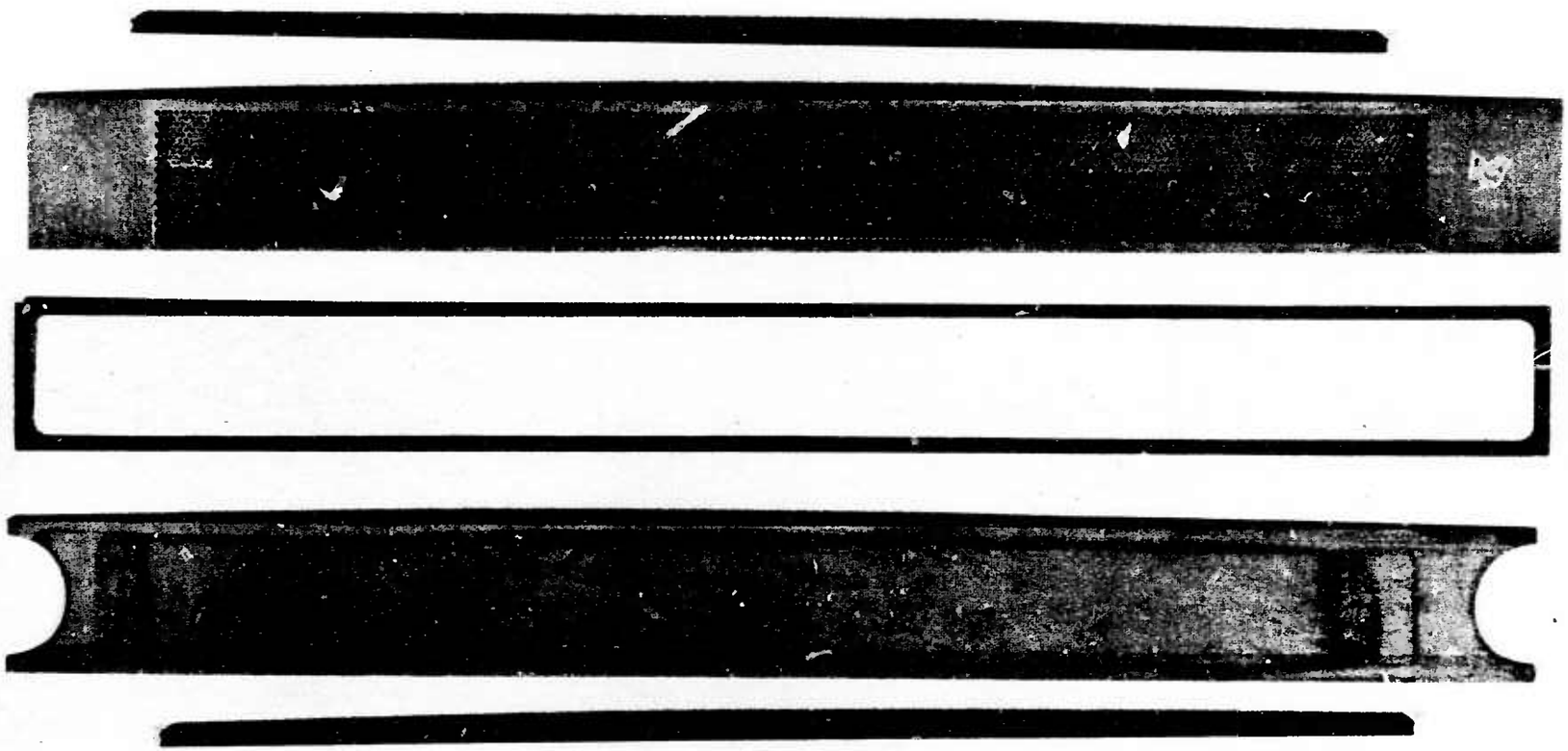

Figure 6. Photograph of Parts for Copper Vapor Injector. From top to bottom these are a side clip, lid, spacer, base, and side clip.

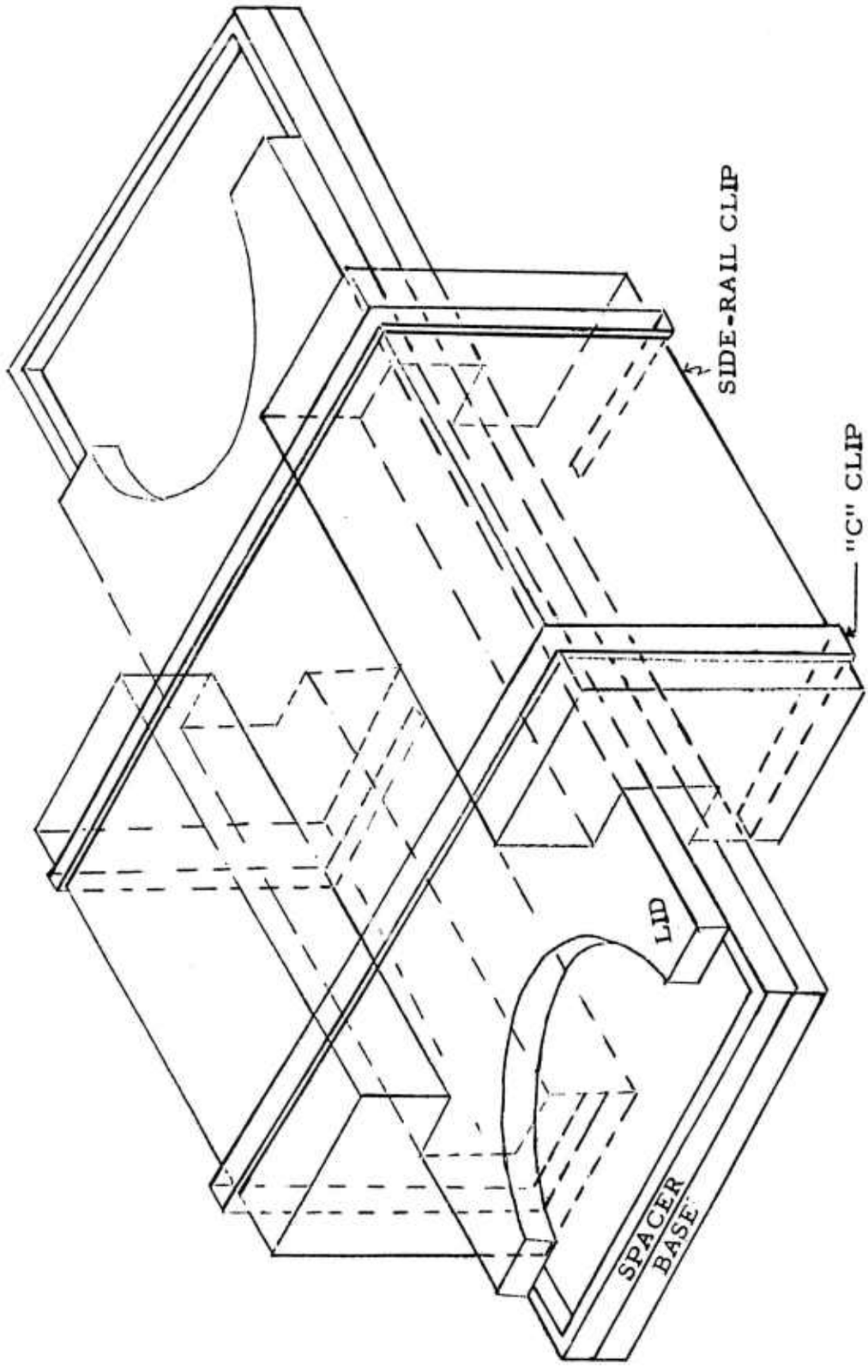

Figure 7. Diagram of Assembled Injector

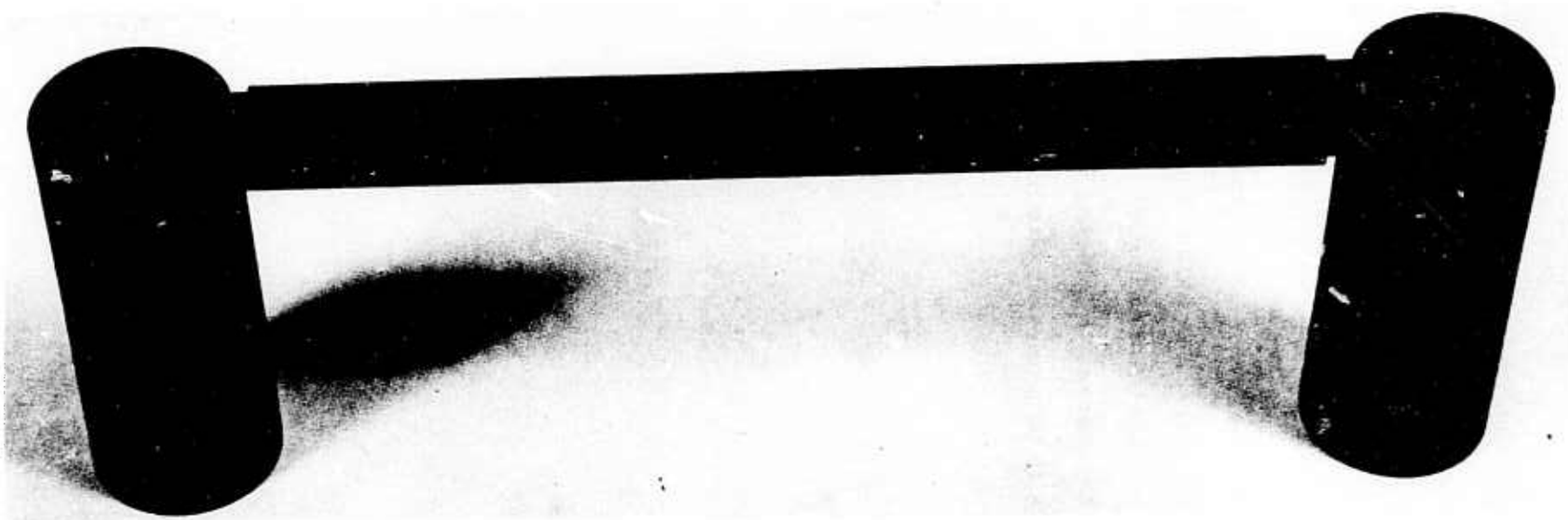

Figure 8. Photograph of Copper Vapor Generator. Injectors has been inserted into reservoir slots.

Reservoir heating can be supplied through resistance loss in the reservoir walls by the main heating current and heat conducted from the injector ends. This was done early in the program. However, the availability of reservoir heaters developed on another program[13] and difficulties associated with controlling reservoir temperatures led to the use of these separate heaters.

The flexibility offered by this reservoir heating technique was needed in order to use injectors B and C (see Table 3). The higher resistance of those two injectors causes them to become unacceptably hot before the main heating current alone melts the copper within the reservoirs. Of course, this higher injector resistance also allows high copper vapor flow densities to be achieved with more modest currents, which was the primary reason for their use.

SECTION VI

ANALYSIS OF GENERATOR OPERATION

A. PREDICTION OF FLOW RATE

The copper vapor flow from the injector into a vaccum can be determined from knowledge of the temperature and the liquid area exposed[21]. The temperature can in turn be computed from knowledge of the power dissipated in the injector, the power radiated, and the power conducted to the reservoirs. When an ambient gas is present losses due to convection must be added.

These last two modes of loss can be neglected. For rare gases at pressures the order of ten torr, convection losses are given[21] by

$$E = \lambda \frac{\Delta T}{d} A$$

where

λ is the thermal conductivity of the gas; for argon, about 4.5×10^{-4} for an average temperature of 10^3 °C.

ΔT is the temperature difference to ambient, about 2×10^3 °C

A is the injector area, 20 cm^2, and

d is the distance to cooled walls, about 5 cm.

As a result only about 3.5 watts will be lost through convection. A technique reported previously[14] was used to compute the temperature distribution within the liquid copper and along the injector. The results are shown on Figure 9 for a condition where the center of the injector is at 1480 °K and the reservoirs at some lower value determined by reservoir conditions. The results of these computations indicated conduction losses to the reservoirs of 20 to 40 watts. This again is small compared to radiation losses and the power delivered to vapor.

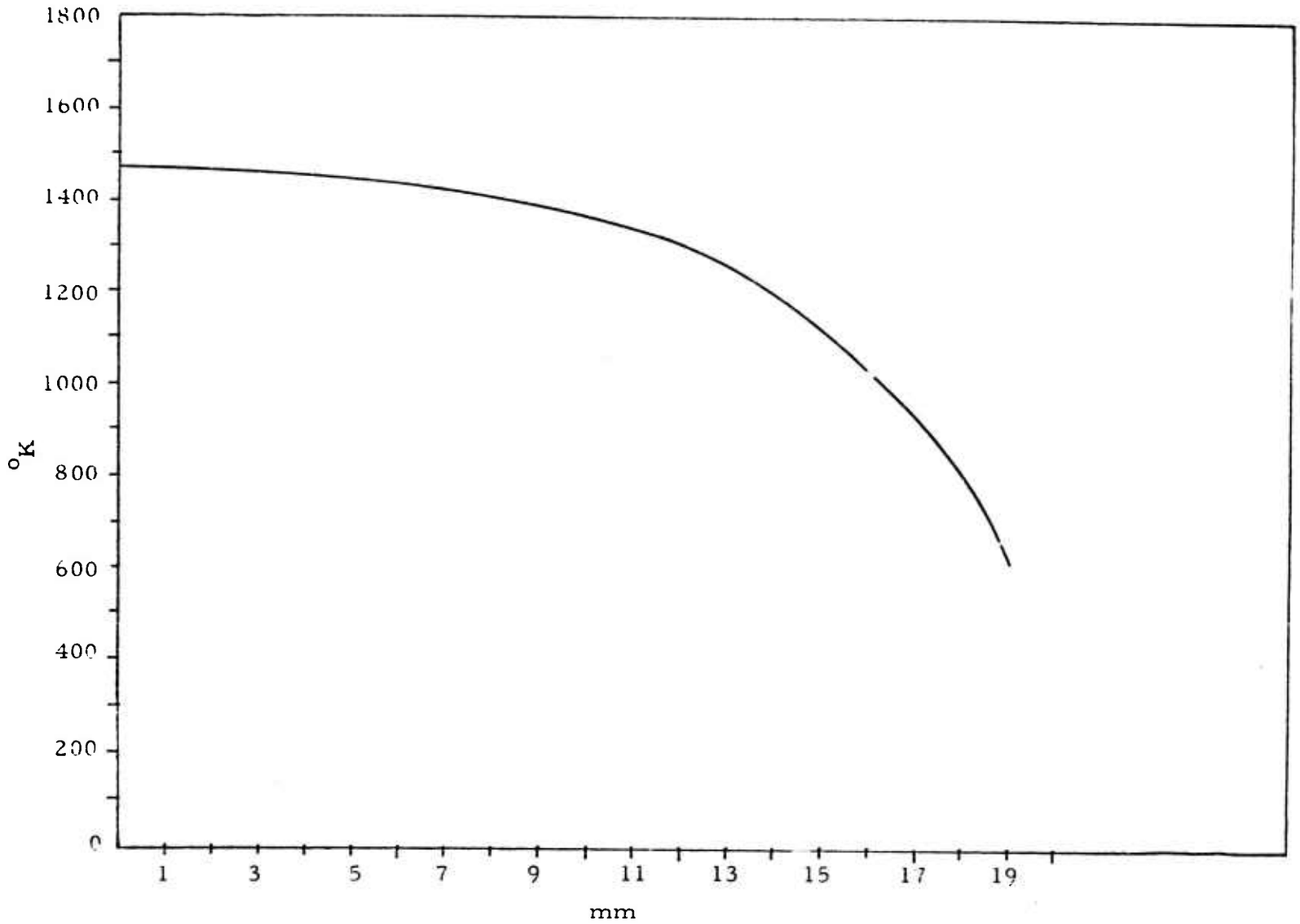

Figure 9. Temperature Distribution Within Injector Along Length

Consequently, only radiation and vaporization were considered when computing injector temperature. The actual procedure was to assume an injector temperature; a vaporization and radiation rate would then follow. The power input needed to maintain the assumed temperature could then be computed.

The flow from each orifice can be expected to follow the form of a supersonic jet expansion. A great deal of work has been done which shows that such an expansion can be described in many ways by a continuum inviscid expansion[22]. Thus the density will fall as the flow from each orifice expands, decreasing the temperature and increasing the flow velocity. When the flow from the 50-percent open area of the injector surface has filled in the empty spaces (area ratio of two), isentropic compressible flow considerations yield[23]

Mach number	2.2
Density ratio	.184
Temperature ratio	.508

The copper atom velocities at this point are given on Table 4 as a function of injector temperature. Beyond this point the expansion will increase much more slowly since the smallest characteristic dimension of the new jet, formed by merging all the small jets, is the order of the distance to the laser cavity where the vapor is to be used.

Table 4. Copper Atom Velocities in Laser Cavity

Copper Atom Velocities	Injector Temperature
7.25×10^4 cm/s	2700 °K
6.97	2500 °K
6.69	2300 °K
6.39	2100 °K
6.08	1900 °K

A high uniformity of vapor should be expected across and along the face of the flow. Geometric interpenetration guarantees such mixing even over distances small compared to a mean free path[2].

Figure 10 gives the predicted density in the closest practical laser cavity (i.e., right after all small jets have merged) as a function of injector temperature for all injector models. The fundamental data were assembled in Reference 2. Figure 11 then follows with the predicted power input requirements needed to maintain a given temperature on injector A. Such information can then be combined to give the predicted copper vapor density within the laser cavity as a function of power into the injector. Figures 12, 13, and 14 show such information for the three injectors used during most of this program. Figure 14 also shows the predicted density just beyond the liquid surface for reference.

The presence of an inert background gas will modify the above results to some degree. A jet expanding into vacuum from a hole will be well directed with very little vapor coming off at large angles to the axis[2, 22, 24] and little decoupling of particle temperatures perpendicular and parallel to the flow. The background gas will cause the jet to become effusive in character once the stagnation pressure of the jet falls below that of the ambient. Radial and translational temperatures will be equal. Furthermore, the copper temperature will fall as the ambient gas is heated and this heat is conducted away. Some effect might also be expected on the net copper flow rate from the injector.

None of these modifications are expected to be significant. The spreading angles could, in principle, grow to 45° but measurements made with a bismuth vapor injector show no major changes[14] (compare with results shown on Figure 21). The low thermal conductivity of the ambient gas (5-30 torr argon or neon) and the fact that the gas near the injector will also be heated by it ensure that the gas in the path of the copper will be near the temperature of the vapor in the copper jet. The overall velocity of the copper flow within the laser cavity will then not change substantially. Furthermore, since the evaporation and condensation rate depends only upon the difference between the ambient vapor pressure, which returns copper to the

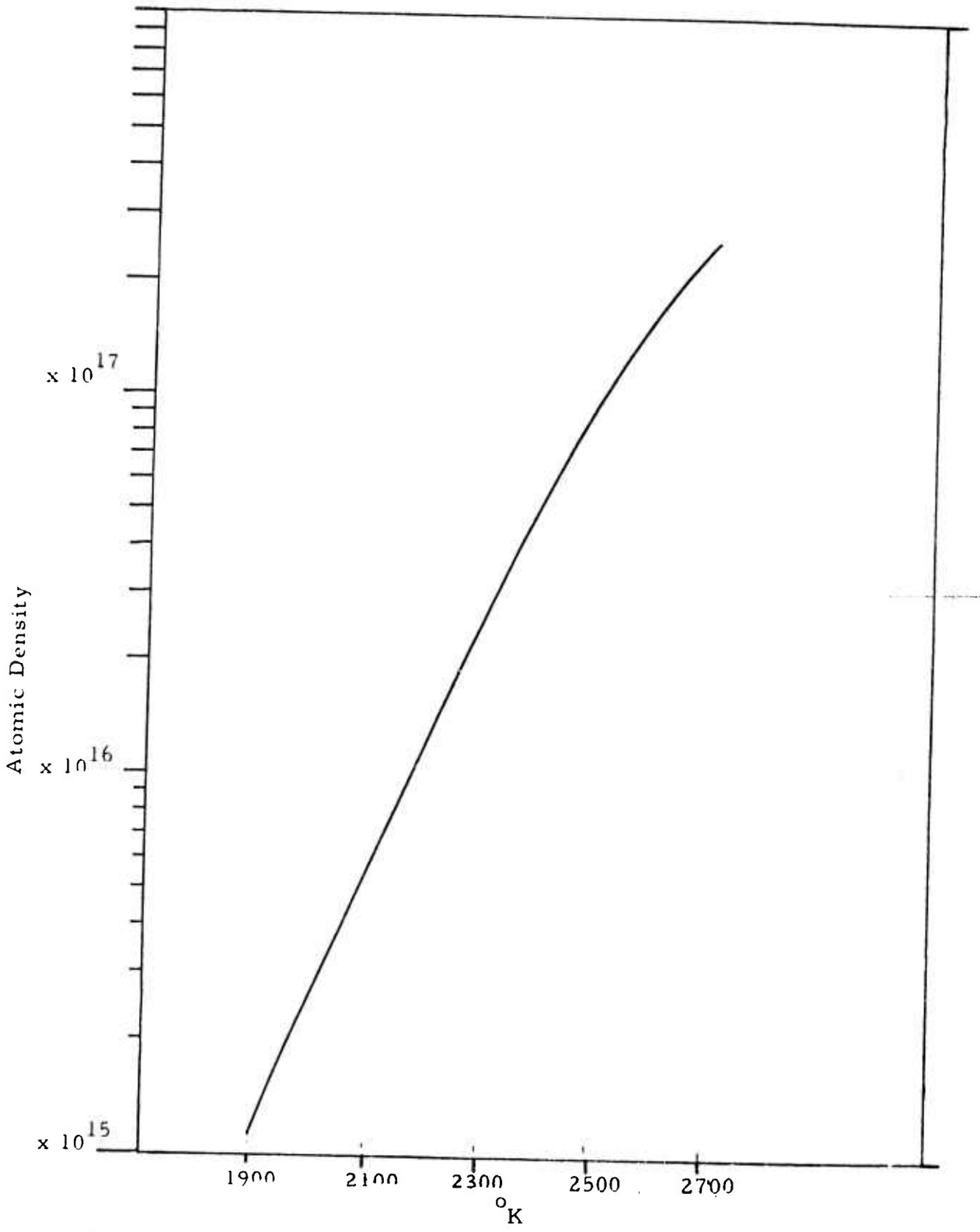

Figure 10. Predicted Copper Vapor Density in Laser Cavity as Function of Injector Temperature

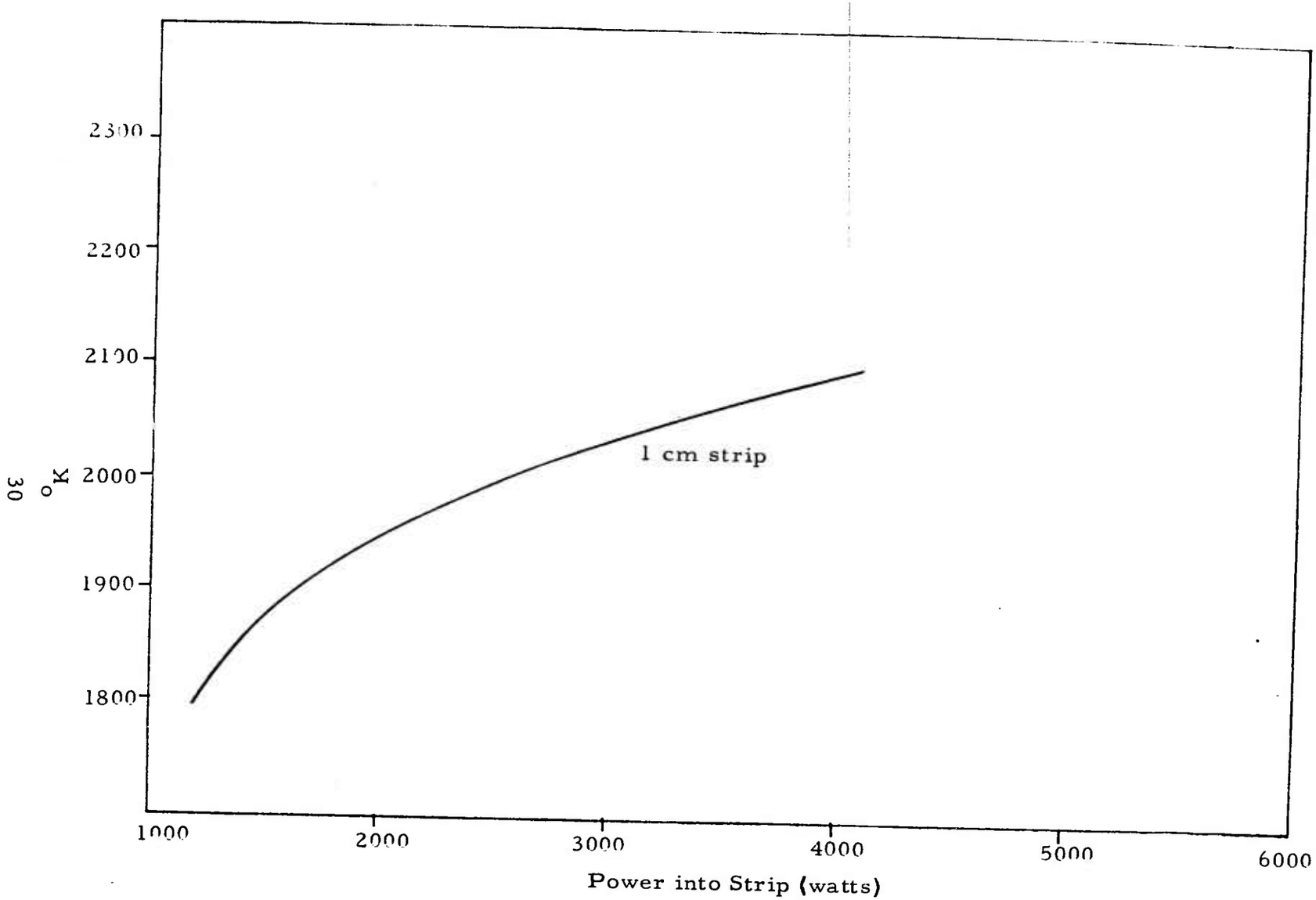

Figure 11. Predicted Power Input Requirements to Maintain a Given Temperature Copper Injector A, .380 Inch Hole Array

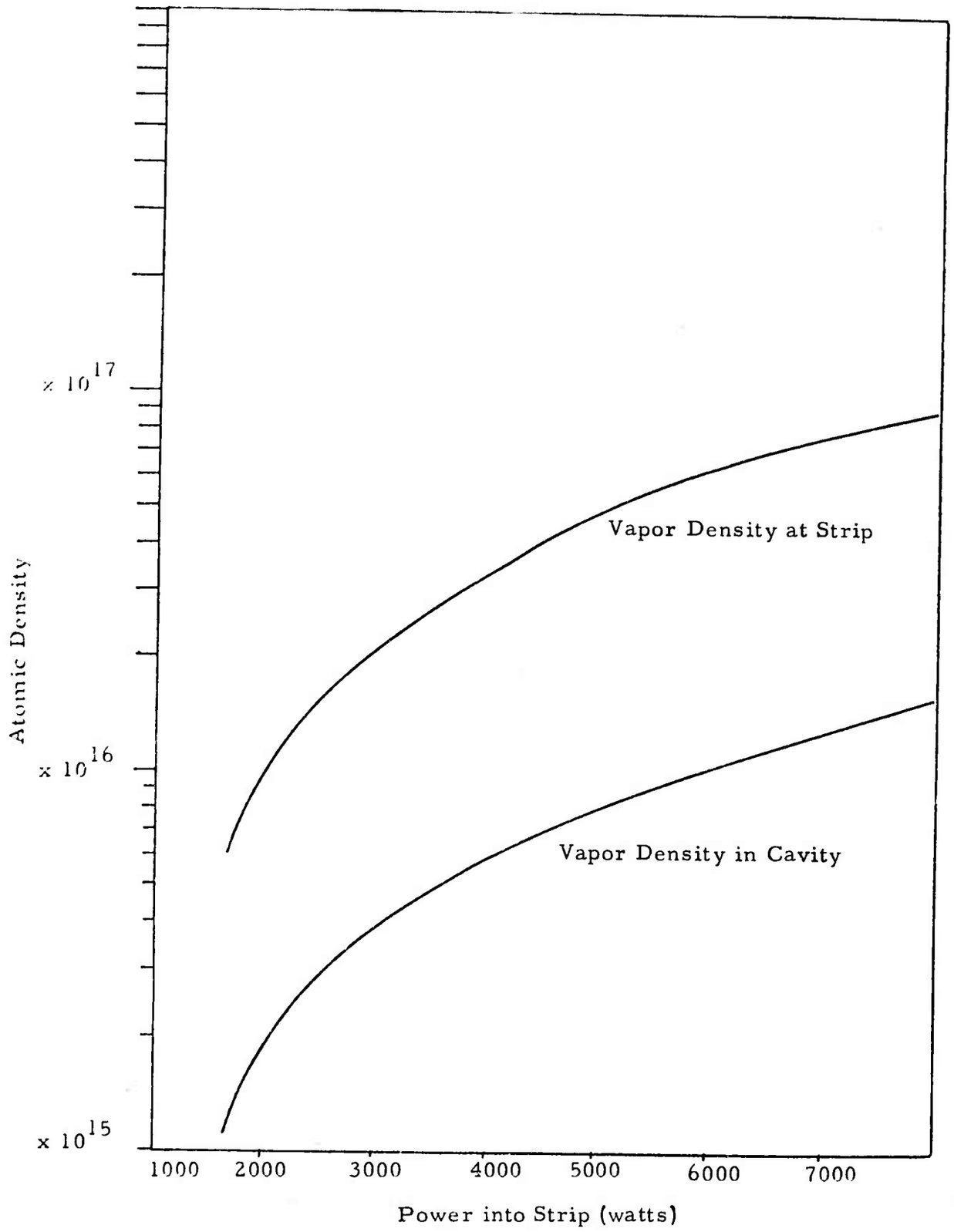

Figure 12. Power Input Requirements Copper Injector A, .380 Inch Hole Array to Produce a Given Vapor Density

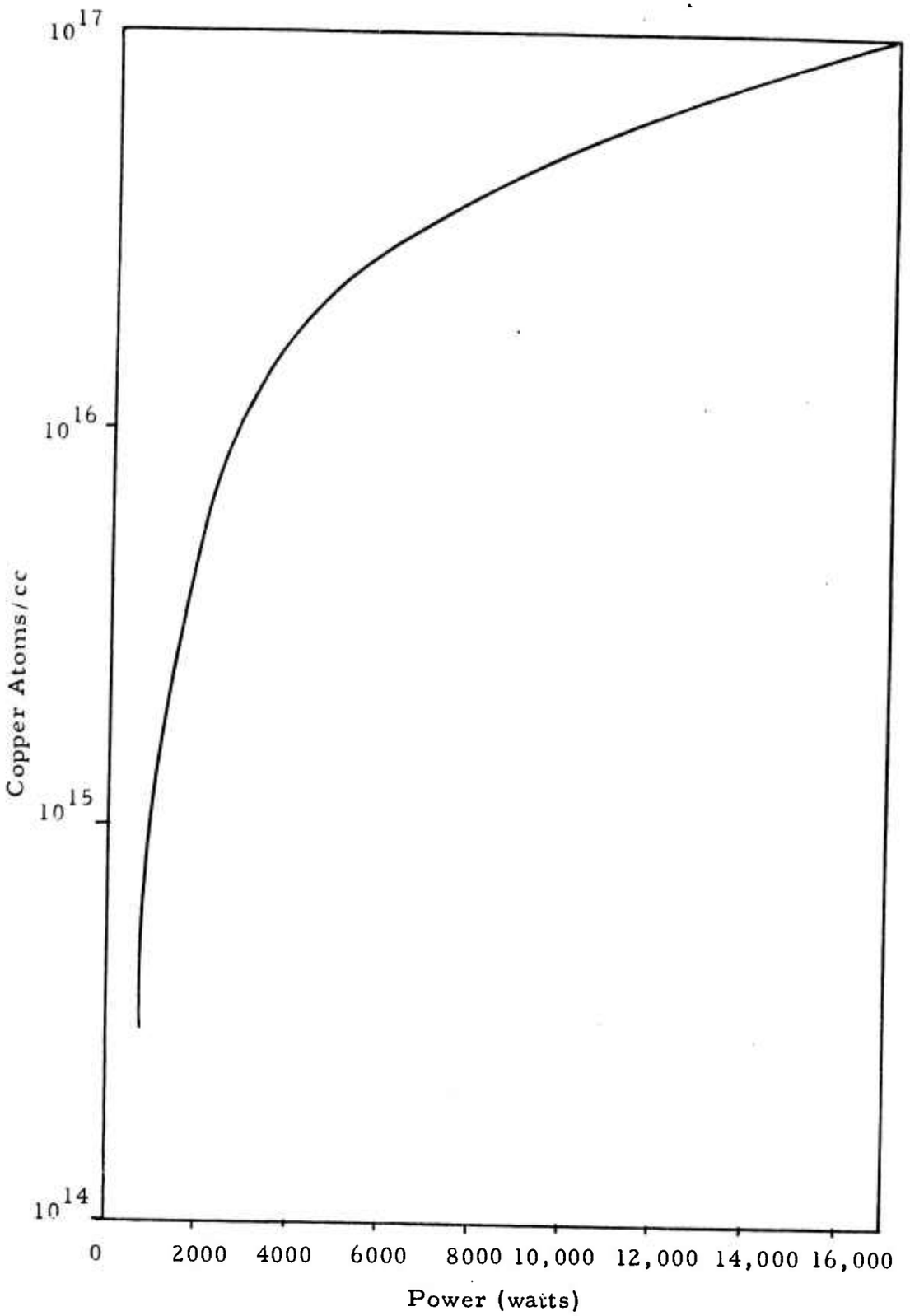

Figure 13. Power Input Requirements Copper Injector B, .165 Inch Hole Array to Produce a Given Vapor Density

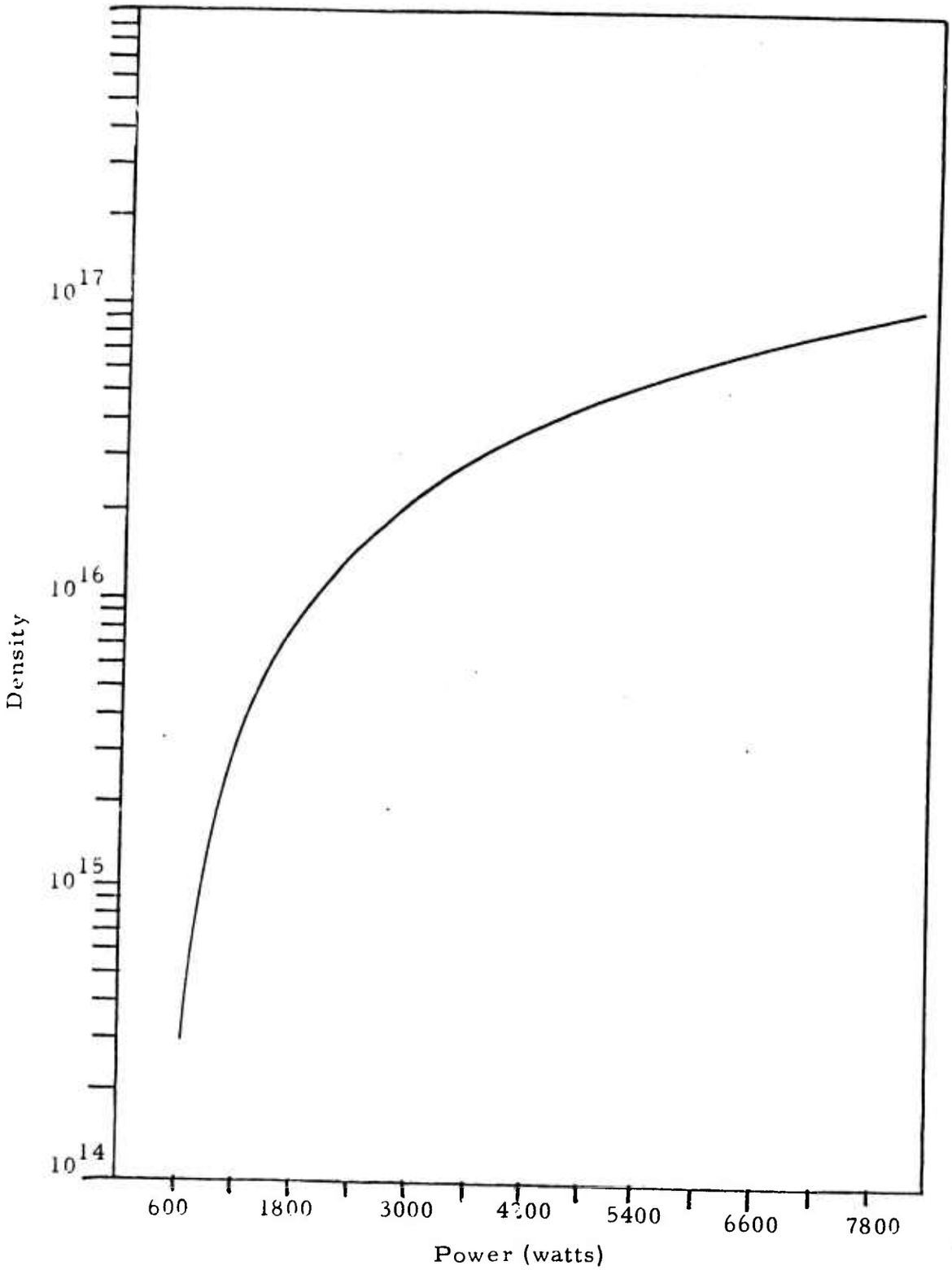

Figure 14. Power Input Requirements Copper Injector C, .067 Inch Hole Array to Produce a Given Vapor Density

liquid, and the pressure corresponding to the liquid temperature, no change in vapor flow rate is expected. Considerations of thermal balance also guarantee this.

B. CHARACTERISTICS OF THE VAPOR

If the copper provided by the copper vapor generator is to be useful for lasing it must overwhelmingly be composed of ground state copper atoms. If droplets, dimers, or excited atoms make up a significant fraction of the flow lasing may not result.

The question of droplet formation will be discussed first. The drop in temperature due to expansion mentioned in the previous section certainly leads to supersaturated conditions. However, the time required for nucleation to occur and droplets to grow could be long compared to the flow times. Recent experiments with ethanol[26] have supported a theory of nucleation time. This theory can be applied to copper to determine the time for droplet formation since the growth time of the droplets after nuclei are formed is small and so can be ignored.

The drop radius at which the transition from slow nucleation to fast condensation takes place is

$$r = \frac{2\sigma m}{kT\rho \ln P_v/P_\infty}$$

where

σ is the surface tension

T is the vapor temperature

P_v/P_∞ is the supersaturation ratio

m is the molecular mass, and

ρ is the bulk material density.

This critical radius is about the same for copper as it is for ethanol, the vapor considered in Reference 26. Consequently, the nucleation rate can be written as

$$J = K \frac{\sigma^{1/2}}{T_m^{1/2} \rho^{1/3}} e^{-K' \frac{\sigma}{T}},$$

where K and K′ contain constants and factors that are the same for both materials. The effects of using copper will be to increase the exponent by a factor of five and to decrease the multiplying coefficient by roughly another factor of five. Consequently, the nucleation rate should decrease substantially. Since times the order of 50 microseconds were needed for the ethanol nuclei to form, copper nucleation can be neglected in the ten to twenty microseconds it takes flow from the injector to the laser cavity.

The dimer fraction is also unlikely to be high. Measurements[27] have indicated less than one part in a thousand at 1110 °C. At higher temperatures the fraction should drop even further.

The use of a metal vapor generator should also reduce this fraction further[14]. Recently performed tests with bismuth have indicated this. Despite the large dimer fraction measured in static systems[27], discharge excitation of the exhaust of a bismuth vapor generator has shown the intensity of dimer band heads to be orders of magnitude weaker than bismuth atom resonance radiation.

Finally, the thermal population of the lower laser state will also be small. The highest temperatures that will be encountered are about 2,500 °K (10^{17} atoms/cc) leading to a lower state population fraction of 2×10^{-3}. This is, of course, an upper limit since as the vapor cools the lower state population will fall. If the atom lower states can follow this temperature drop the population will be about 10^{-4}. Lower injector temperatures will correspond to even smaller lower state populations.

Clearly, the flow of a copper vapor generator should be predominantly composed of ground state copper atoms.

C. LIQUID FLOW

In order to maintain the flow rates described in Section VI-A adequate liquid copper must be supplied from the reservoirs to the injector. The driving force for this liquid flow will be the wetting between the carbide film and the copper since the only applied pressure will be the few cm head in the reservoir. This wetting force will, of course, be balanced by viscous forces. Assuming that the injector flow can be approximated by that between two parallel planes, the steady pressure balance is

$$\frac{12\,\mu V \ell}{T^2} = \frac{4\gamma}{T} \cos\theta.$$

The viscous forces on the left have been equated to the wetting forces on the right, and

μ = the viscosity of copper = 3×10^{-2} poise

γ = the surface tension of copper = 1.1×10^{3} dynes/cm

θ = the wetting angle

ℓ = the average length of channel fed by each reservoir = 2.5 cm, and

V = the fluid velocity.

Solving for V

$$V = \frac{T\gamma \cos\theta}{3\,\mu\ell} = 4.89 \times 10^{3}\, T \cos\theta$$

which makes the mass flow rate from each reservoir,

$$M = 4.10 \times 10^{4}\, T^2\, W \cos\theta.$$

The mass flow rate needed to achieve 10^{17} atoms/cc and the deliverable mass flows available with ideal wetting ($\cos\theta = 1$) are listed in Table 5 for several injector cavities.

It can be seen that even with ideal wetting only .0075 inch thick injector cavities can supply enough copper when the cavity length is 10 cm. Reduction to a cavity thickness of .005 inch makes the liquid mass flows inadequate. Lower vapor densities can be supplied easily, of course.

Reduction of cos θ much below one, through incomplete wetting, could eliminate even these flows. However, the measurements given in Section V indicate that this will not be the case with the carbide wetting films chosen.

Table 5. Injector Capabilities for High Mass Flow (10^{17} atoms/cc in Laser Cavity)

Injector Cavity Width	Injector Cavity Thickness	Power Needed to Produce 10^{17} atoms/cc in Laser Cavity	Needed* Mass Flow for 10^{17} atoms/cc	Deliverable Mass Flow*
1 cm	.005"	1.28×10^5 watts	20 gms/sec	13.2
	.0075"			29.7
.5 cm	.005"	$.64 \times 10^5$ watts	10 gms/sec	6.6
	.0075"			14.8

*Both reservoirs 10 cm long injector

D. CONDENSATION AT THE CATCHER

After the copper vapor has been used in the laser cavity it can flow to a cooled surface where it may be removed by condensation. Ideally, the metal atoms will have a very high sticking coefficient and very few will be reflected back into the laser to coat electrode insulators, windows, etc. or in anyway affecting the flow upstream[28]. Since copper is such a good thermal conductor a thick layer could build up without affecting heat transfer.

In actual practice the sticking coefficient is not likely to be ideal. Substantial reflection has often been found when metal atoms are incident upon surfaces with temperatures far below their freezing points[29]. Furthermore, high directed velocities have also been found to create fewer condensation nuclei[30]. There

has been some indication that metals would stick best to substrates of a similar freshly deposited metal, but even there 10 to 20 percent reflection was common[29].

As a result, in order to gain information about condensation properties in the most easily interpretable manner, flat, water-cooled, stainless steel and copper catchers were used with other materials occasionally interposed.

SECTION VII

DISCHARGE DESIGN

A. PULSE TIME AND DISCHARGE MODE

The electrical discharge pulse used to cause the inversion is as important in laser operation as the vapor itself. It must

1. deposit enough energy in the gas to excite the number of atoms desired,

2. have peak current densities sufficient to excite the number of atoms desired in the pulse time available,

3. be shorter than the spontaneous decay time of the upper laser state,

4. be comparable to or shorter than the lasing time so that no electrical energy is wasted.

The first three will be met to some degree any time lasing is achieved. However, if high efficiency and high laser energy per unit volume of the cavity is to be achieved, the fourth condition must be achieved and the first and third must be optimized upon. All of this can be done by proper discharge circuit design.

Some information can be gained about such a design by considering certain fundamental requirements. Excitation of all the copper atoms present would take 6.2×10^{-19} n joules/cc, where n is the number of copper atoms per cc. It also has been indicated that current densities of up to 10^4 amp/cm^2 would be needed to excite such a large fraction of the copper atoms[2, 31]. Both these conditions can be written as

$$\frac{1}{2} \quad CV^2 = \alpha n$$

and

$$\frac{CV}{\tau} = J$$

where it is assumed that one cc of laser cavity volume presents one cm^2 of discharge area and

C is the storage capacitance

V is the initial voltage

α is the energy per atom needed

τ is the discharge pulse width, and

J is the current density.

Simultaneous solution of these equations shows that

$$C = \frac{2 \alpha n}{V^2}$$

and

$$\tau = \frac{2 \alpha n}{V J}$$

The discharge time needed can also be arrived at by noting that the number of electron-atom collisions per second is given by

$$\frac{\nu}{n} \tau' = 1 = \sigma n_e \overline{V} \tau'$$

or

$$\tau' = \frac{e}{\sigma J} .$$

Assuming a voltage of 10^4 volts, a vapor density of 10^{17} atoms/cc, and noting the value $\alpha = 6.2 \times 10^{-19}$ given above, then

$$C = 1.2 \times 10^{-9} \text{ farads}$$

$$\tau = 1.2 \times 10^{-9} \text{ seconds.}$$

In addition assuming $\sigma = 9 \times 10^{-15}$ then[32]

$$\tau' = 1.4 \times 10^{-9}$$

in agreement with τ. Longer pulse times than 1.2×10^{-9} seconds will then lead to lower current densities and a smaller excited fraction.

Unfortunately, such short discharge pulses will be very difficult to obtain without special effort beyond the scope of this program. For instance, the inductance needed with 1.2×10^{-9} farads to produce a half period of 1.4×10^{-9} seconds is 1.8×10^{-10} henrys. A coaxial line has an inductance given by

$$L = 2 \times 10^{-7} \ln \frac{r_o}{r} \quad \text{henrys/m}$$

and so, if the discharge took the form of the central conductor of such a line (i.e., longitudinal discharge), assuming a practically realizable radius ratio of two, the discharge could only be .13 cm long. An improvement can be obtained by using a series of transverse discharges. Each will be shorter than the longitudinal discharge through the same volume by the aspect ratio of the laser cavity. The number of parallel circuits involved will also be equal to that ratio. Thus, in principle, a laser cavity pumped by transverse discharges can have two orders of magnitude smaller inductance than one pumped by a longitudinal discharge.

One advantage of a longitudinal discharge is that with a large apsect ratio the area through which current flows is smaller compared to the volume being excited than was assumed above. For this reason the pulse width, τ, needed will be larger than computed. A similar result can be obtained with a transverse discharge by making the thickness of the discharge small.

Ultra-low inductance discharge circuits can only result if the discharge and the current return are built into a single closely spaced unit. Current thinking leans to a design integral with the copper vapor generator and the vacuum chamber walls. The initial laser design described in Appendix V, dictated a flanged port

chamber, incompatible with such integral circuitry. As a result only a limited improvement in the state-of-the-art could be expected in this area.

That chamber did allow a longitudinal discharge to be applied to a modest volume with substantial gain length. Early tests in which gain was limited by low vapor density benefited from that configuration. Later tests using a single transverse discharge were used to investigate shorter pulse times, small volumes and high current densities.

Ultimately an ultra-low inductance integrated discharge circuit laser is needed. Only in this way can the full promise of this laser system be realized.

B. SWITCHING

Despite early concern that a simple series switch would

1. not lead to uniform discharge currents within laser cavity,
2. would unacceptably increase the circuit inductance and slow the discharge, and
3. could not operate at the high repetition rates needed,

all laser tests have been operated in this way. The development of a high repetition rate quenching spark gap is largely responsible for this choice[14]. This device has demonstrated 250 KHz repetition rates, less than two nanosecond rise times, and peak currents of several thousand amps. Furthermore, if suitable electrodes were used, uniform discharges resulted. The discharge times are too small for anode or cathode spot formation.

SECTION VIII
EXPERIMENT DESIGN

A. LASER EXPERIMENT

A desire for flexibility dictated that all components of the laser be removable. Major modifications to both the copper vapor generator and the discharge circuits could then be accommodated within the same structure. Appendix V discusses this choice in light of the discharge design first contemplated.

This structure was based upon a rectangular box (see Figure 15) with removable bottom and top. The walls were cooled by water flowing through copper tubing. Three flanged ports were available on each long side for pumping, gauges, and electrodes. One pair of electrodes can be seen within the box. One flanged port was present on each end for Brewster angle laser windows. These windows were on the axis of the box.

The removable box top (see Figure 16) had two flanged tubes standing on it enclosing the copper vapor generator reservoirs. These reservoirs extended down into the box itself where the injector strip was inserted between them as described earlier. The reservoirs were mechanically supported, filled with new copper, and supplied with heating current at the flanges. Radiation shields were hung around the reservoirs to reduce thermal losses as described in Appendix IV. Wires were also connected to the reservoir bottoms to allow measurement of the voltage drop in the injector strip and in each of the reservoirs.

The bottom of the box was a simple, hollow-core, water-cooled stainless steel plate. The copper vapor was largely condensed there, though some deposited on the walls.

The assembled laser can be seen in Figure 17. A schematic of the laser experiment shown on Figure 18 identifies components in the photograph.

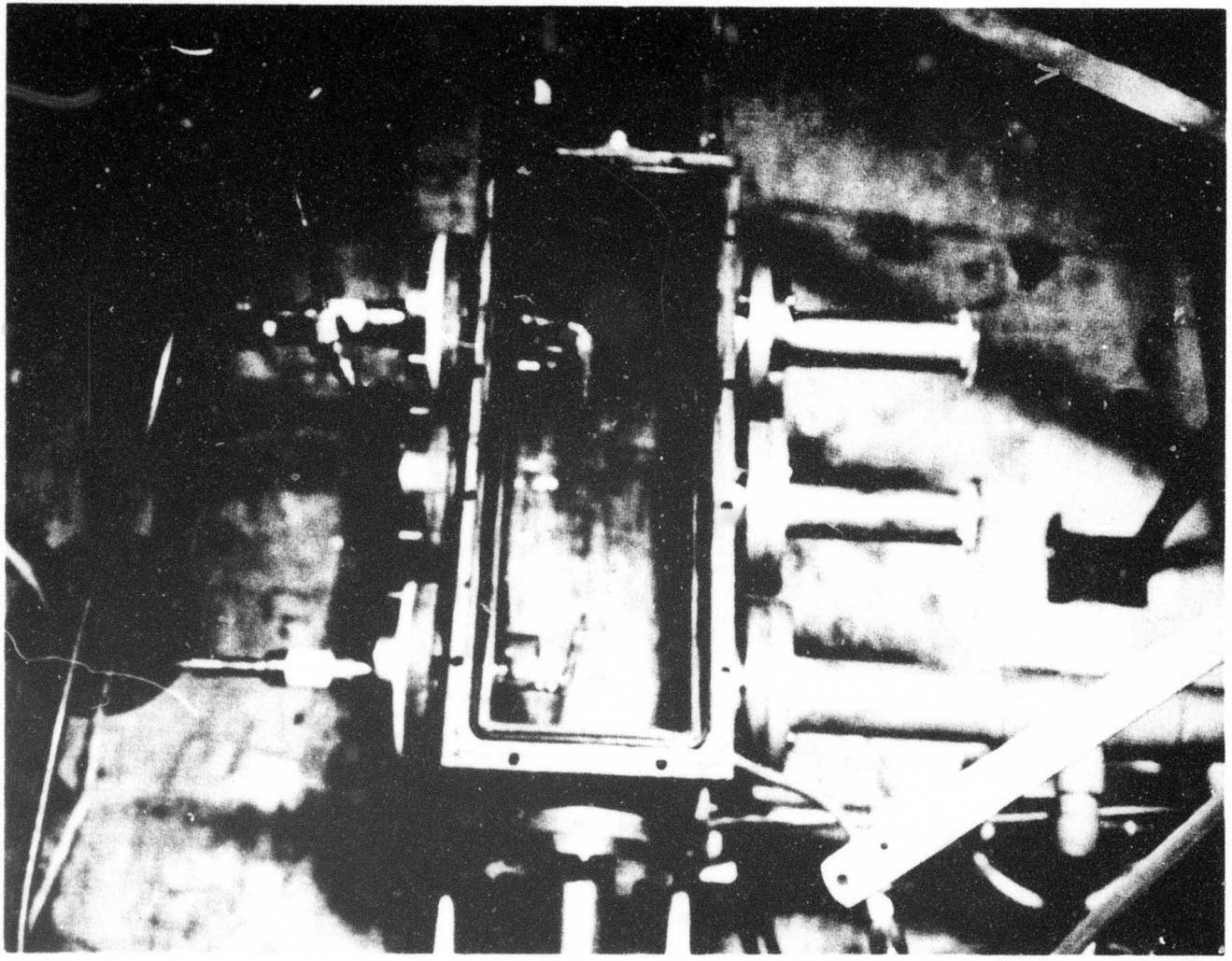

Figure 15. Photograph of Laser Box without Top. Longitudinal discharge electrodes have been installed.

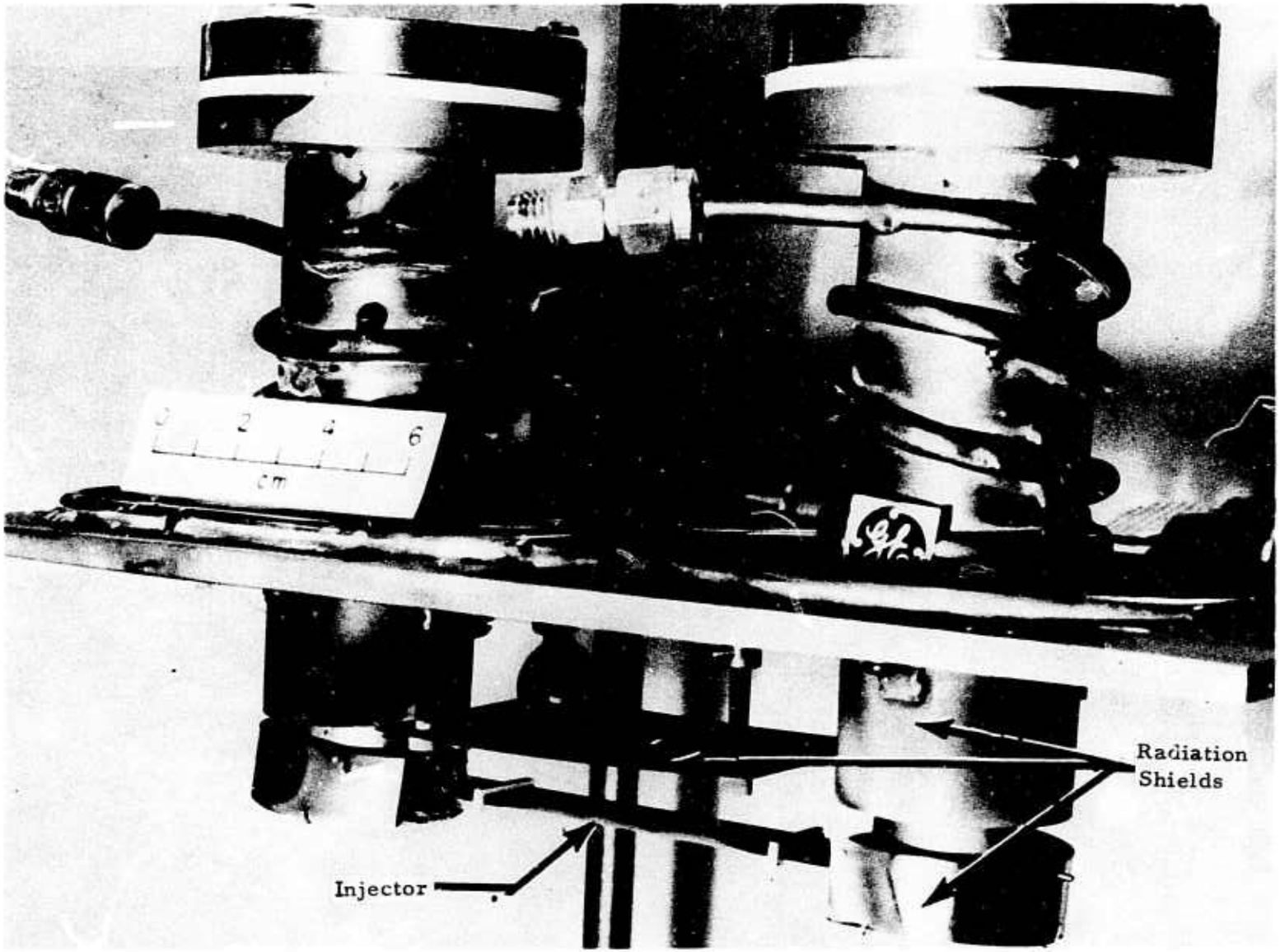

Figure 16. Copper Vapor Generator Assembly for Copper Vapor Laser. This assembly is mounted on top of laser structure shown in Figure 15.

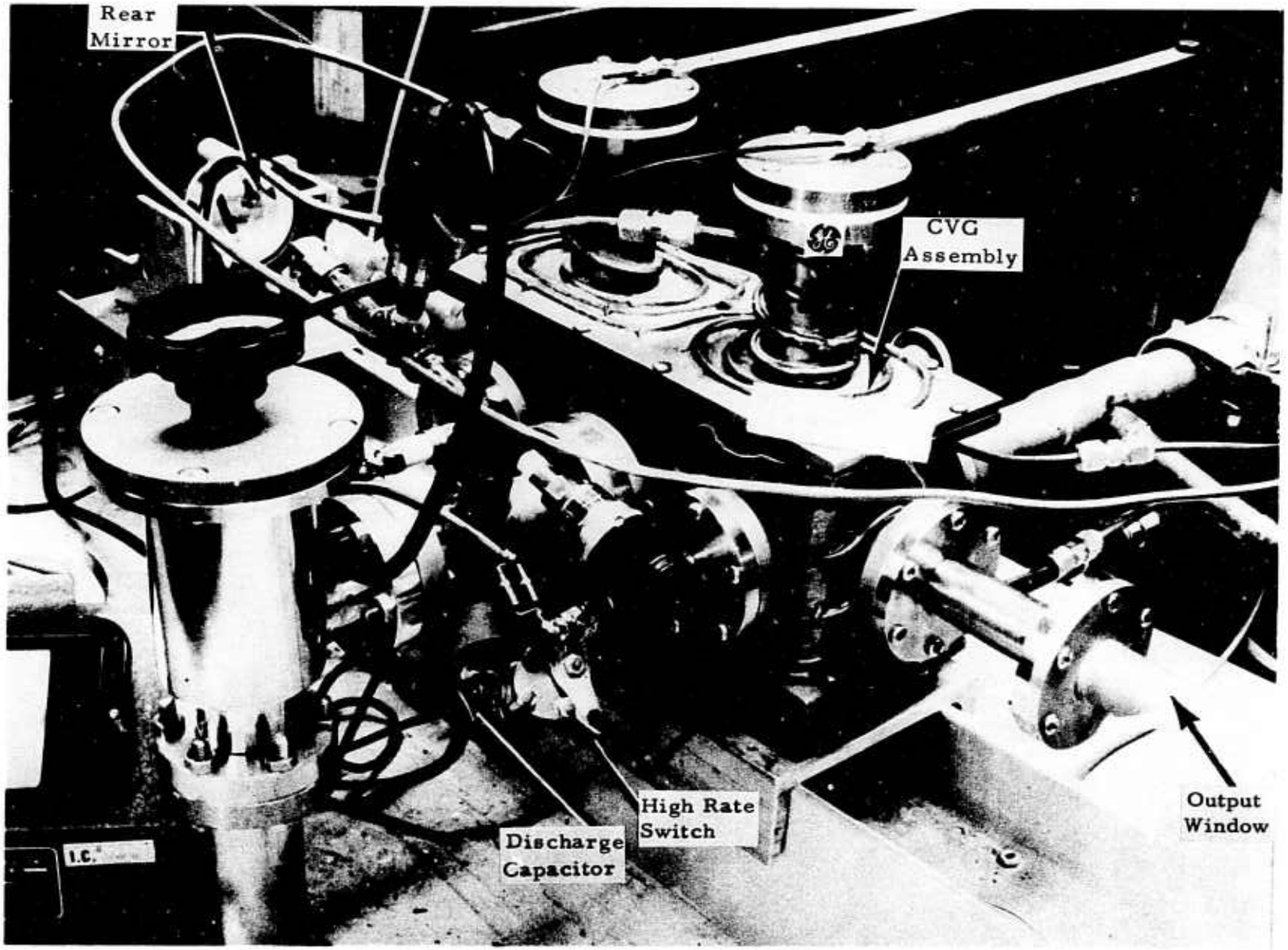

Figure 17. Copper Vapor Laser. Set up for longitudinal discharge operation.

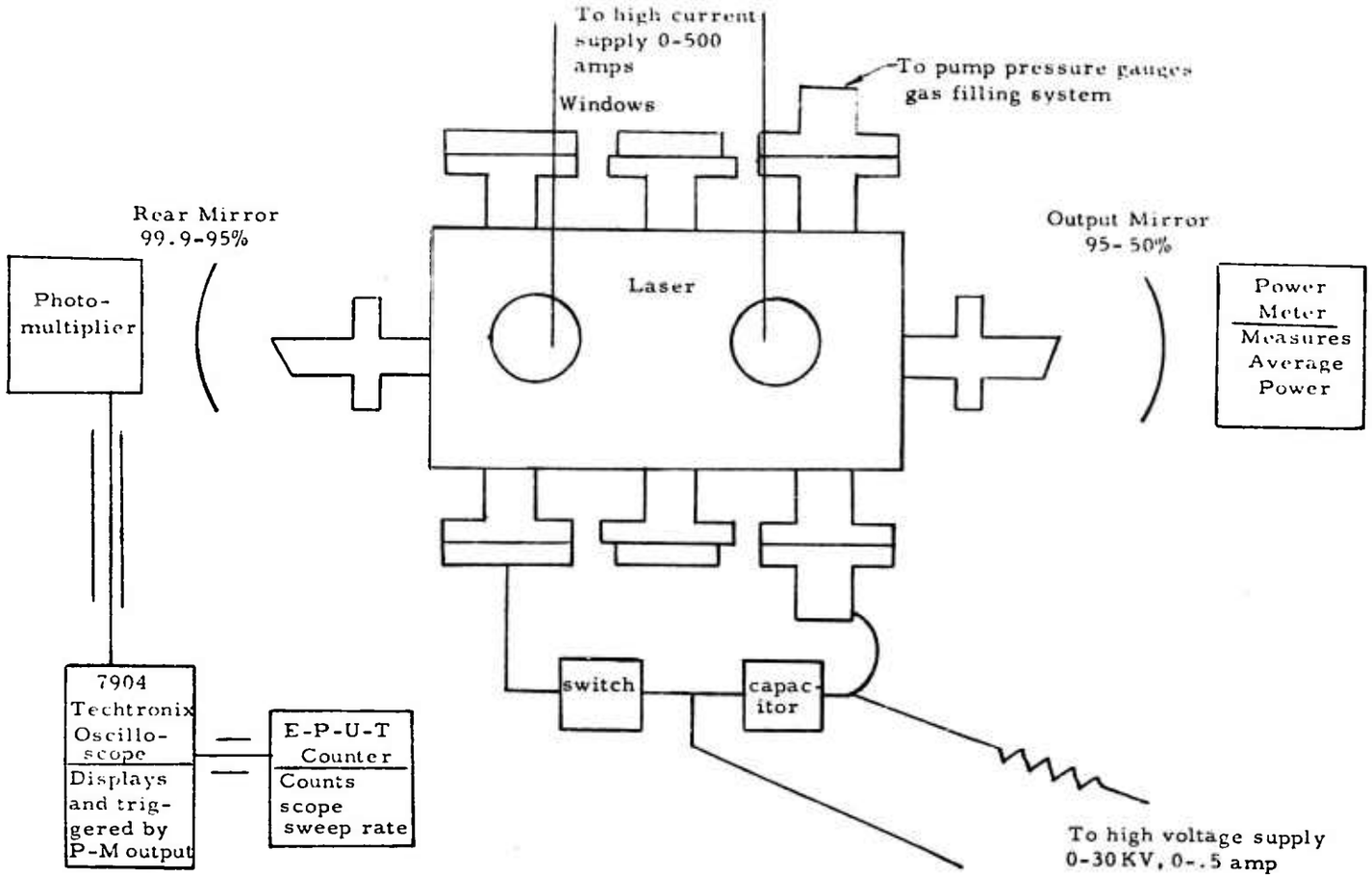

Figure 18. Schematic of Laser Experiment

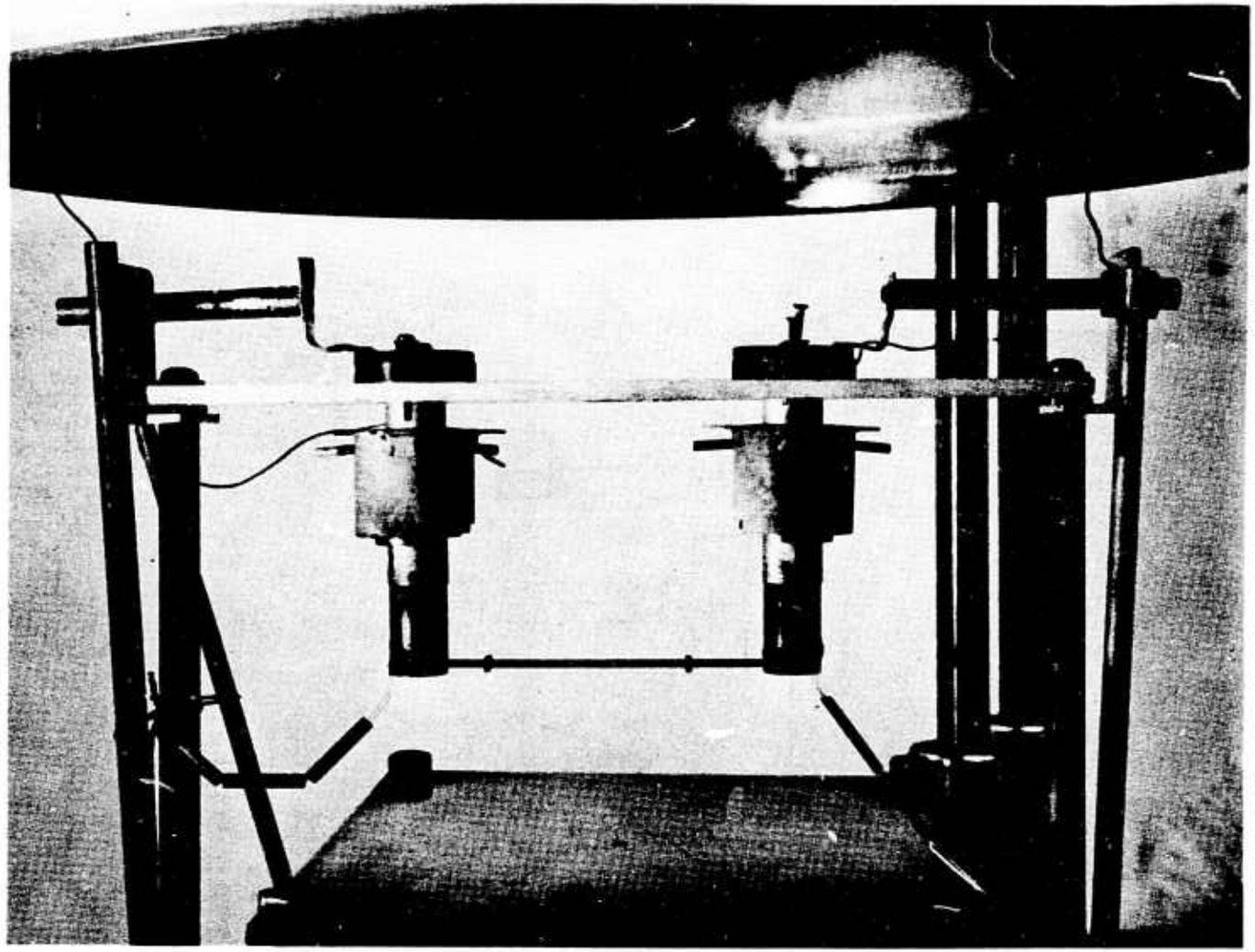

Figure 19. Copper Vapor Generator on Bell Jar Test Stand. Radiation shields have been raised so that reservoirs can be seen. Wires attached to reservoir bottoms are used to measure reservoir temperatures and the voltage drop across the injector.

Ambient pressure was maintained in the range of one micron. Argon, Neon, or Krypton was generally admitted to a pressure of more than five torr to carry the discharge currents.

B. TEST STAND

A photograph of the bell jar system used for checkout of the copper vapor generators is shown in Figure 19. The fundamental advantage of this system over that of the laser is that the large chamber and the large distance to the high current feed-throughs minimize thermal problems to a degree not possible in the present laser. In addition large windows are available in this system for viewing of the whole generator. Analysis of generator operation is very difficult without such a total view.

C. MIRRORS AND SENSORS FOR LASER

The optical cavity is two 10 meter radius mirrors separated by one meter. One mirror has maximum reflectivity (~100 percent) at 5105 Å and 55 percent at 5782 Å. The output mirror can be chosen to be either 3, 10 or 50 percent transmission at 5105 Å. Of these three mirrors only the transmission of the three percent one is known at 5782 Å, and this is 13 percent.

The spontaneous or laser emission is monitored by focusing the light from the laser cavity on the entrance slit of a Jarrell Ash 1/2 meter Ebert monochromator. The intensity at the output slit is detected by a 1P28 phototube with a divider chain designed for fast pulse operation. The phototube signal is displayed on a Tektronix 7904 oscilloscope for waveform determination or presented to a Keithly Model 410 micro-micro ammeter for time averaged measurements.

The sawtooth output of the scope drives an event-per-unit-time meter to monitor the current or laser pulse repetition rate. A calibrated Rogowski coil current probe measures the amplitude and time dependence of the pulsed current discharge in the laser cavity.

SECTION IX
COPPER VAPOR GENERATOR TESTS

A. SUMMARY

A large number of tests have been performed developing and investigating the copper vapor generator described earlier. A summary is given in Appendix VI. As a result, copper vapor flows suitable for lasing can be produced reliably from a given generator for periods the order of hours. Injector temperatures over 2400 ^{o}K with corresponding vapor densities near 10^{17} atoms/cc have also been attained for shorter periods. In addition, measurements of deposited films indicate flow uniformity of a few percent and confinement of the flow within the ranges defined by theory. The temperature and velocity of the copper vapor can be inferred from this spreading and were found to respectively fall below 1400 ^{o}K and in the range of 6-7 x 10^{4} cm/sec. The following sections discuss these characteristics in greater detail.

B. PRELIMINARY OPERATION

Operation of a copper vapor generator of the optimum design began with an empty injector and each reservoir loaded with about 20 grams of solid copper. The volume around the injector and within the reservoirs was then evacuated to pressures on the order of 1 micron or below. Reservoir heaters then raised the reservoir temperatures close to the melting point of copper. The main heating current was then raised to a level that brought the injector and the reservoirs above the melting point of copper. The liquid then wet the carbide surface extending into the reservoirs and was drawn into the injector cavity. The resistance of the injector dropped during this filling, and so the applied voltage had to be reduced if the injector temperature was to be kept from rising. Once the injector was filled, as evidenced by a stabilized resistance, the system could be cooled and run another time or the current could be raised to levels neeeded for vapor injection immediately.

A few minutes operation at high temperature generally resulted in a bulge in the thin graphite sheets forming the injector causing the resistance to drop further. Injector A would generally reach .010 to .016 ohm and Injectors B and C .022 to 0.027 ohm. This resistance change required an increase in the current needed to produce a given injector temperature.

During high-current operation the reservoir resistance and conduction from the injector provided additional heat. The reservoir heaters could then be turned down or off. It should also be noted that injector designs of sufficiently low resistance while empty could be used without separate reservoir heaters. The same current that heated the injector heated the reservoirs. Injectors of design A and bismuth vapor injectors described elsewhere[14] have been operated in this way.

One result of not having independent reservoir heaters was that both heaters may not have been at the same temperature. When this temperature differential was maintained for any significant period large liquid flows were observed to take place between the reservoirs[34]. A temperature difference of 1 to 2 hundred degrees generally was sufficient for several grams per minute of liquid copper to flow from the hot reservoir to the cold reservoir. Of course, as soon as one reservoir ran low on copper it became more resistive and hotter, increasing the flow from it until it was empty. The end of the injector closest to the empty reservoir would then find itself empty and far more resistive than the rest of the injector. Overheating and failure would often result. Proper temperature balance through careful reservoir design and separate heaters solved this problem.

C. OPERATING DURING VAPOR PRODUCTION

Currents sufficient to heat the injector to 1800 ^{o}K or above, produced significant vapor flow. Most of that flow was contained in a well defined stream leaving the injector holes. The stream expanded and impinged upon the cooled catcher. Under the proper conditions a film adhered to a substrate placed upon the catcher so that the stream and its uniformity could be measured.

Figure 20 is a photograph of a series of sapphire wafers used as the substrate for such a measurement. The extent of the flow can be seen clearly. The absence of film can also be seen in certain locations. This is due to the critical nature of the substrate temperature. When the substrate temperature was very low, as with the cooled catchers themselves, only very thin films would remain intact. Films approaching .001 inch and larger would crack and separate from the substrate. A high thermal conductivity material, such as sapphire, when placed on the cooled catcher would have a surface temperature dependent upon the thermal flux on to it (radiation and heat of condensation of the vapor) and the intimacy of contact with the cooled surface it rests upon. A proper heat balance would lead to high substrate temperatures but below the melting point of copper. Adhering, intact films would result[33]. Of course, if the thermal balance is improper the surface of several of the sapphire wafers would not have the proper temperature, probably due to the condition of the surface beneath them.

The number of wafers that retained the film properly was, however, generally adequate to establish the dimensions of the stream and its uniformity. Figure 21 gives the stream width as a function of the distance from the injector as determined from several such sapphire wafer arrays. These correspond well with the spreading expected from theory for flow into a vacuum[9, 10] or diffusion into a low pressure gas. This measurement is sufficient to allow determination of the vapor density, temperature and velocity as a function of the distance from the injector. Figure 22 gives this information scaled for initial temperature and density. These initial conditions will be discussed below and on Table 6.

Figure 23 gives the film thickness along a line parallel to the injector axis as an indication of integrated flow uniformity. Here, the mean deviation is the order of two percent, within measurement uncertainty. Measurements have also been made over lengths the order of .75 inch which the measured deviation was zero, indicating even better uniformity. The two percent measurement uncertainty was still operative, however.

Table 6. Characteristics of Copper Vapor Generator Operation

Injector Type	Power (watts)	Time at Power (seconds)	Density in Laser Cavity (atoms/cc)		Copper Mass Injected (gms)	
			Computed	Experiment	Computed	Measured
C	920	60	3.4×10^{14}	2.5×10^{14}	.08	
	970	600	4.4×10^{14}	3.3×10^{14}	.15	
	1020	1440	5.5×10^{14}	4.1×10^{14}	5.00	
	1060	570	6.5×10^{14}	4.9×10^{14}	2.50	
	1300	60	1.4×10^{15}	1.1×10^{15}	.60	
					8.33	6.25
B	1200	30	1.0×10^{15}	8.5×10^{14}	.8	
	1300	30	1.3×10^{15}	1.1×10^{15}	1.03	
	1400	150	1.8×10^{15}	1.5×10^{15}	7.12	
					8.95	7.6
A	1400	60	3×10^{14}	2.9×10^{14}	1.13	
	1540	15	1×10^{15}	9.7×10^{14}	.94	
	1800	15	3×10^{15}	2.9×10^{15}	1.35	
					3.42	3.3
C	6000	7	6.2×10^{16}	1.67×10^{17}	6.6	11

Vapor temperature is $880^{\circ} - 960^{\circ}K$ except last entry which is $1200^{\circ}K$

Vapor velocity is 6×10^{4} cm/sec except for last entry which is 7×10^{4} cm/sec

Measurement of the deposited film as a means of establishing the amount of vapor flow, is open to some question. The sticking coefficient of copper on even cold copper is not ideal. Substantial reflection of the primary copper vapor stream occurred so that supposedly shadowed locations were often coated with copper. The bell jar window was ideally situated for deposition of these reflected atoms. Coatings of over 10^3 Å were observed. Comparison of the material lost from the reservoirs, that deposited on the catcher, and an estimate of that reflected to other surfaces, gave a rough accounting of all material. The reflected component was found in this way to be substantial but not dominant (e.g., less than 25 percent, generally much less). Consequently, measurement of the copper lost from the reservoirs was generally used as a measure of the amount of metal vaporized.

Knowledge of the time the injector was at a given power level can be coupled with the vaporized mass to give a measure of the mass flow rate. Since the area available for vaporization is fixed the injector temperature follows. Furthermore, vapor stream dimensions from Figure 21 then allow determination of the expansion ratio (at least two), and flow velocity temperature and density, follow through the use of the gas laws, as described in Section VI. Table 6 lists several runs, with computed and measured total flows and vapor density. Figures 12, 13, and 14 were used. Included are generators differing in dimensions, constructional details and filling procedures. Appendix VI lists more runs.

Agreement lies well within uncertainties of vapor pressure[27] and mass determination. As a measure of the efficiency of vapor production obtained the energry required to produce each cc of vapor is compared with theory on Figure 24. The characteristics of the vapor given in Table 6 are well within ranges of interest for copper vapor laser applications[1-8].

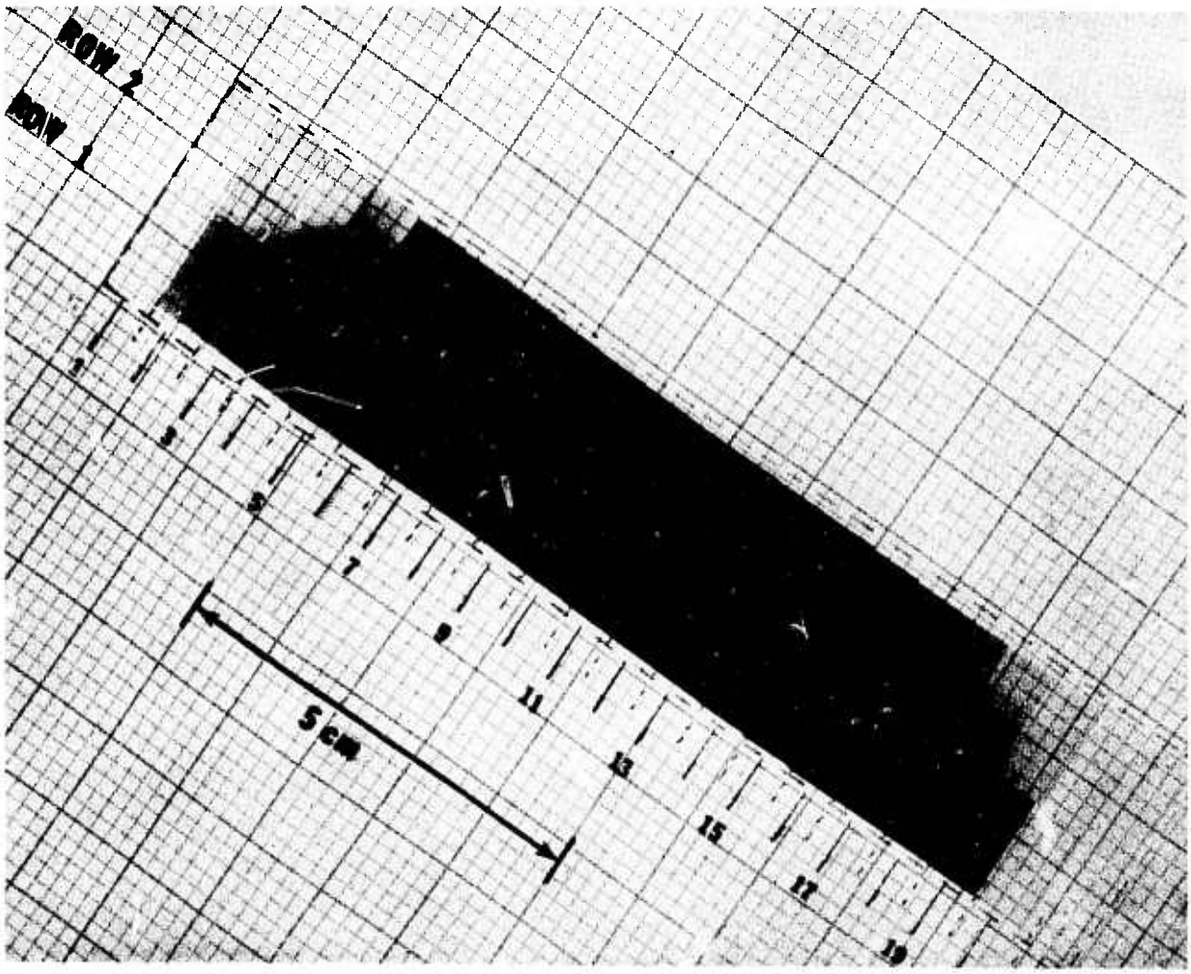

Figure 20. Photograph of Sapphire Wafers with Deposited Copper
The effect of different thermal contact between individual wafers and the cooled surface they rest upon is reflected in the great variation in deposit found on some adjacent wafers.

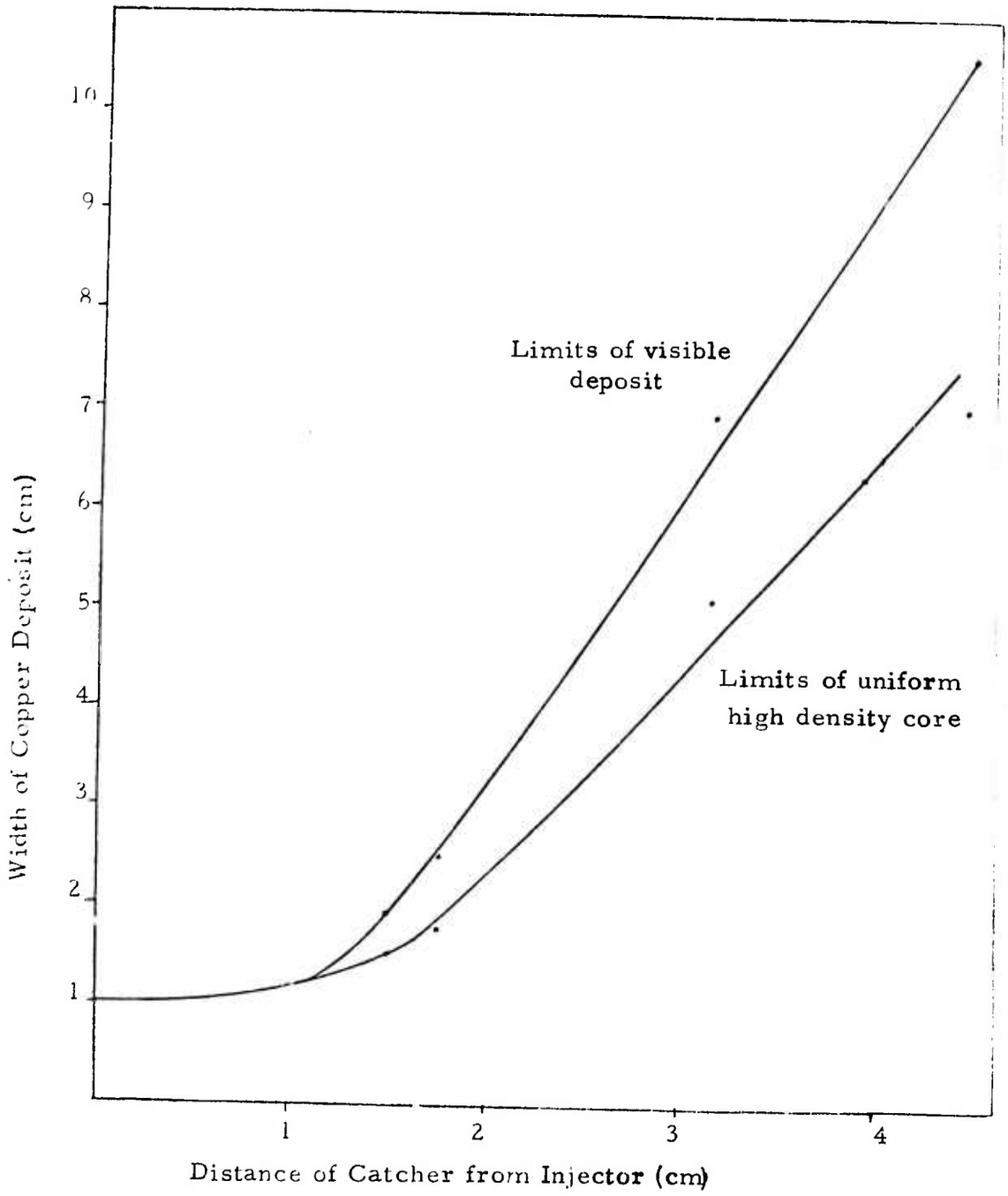

Figure 21. Width of Vapor Stream as Function of Distance from Injector

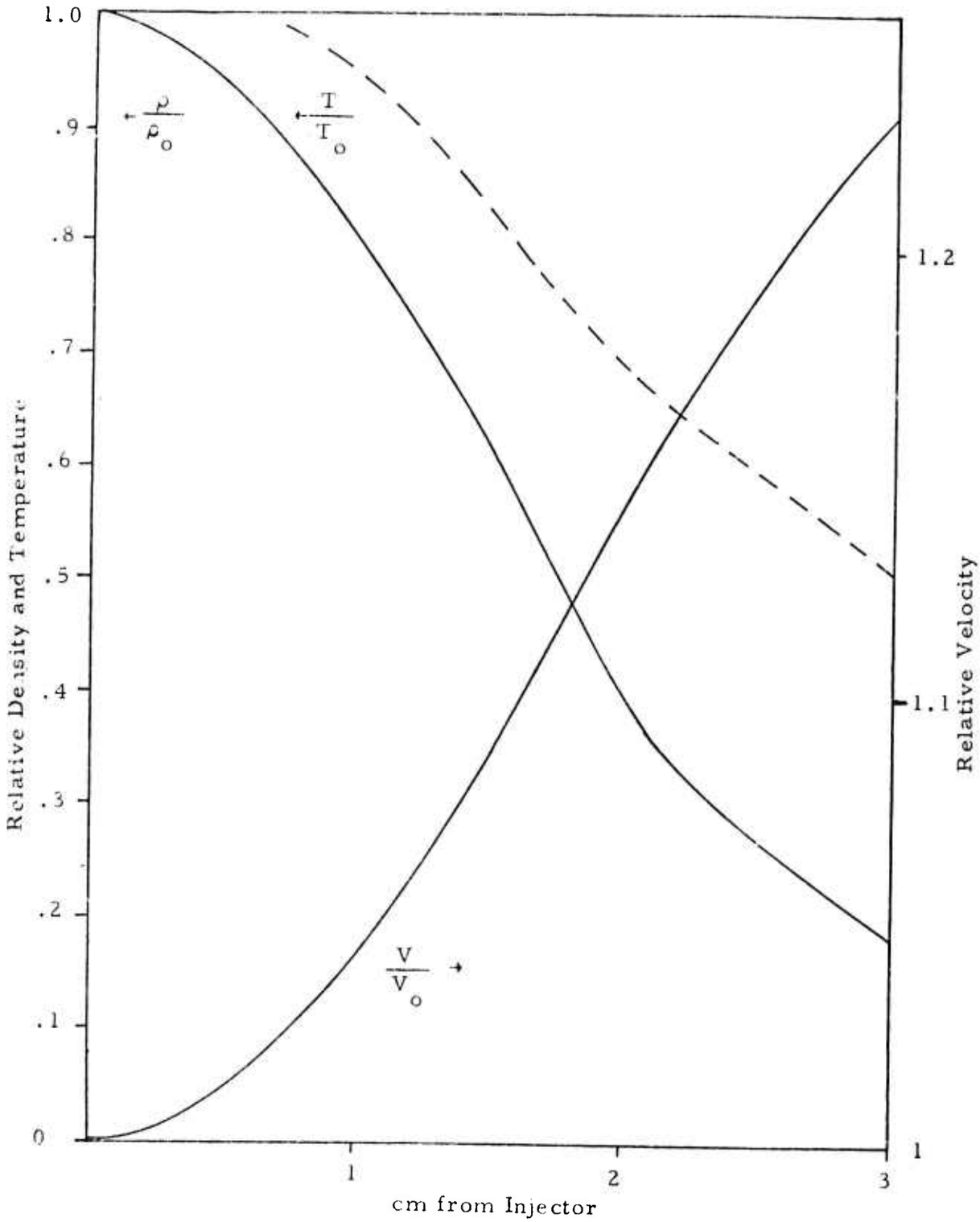

Figure 22. Vapor Density, Temperature, and Velocity as Function of Distance from Injector A. Scale constants ρ_o, T_o, and V_o are values obtained just beyond injector surface after merging of individual jets from holes. See Figure 12, Table 4, and page 27.

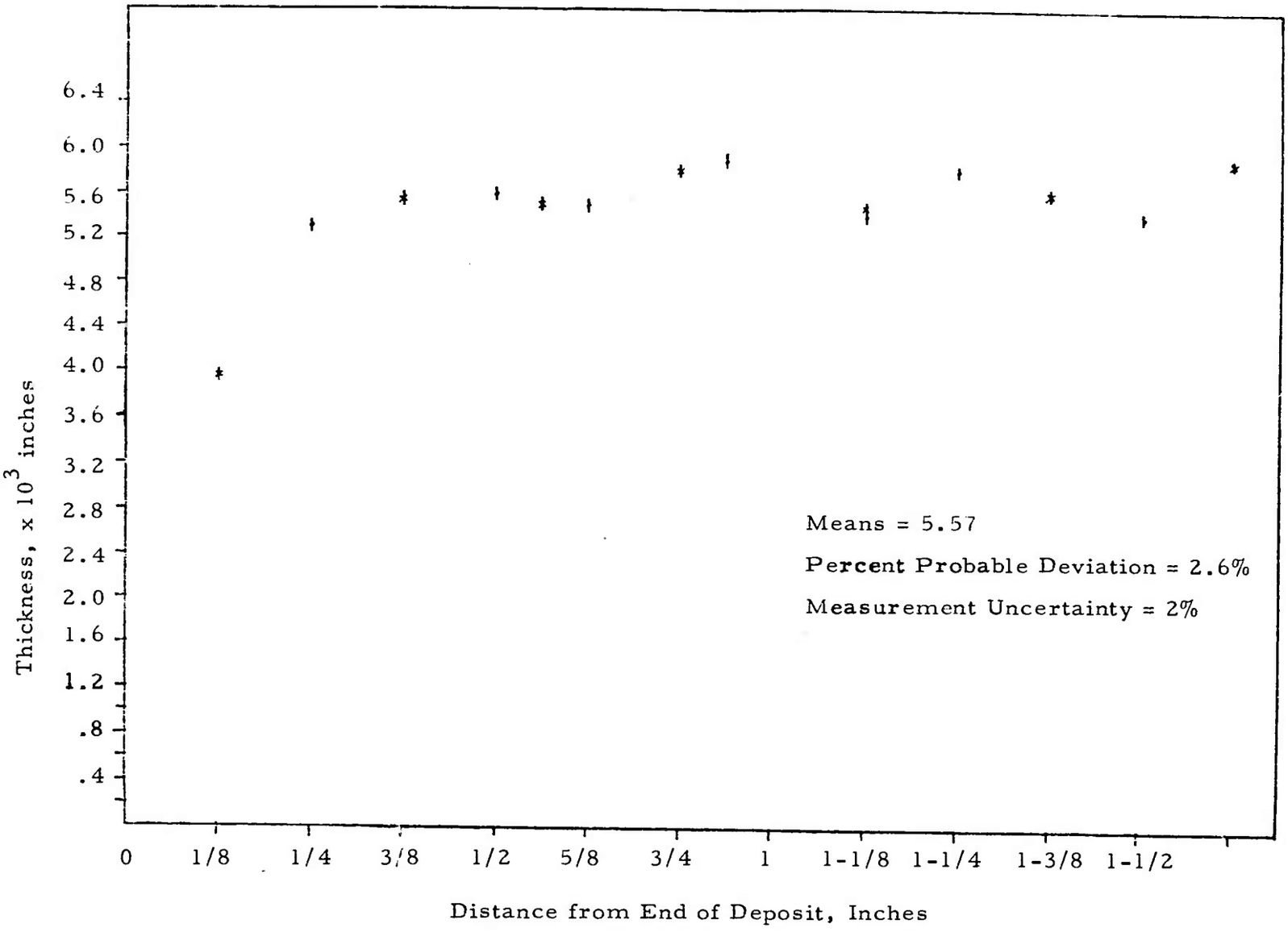

Figure 23. Copper Film Thickness Along Line Parallel to Injector Axis

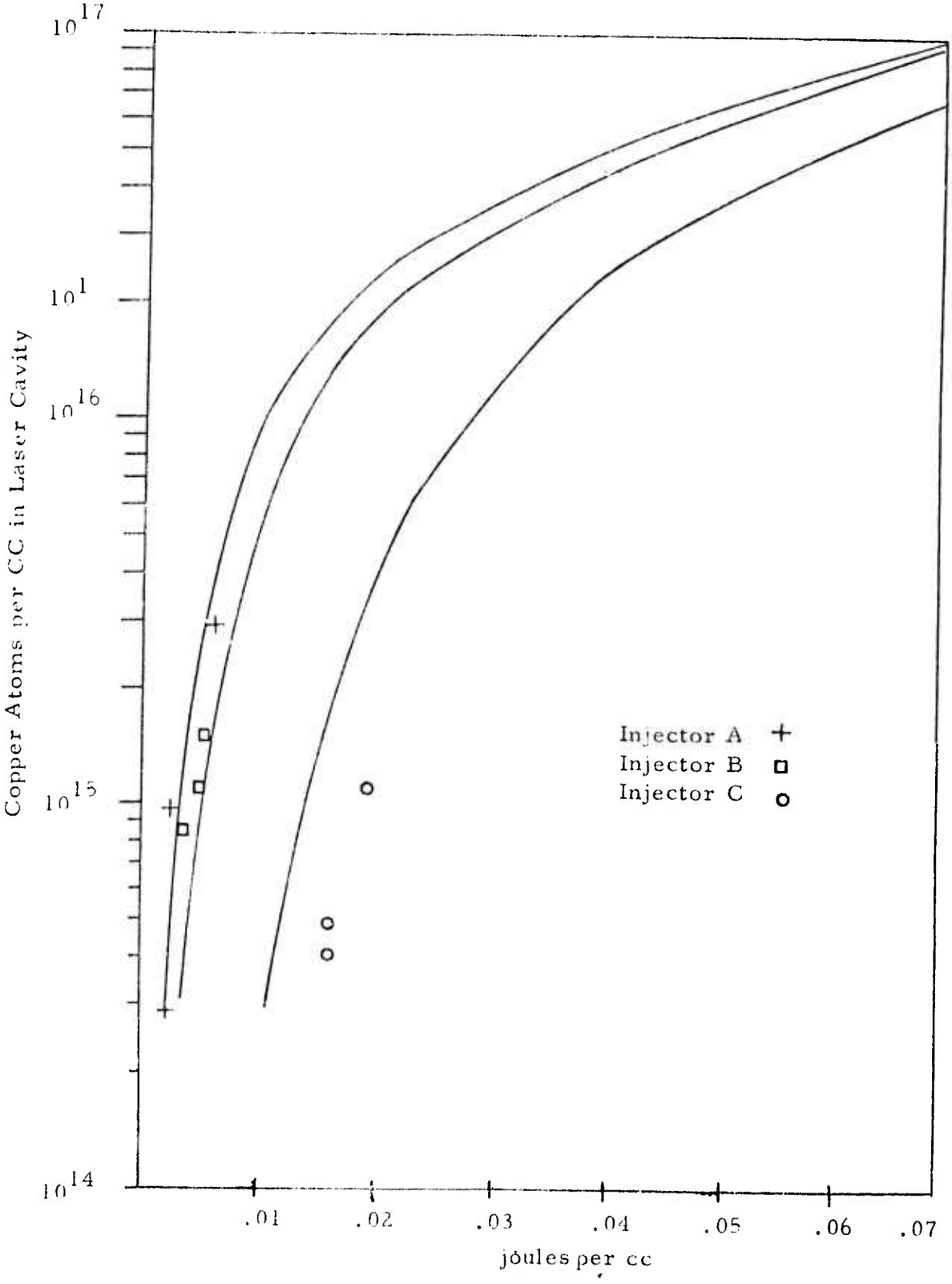

Figure 24. Energy Required to Produce Copper Vapor per Unit Volume as a Function of Density. Theory from Figures 12, 13, and 14 and experiment from Table 6.

SECTION X

LASER TESTS

A. HISTORICAL OUTLINE

Following the deveopment and successful testing of a copper vapor generator in a bell jar, the unit was placed in the laser system to demonstrate its capability as a source of copper for laser operation. Three different methods were used to excite an electrical discharge to produce the population inversion in the copper vapor. These were: 1) pulsed transverse electron beam, 2) cold cathode longitudinal overvoltage, and 3) cold cathode transverse voltage.

The first experiments were performed with the electron beam excitation. The anode was charged to a high positive potential (several kV), and the discharge was initiated by pulsing the electron source negative to overcome the retarding effect of a grounded screen grid. This method proved unsuccessful, however, because the conductivity of the copper vapor was too large and thus would not stand off the high anode voltage. (The reader is referred to Appendix V for a more detailed treatment of this phase of the work.)

This was followed by cold-cathode overvoltage techniques with electrodes placed both longitudinally and transversely to the vapor sheet. In this method a fast quenching spark gap switch[14] was used to discharge the energy storage capacitor into the laser cavity. Injector strips of widths 0.97, 0.42 and 0.16 cm have been used. The tests demonstrated lasing action with both electrode configurations. The results are described in more detail below.

B. OBJECTIVES OF LONGITUDINAL AND TRANSVERSE DISCHARGES

The longitudinal electrode configuration was chosen for the initial experiments to demonstrate lasing. The choice was made to provide maximum gain length (10 cm) and discharge conditions similar to other copper systems known to lase. A one cm wide injector strip (A on Table 3) was used for the vaporization of copper.

Argon buffer gas at filling pressures in the range of 5 to 10 torr was used to carry the electrical discharge and to minimize copper deposition on the Brewster and viewing windows.

Lasing was demonstrated with this configuration. The numerical results are tabulated and discussed in Section X.E. There were, however, several difficulties encountered which presented limitations.

The Argon discharge (see Figure 25) can be qualitatively described at these pressures as a diffuse glow with the beginnings of a strong glow or weak arc on a direct line between electrodes. The rise time was the order of 50-60 nanoseconds. The large electrode spacing consequently allowed the discharge to follow shorter paths along the injector strip or along the walls of the metal box rather than through the gas and thus reduced the current density in the laser cavity. This problem was remedied to some extent when insulators were placed so as to block discharges to the walls.

Thermal phenomena led to a limitation in use of the wide injector. Its low resistance required very large injector currents to produce high copper atom number densities in the cavity. Currents in the range of 400-450 amperes were necessary to reach laser threshold. At these high currents all electrical contacts, both internal and external to the laser, caused practical difficulties from overheating.

In an attempt to overcome these limitations the system was switched to a transverse electrode arrangement and the 0.42 and 0.16 cm (B and C in Table 3) injector strips.

The transverse discharge electrodes provided a much more localized discharge that reduced current to the wall and increased current density. Furthermore, the circuit inductance was decreased and, as expected, a faster rise time discharge was observed. The narrower injector strips produced the copper vapor densities required with lower injector currents.

Two transverse electrodes three or four cm long were located in the center of the optical cavity 0.45 to 1.5 cm below the injector and with separation of 0.50 to

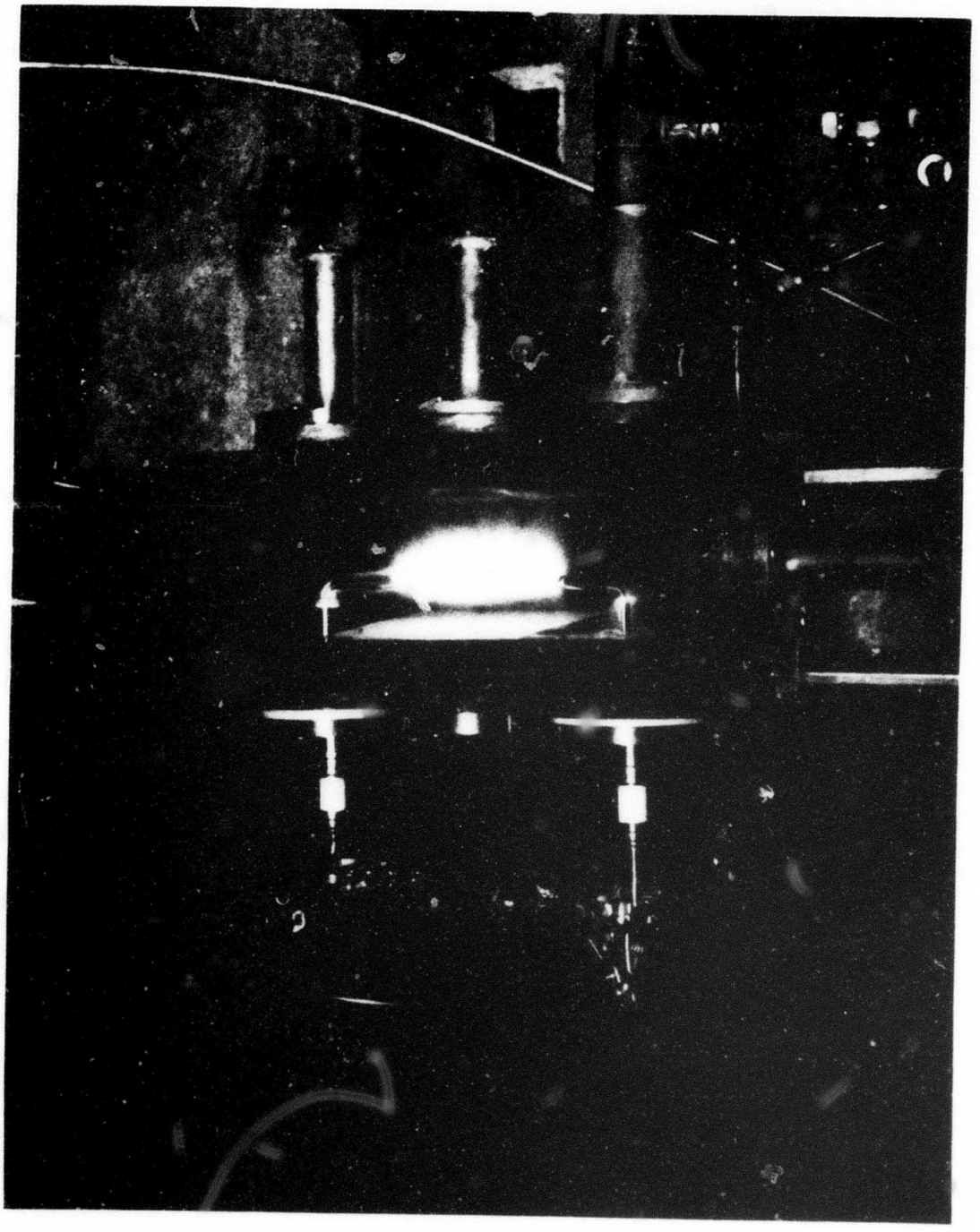

Figure 25. Longitudinal Discharge. The copper vapor generator assembly has been removed from on top of the laser and replaced with a glass plate.

2 cm. These dimensions were a compromise chosen to minimize the amount of discharge going to the injector strip and copper accumulation on the electrodes. Too narrow a spacing was also likely to increase the field strength and electron temperature unacceptably. The small excited volume limited the total power output but was ideal for investigation of large energy per unit volume phenomena, the principal effort of this part of the program.

Lasing was demonstrated and the limitations observed with the longitudinal configuration were substantially reduced. Currents in the injector of the order of 200 and 180 amps became sufficient to produce lasing respectively in Argon and Neon. Section X.E describes results.

C. POWER MEASUREMENTS: POWER METER AND CALIBRATION OF PHOTOTUBE

In this section we describe briefly the methods used to measure the output power of the laser. The results of these measurements are described fully in Section 10.5.

Initially, the average power of the laser was measured by a Scientec Model 3600 Disc Calorimeter. The output beam was directed across the laboratory to the calorimeter by a first surface mirror. Simultaneously a small fraction of the beam transmitted by the maximum reflectivity mirror was directed into a monochromator, detected by a phototube and displayed on an oscilloscope. The laser pulse shape was recorded photographically with camera shutter speeds of 1/10 sec or longer so that the traces are averages of many pulses.

The number of laser pulses per second is monitored by the events-per-unit-time meter. This device is triggered (and counts) each pulse at the gate-out of the scope. Because the scope is triggered internally only on each laser pulse the EPUT meter then counts laser pulses directly and not discharge pulses. Thus, from this data we have average power and energy per pulse, and the peak power during the pulse can be calculated. Measurements performed at different repetition rates showed that inidividual pulse characteristics did not change.

Unfortunately, the average power levels of the present laser required the most sensitive scale of the calorimeter be used. On this scale the drift and fluctuations of the meter due to electrical interference from the spark gap was significant, and meaningful power measurement could only be obtained with the longitudinal discharge.

Instead a calibrated photomultiplier tube was substituted to measure the average power when the transverse discharge was used. The calibration was done in this laboratory with an EOH Model L101 spectral irradiance standard[35] and a (calibrated) narrow band filter in the 5100 Å region. Simultaneously, neutral density filters were calibrated and the region of linear output of the phototube determined. As mentioned above, the divider chain of the tube was designed for fast pulse operation to avoid saturation by the laser pulses. The time averaged output of the tube was measured by the Keithly micro-micro-ammeter. The calibrations permitted direct conversion of anode current to average laser power output. The results of the measurements are discussed in detail in Section X.E.

D. KINETICS

A theoretical model for the copper vapor laser involves a qualitative interpretation of equations 1 and 2 presented below along with the energy level diagram shown in Figure 1.

$$\frac{dN_3}{dt} = N_e N_1 \overline{\sigma_{13} V_e} - \frac{N_3}{\tau_{31}} - \frac{N_3}{\tau_{32}} - P \qquad (1)$$

$$\frac{dN_2}{dt} = N_e N_1 \overline{\sigma_{12} V_e} - \frac{N_2}{\tau_{21}} + \frac{N_3}{\tau_{31}} + P \qquad (2)$$

Here

N_a is number of atoms per unit volume in state a

σ_{ab} is the cross section for excitation by electron collision from state a to b

τ_{ab} the spontaneous emission lifetime between states a and b

P the stimulated emission rate

and subscripts

1 represents the copper atom ground state

2 the first excited state that is metastable, and

3 the second excited state which is resonant with state number 1.

In order to facilitate interpretations, several terms in equations 1 and 2 can be eliminated. The second term in equation 1 represents the radiative transition from level 3 to level 1. This radiation is trapped which in effect causes τ_{31} to become very large relative to τ_{32}. Furthermore under lasing conditions, P dominates the spontaneous emission term controlled by τ_{32}. Finally level #2, the lower laser state, is a metastable and hence τ_{21} is very large. Rewritting equations 1 and 2 below and replacing P by N_3/τ_{stim}, the results shown below are derived.

$$\frac{dN_3}{dt} = N_e N_1 \overline{\sigma_{13} V_e} - \frac{N_3}{\tau_{stim}} \tag{1a}$$

$$\frac{dN_2}{dt} = N_e N_1 \overline{\sigma_{12} V_e} + \frac{N_3}{\tau_{stim}} \tag{2a}$$

Subtracting equation 2a from 1a;

$$\frac{d(N_3 - N_2)}{dt} = N_e N_1 \left\{ \overline{\sigma_{13} V_e} - \sigma_{12} V_e \right\} - \frac{2N_3}{\tau_{stim}} \tag{3}$$

To produce a population inversion:

$$N_e N_1 \left\{ \sigma_{13} V_e - \sigma_{12} V_e \right\} > \frac{2N_3}{\tau_{stim}} \tag{4}$$

In copper, the cross section σ_{13} is considerably larger than σ_{12} which means the upper copper laser state will be pumped by direct electron collision faster than the lower laser state. It is this difference in pumping rate as well as the magnitude of σ_{13} that enables copper to lase at 5105 Å.

Returning to equation 1a, at some point in time the excitation rate dN_3/dt must be zero.

$$\frac{dN_3}{dt} = 0 = N_e N_1 \overline{\sigma_{13} V_e} - \frac{N_3}{\tau_{stim}} \tag{5}$$

$$N_3 = N_e N_1 \overline{\sigma_{13} V_e} \tau_{stim} . \tag{6}$$

This value of N_3 represents the highest concentration of excited copper atoms. It is a function of the copper density, N_1, the electron density, N_e, the excitation cross section and electron velocity. Since σ_{13} is strongly dependent upon the electron energy, the total electron density is not important. What is important is the density of electrons in the energy range that σ_{13} is large. For copper this energy range is between 2.5 ev and 10 ev.

The laser intensity is directly dependent upon N_3 as is illustrated in equation 7 below.

$$E = .6 N_3 V h\upsilon \tag{7}$$

$$E/V = .6 N_e N_1 \overline{\sigma_{13} V_e} \tau_{stim} h\nu \tag{8}$$

E = laser energy

V = laser volume

$h\upsilon$ = photon energy.

Equation 8 illustrates the importance of high electron densities (N_e) and copper densities (N_1) for achieving high laser power densities. It is apparent that increasing

the volume will increase the total power output of the laser. Electron densities can be increased by increasing the electric current through the discharge. This can be accomplished by using larger capacitors at higher voltage, while not increasing your electron temperature to the point where the copper excitation cross section has significantly fallen. Alternatively, rather than increasing the capacitance and voltage, a smaller volume of gas can be excited. This is precisely what is done in a transverse discharge as opposed to a longitudinal discharge.

E. LASER MEASUREMENTS

1. Longitudinal Discharge Laser

The first demonstration of lasing was accomplished with a longitudinal electrical discharge. A photograph of such a discharge can be seen in Figure 25 where the generator assembly has been replaced with a glass plate. A wide injector strip (injector A on Table 3) was used for the vaporization of copper. This electrode configuration was chosen for the initial experiments, as indicated earlier, to provide maximum gain length (10 cm) and discharge conditions most nearly alike other previous systems known to lase.

Table 7. Typical Early Longitudinal Discharge Laser Parameters

Parameter	Value
Discharge	Longitudinal, 10 amp/cm^2
Gain Length	10 cm
Discharge Energy	Capacity 2.5 nf - Voltage 4-8 kV
Injector Power	1.4 kW
Copper Atom Density	1.2×10^{14}/cm^3
Buffer Gas	Argon 1.5-2.0 torr

Table 7 presents typical parameters for a laser run in this configuration. The resulting output beam was circular with a diameter determined by the 1/2" and 3/4" apertures whose primary purpose was to restrict copper deposition on the Brewster windows. A photograph of the laser spot in the near field showed it to be well defined and to have lowest order symmetry. Densitometer traces were taken of the photograph and are shown in Figure 26.

The laser power was measured by a Scientec calorimeter as described in Section X.B. It should be noted that for each configuration the steady readings that have been recorded were maintained for durations up to several minutes. During these periods, however, there were bursts of less than one second duration in which the laser power increased substantially. Unfortunately, these could not be measured because of the three second response time of the calorimeter. They were correlated though with obvious changes in the character of the electrical discharge as observed visually from the side viewing ports. The indications thus are that, at present, the output power is limited by discharge characteristics.

Table 8 lists longitudinal discharge laser output characteristics. It can be seen that, as expected, values are similar to those obtained elsewhere with similar discharge current densities[1]. The fact that the working medium is flowing has little effect.

Table 8. Longitudinal Discharge Laser

Characteristic	Value
Average power	6×10^{-3} w
Repetition Rate	700
FWHM	30 ns
Peak Power	0.54 KW
Pulse Energy (in cavity)	2×10^{-3} j/liter
Copper Density	$1.2 \times 10^{14}/cm^3$
% Copper Atoms Lasing	4.3%
Efficiency (electrical)	0.2% (1.0%)*

*The efficiency of 1% is based on an estimate of the fraction of stored electrical energy deposited in the optical cavity during the discharge.

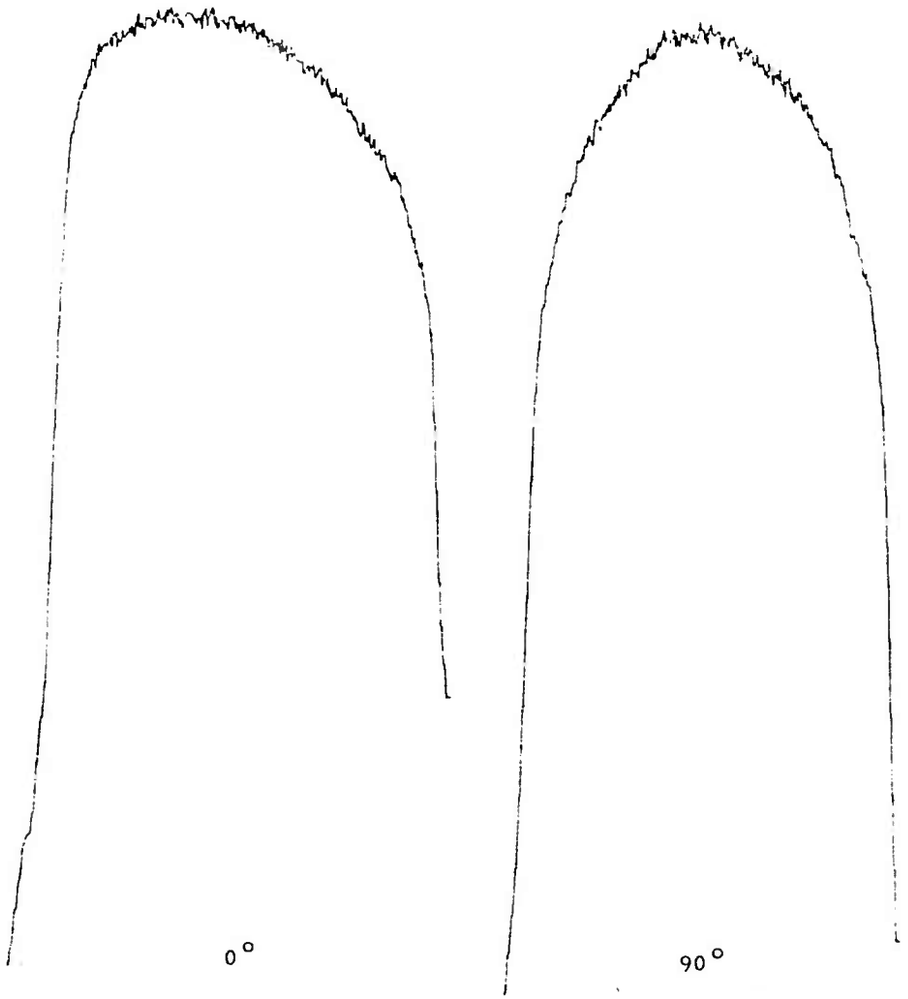

Figure 26. Densitometer Traces of Photograph of Laser Spot

2. Transverse Discharge Laser

As has been described above, the electrode configuration of the laser was changed to a transverse orientation to localize the discharge, produce higher current densities and faster rising current pulses.

The first electrodes consisted of two "T" electrodes made of 1/8" molybdenum rod and machined sheet brought in from opposite sides of the laser box with the return electrical path external to the box. Although lasing was achieved,this configuration had several drawbacks. These were extraneous discharges to the walls of the chambers, long risetime current pulses (up to 120 nsec.) and non-uniform discharges between the electrodes along the gain length and from pulse-to-pulse. Thus, the laser was unsteady, did not lase with each current pulse, and required relatively high copper densities for threshold.

Ultimate major electrode changes consisted of three modifications.

1. Glass insulators encircled the electrode feed-throughs reducing extraneous discharges.

2. The electrode return path was made internal to the laser box producing lower inductance.

3. Stainless steel razor blades replaced the molybdenum as electrode material.

These alterations produced significant improvements. The extraneous discharges to the walls were reduced, but not eliminated. The current pulse had a relatively fast rise time (40 nsec.) and the discharge between the electrodes became more uniform. The laser fired on every current pulse and threshold was reduced to the range of 6×10^{13} atoms/sec. Results for this electrode configuration appear under the caption "old electrodes" in Figures 27, 28 and 29.

A final alteration involved further improvement of the glass insulators and shaping of the electrodes reduce extraneous discharges to the walls further. This produced marked improvements as illustrated in Figures 27, 28 and 29 under the caption "new electrodes".. The most noticeable changes were the lasing at 5782 Å

and superradiant emission at 5105 Å with one mirror while using copper densities of only 4×10^{14} cm^{-3}. Table 9 lists characteristic parameters used while testing this mode of laser operation.

Table 9. Typical Transverse Discharge Laser Parameters

Parameter	Value
Discharge	Transverse, ~200 amps/cm^2
Gain Length	4 cm
Discharge Energy	Capacity .5-7 nf - Voltage 3-9 kV
Injector Strip Power	2.0 kW
Copper Atom Density	$4.0 \times 10^{+14}/cm^3$
Buffer Gas	Argon 4.0-10.0 torr Neon 20.0-85.0 torr

The output beam from the transverse discharge copper vapor laser had a rectangular to elliptical cross section (13 mm x 3 mm) which corresponds to the region of the most intense discharge in the buffer gas. The beam divergence was measured to be 0.6 milliradians.

Using a calibrated photomultiplier as outlined in Section X.B, power measurements were obtained for the transverse discharge laser. The results of these measurements are shown in Figures 27, 28 and Table 10.

To determine the energy density per unit volume (joules/liter) as presented in Figure 27 the output energy per pulse was first measured. This was divided by the laser volume which was taken to be the product of the gain length (4 cm) times the laser spot area measured at the output mirror. This resulted in the output energy per unit volume. However, this output energy density represented only three percent of the energy in the cavity because the reflectivity of the output mirror was 97 percent. Therefore, the output energy density was multiplied by 33.3 to determine the energy per unit volume in the cavity. This latter number is shown in Figure 27 and Table 10.

Table 10. Transverse Discharge Laser Characteristics

Characteristic	Value
Average Power (In Cavity)	1.0×10^{-2} watts*
Repetition Rate (In Cavity)	141 pps (3,000)**
FWHM	30 nsec
Peak Power (In Cavity)	2.8 KW
Pulse Energy (in cavity)	.055 joules/liter
Copper Density	4×10^{14}
Percent Copper Atoms Lasing	33%***
Discharge Efficiency	.6%
Gain	120 db/m

* At 5105 Å. Emission at 5782 Å would increase this further.

** Highest level, without power measurement.

*** The equivalent of 565 Kj/lb of copper.

In order to extract a larger fraction of this energy a higher gain laser must be built by either increasing the gain length or the vapor density. Then the coupling fraction could be increased. Walter has shown up to 96 percent coupling can be used. In the present system a ten percent transmission mirror produced 3.3 times more power out than the three percent mirror, whereas a 50 percent mirror resulted in only five times more power out. Increased coupling can be used to increase the output power only until the radiation intensity within the cavity has been reduced to a point that the remaining gain is insufficient to extract the available inversion. Hence, with the ten percent mirror the system was still undercoupled, the intercavity radiation intensity was sufficient, but with the 50 percent mirror it was over-

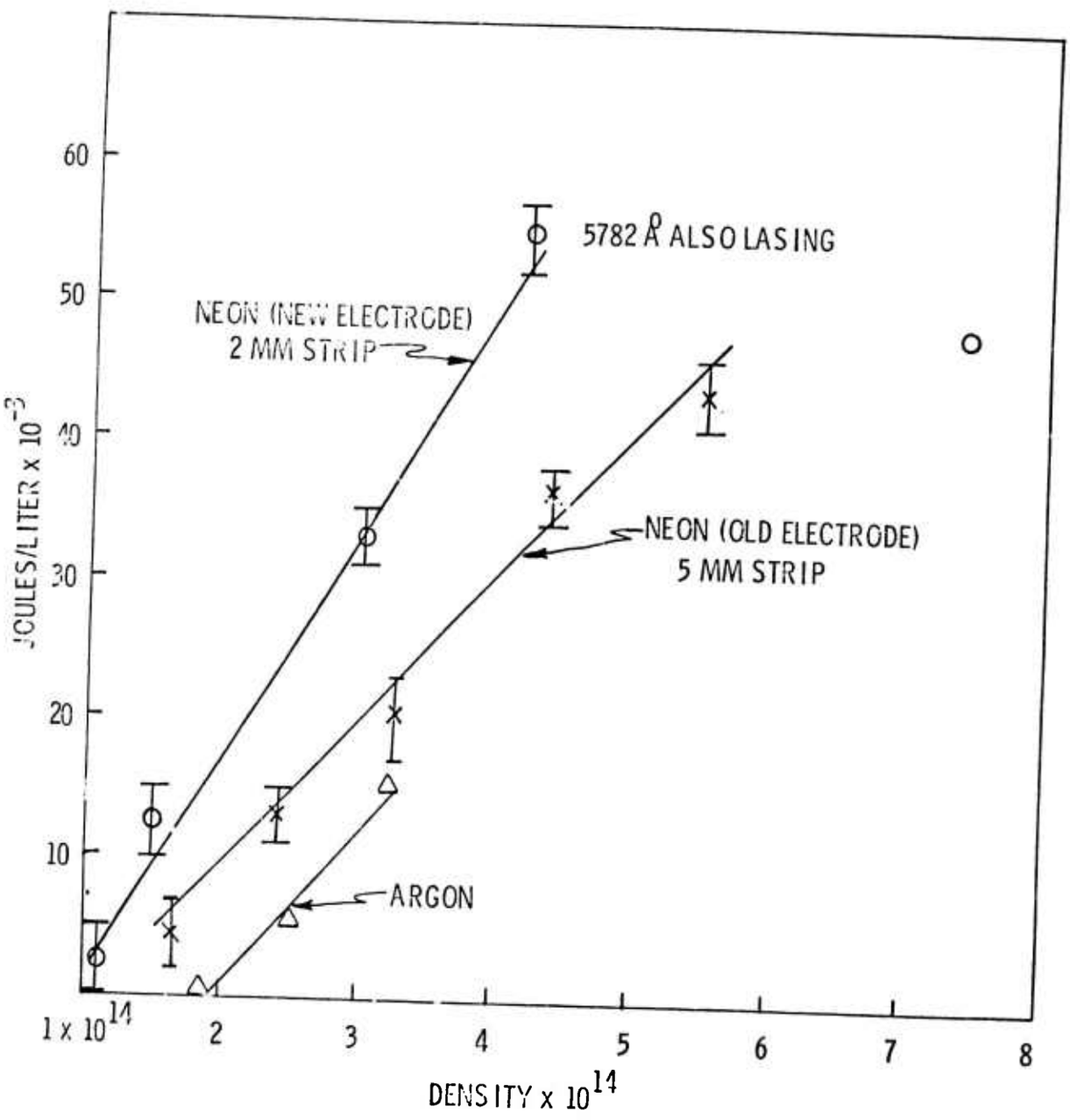

Figure 27. Lasing Energy at 5105 Å per Unit Laser Cavity Volume as Function of Copper Atom Density. Transverse discharge configuration, see Tables 9 and 10. Buffer gas and electrode specified.

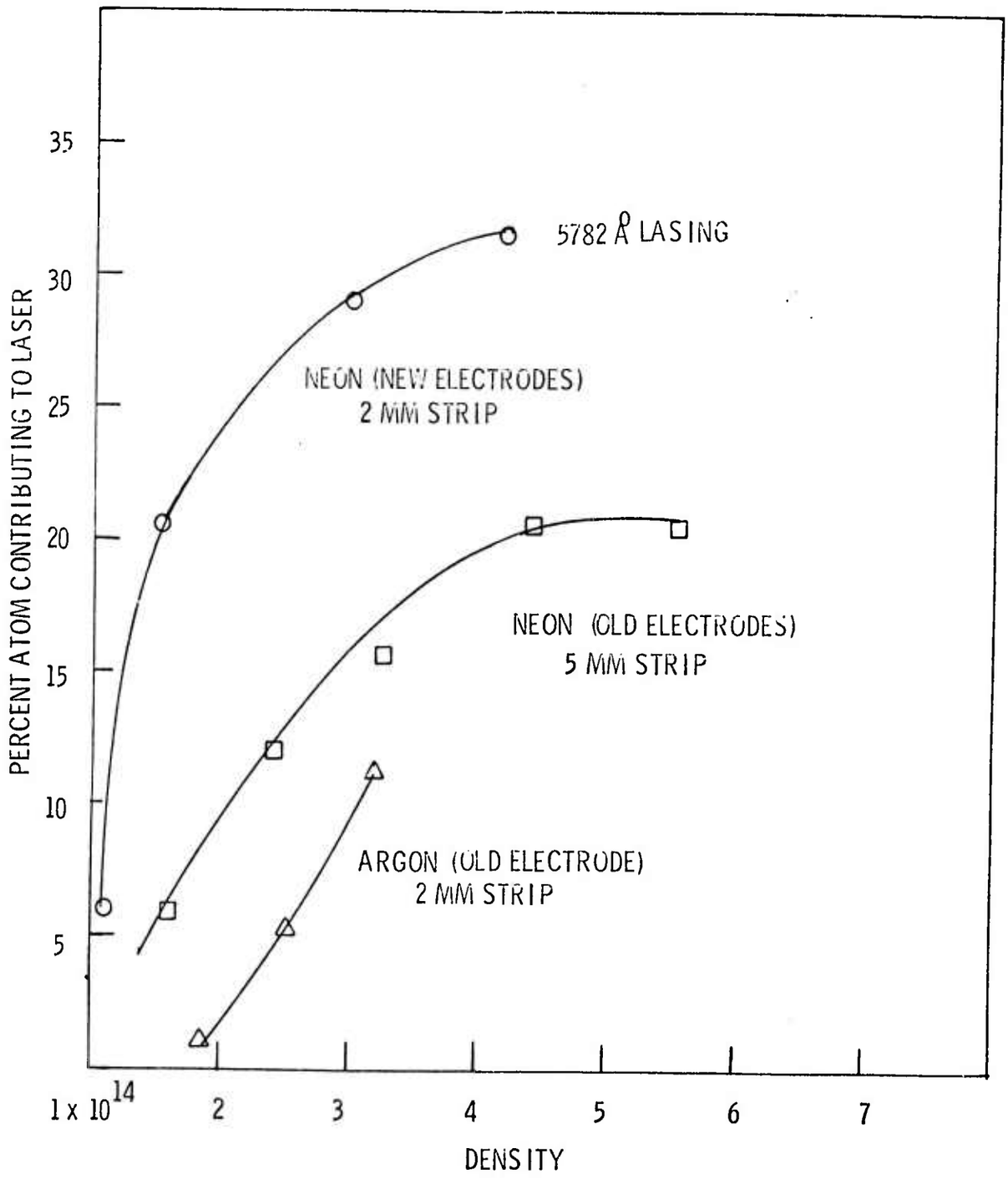

Figure 28. Fraction of Copper Atoms Lasing at 5105 Å as Function of Copper Atom Density. Transverse discharge configuration, see Tables 9 and 10. Buffer gas and electrodes specified.

coupled. Clearly, optimum coupling does not permit extraction of all the energy density shown in Figure 27. However, since the gain of the medium can be increased relative to losses by increasing laser length or vapor density, the optimum coupling fraction can be increased. A system 40 cm long would have much higher gain than one of four cm and,assuming a linear increase in gain, the optimum coupling would approach 100 percent transmission, then enabling extraction of nearly all the energy available.

The laser volume used to determine the energy density was based on a gain length of four cm. Observations of the electrical discharge length are impossible with the CVG in place, but with it removed and a glass plate placed over the laser box, the discharge could be studied. In both argon, and neon, the most intense portion of the discharge occurs over a length less than four cm depending upon the physical condition of the electrodes and their insulators. That is, when the electrodes and insulators covering the vacuum feed-throughs become coated with copper, the discharge is no longer uniform over the four cm electrode length and also substantial portion of the discharge goes to the wall of the laser box. Thus, using four cm to determine the laser volume gives a lower energy/volume than may actually exist. In some cases it may be as much as 50 percent low.

A second factor reducing the measurement of energy density again concerns the laser volume. The cross sectional area of the volume is determined directly from the laser spot size. Using this area, gives an accurate energy density if the laser power is uniform over this area. Observations indicate that the power is not uniform over the spot. Hence, the energy densities listed in Tables 5 and 6 are averages and the peak energy density is much higher.

Other buffer gases were used to produce lasing. We were unable to obtain lasing with nitrogen or helium, but did succeed in krypton. Qualitiatively krypton is slightly poorer than argon as a buffer gas.

As the power was increased in the injector strip in order to achieve higher copper densities, meaningful laser data became unattainable due to a variety of reasons. Thermal problems, outgassing of the walls of the chambers, and ineffective catching of the copper downstream all led to unreliable and unsteady lasing. Such thermal effects and strong interactions with copper reflected from the catcher are not a fundamental condition because they were not observed when copper vapor generators were operated in the bell jar test facility. Indications of fundamental behavior are that the laser power increases with density as shown on Figure 27. (In one set of uncalibrated measuremens an increase in density of two orders of magnitude produced a factor of 200 increase in laser output.) However, the percentage of copper atoms utilized levels off. This is shown on Figure 28 which was computed from data on Figure 27. In the future high density (10^{17}/cc) copper operations should demonstrate extraction of almost 10 joules per liter.

Finally, the efficiency of the system was determined. Most of the data was recorded using a 5 nf capacitor and 4.5 KV spark gap. It has been observed, however, that no reduction in laser power per pulse occurred if a 3 KV spark gap was used and also a 2.5 nf capacitor. Using these latter components, a maximum efficiency of 0.64 percent has been measured.

Further increase in discharge efficiency could be obtained by increasing the length of the discharge (width of the laser volume). The volume that the current flows through would increase and better use could be made of the available energy (see equation 8, Section X.D). Increase of the vapor density would have a similar effect. Experiments have shown that within the modest range of densities and discharge lengths used the expected efficiency increase has been found. Furthermore, expectation of over 15 percent discharge efficiency has been indicated under some high density conditions by computer simulations[31].

Current understanding of the processes taking place is still in an early stage. An effort is now underway[36] trying to correlate the discharge current, the lasing pulse and spontaneous emission from all atomic levels involved with the lasing process (see Figure 29).

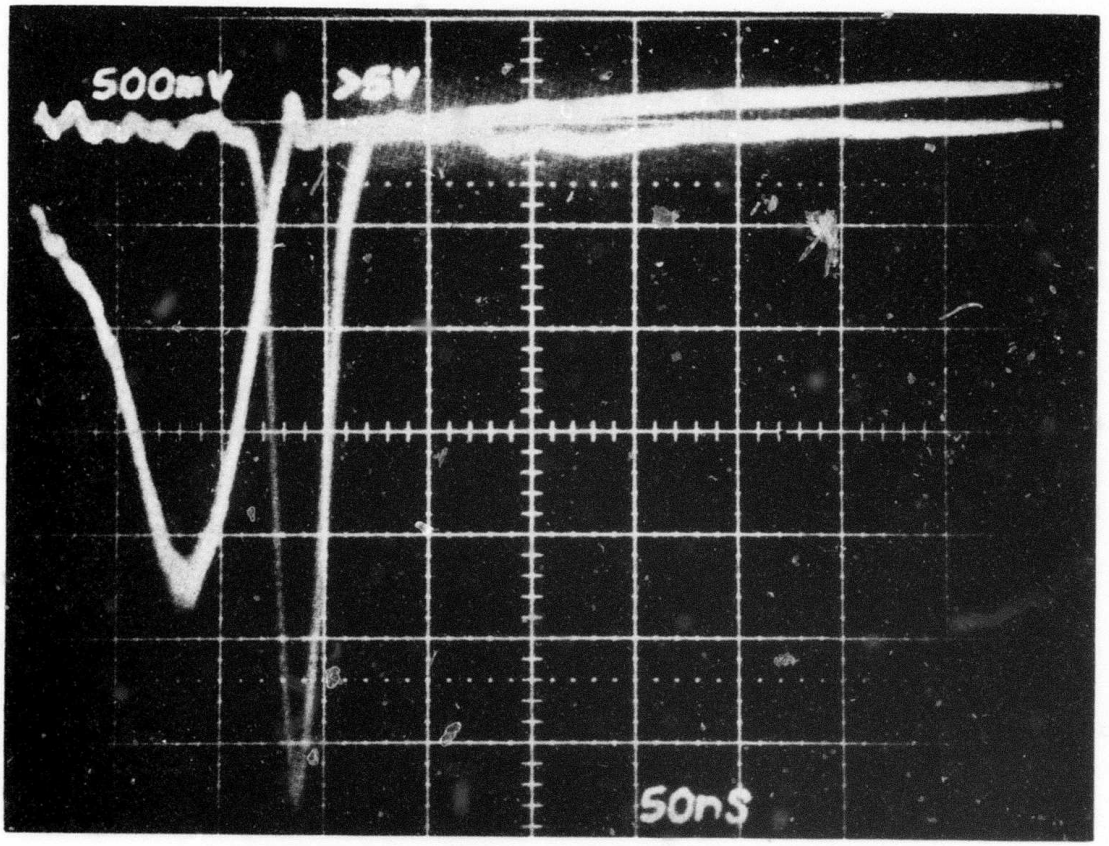

Figure 29. Oscilloscope Trace of Discharge Current and Laser Pulse, Uncalibrated Amplitudes.

SECTION XI
EXPERIMENT SUMMARY

High expectations for the copper vapor generator and its associated laser have been supported. The generator has been tested for hours at a time while producing densities the order of 10^{14} atoms/cc. Vapor densities the order of 10^{17} atoms/cc have been produced for about ten seconds. Vapor uniformity across the laser cavity was measured to be better than about two percent. Vapor velocity and temperature were found to be 7×10^{4} m/sec and 1400 ^{o}K or below in the same region.

Copper vapor lasers were operated using this vapor source with both longitudinal and transverse discharge configurations. As expected, the performance of the longitudinal discharge device was similar to those reported earlier in the literature. The transverse discharge device, however, demonstrated substantially improved characteristics. Almost 33 percent of the copper atoms available were made to lase. This is the equivalent of 565 Kj/lb of copper. Almost .1 j/liter of lasing atoms were produced at 5105 $\mathring{A}$ using only 4×10^{14} atoms/cc. Discharge efficiencies of about .6 percent were obtained. Overall efficiencies were the same since the energy required to produce the vapor was always much smaller than the capacitor energy (see Table 9 and Figure 24) because of the low discharge efficiency. Other results of interest found during this study, such as the high gain (120 db/m) superradiance, and operation at high rates (3,000 pps) were also entirely as expected.

The limitations on generator operating time and maximum density in the laser due to reservoir volume and particularly thermal effects, and on current rise time due to the inductance of the circuit, prevented reaching the .25 j/l and ten percent efficiency expectations. Improvements on the generator are needed to reach the high densities for reasonable periods but these are expected to be straightforward. Discharge optimization to a clean 10-20 nanosecond pulse may be much more difficult. However, the indication of these tests is that over ten percent efficiency and ten joules per liter should be achievable once those problems are solved.

SECTION XII
RECOMMENDATIONS

The importance of electrical circuit design is clearly demonstrated by the results just described. A major effort is thus needed in this area. Included must be an integrated electrode design that will prevent discharges anywhere but through the laser cavity, low impedance transmission line construction that will produce 10 to 20 nanosecond discharges, and a larger volume of excitation. The last two are expected to be particularly important.

Improvements in copper vapor generator operation should be directed toward high density and long term operation. For instance, reservoir capacity must be expanded or some mechanism for a continuous copper feed provided so that there is enough run time at high density. Recirculation should ultimately be provided as the ideal solution. Proper catching of the copper vapor stream is also necessary so that adverse interaction with subsequent flow can be avoided.

Adequate thermal design for the laser is associated with discharge dissipation as well as the copper vapor generator and will have a dominant effect in the near future. Some of the most severe limitations of the current system are related to just such considerations.

Finally, understanding of the kinetic processes taking place must be improved if the full promise of the device is to be realized. Indications of a lack of simultaneity between discharge current and lasing action have been recently indicated[36]. The large fraction of atoms made to lase required more full explanation than the simple model originally suggested[2].

Once these problems are in hand and the supporting technologies (e.g. high repetition rate quenching spark gaps) have proven fully successful, there is every reason to believe that the full promise of this device can be realized. The results of the tests conducted thus far fully support all early expectations[2].

APPENDIX I

EARLY GENERATOR DESIGNS

A. ONE MM WIDE STRIP INJECTOR

Initial operation was conducted with an injector similar to that described in Reference 2 and shown on Figures A-1 and A-2. The channel was .063 inch by .060 inch cross section, 10.8 cm long, and had two rows of .009 inch holes extending along 10 cm (388 holes) spaced so that the width of the hole array was 1 mm. This channel had a cover fixed upon it with graphite cement. A space of .015 inch was left between the cover and the channel wall which had holes in it, to accommodate the copper. This assembly was then inserted into a pair of graphite elbows which were then cemented into the bottom of two zirconium oxide reservoir tubes, as shown on Figure A-3. Molybdenum rods were suspended into the reservoirs to carry the current.

The inside of the channel cover had a film of tantalum sputtered upon it. Upon heating this thin film converted to tantalum carbide. Early experiments were conducted which showed that liquid copper wet such a film, was drawn into the channel, and was injected as vapor.

Materials analysis also uncovered interesting informating regarding the use of graphite cement on the injector. Photomicrographs were taken of a sectioned injector from which copper had been boiled off, as shown on Figures A-4 and A-5.

Copper droplets remaining show up as the light colored material and the graphite as dark or gray. Some graphite cement had squeezed into the channel and is clearly visible around it in Figure A-4 as a darker substance of non-uniform granularity. All inside surfaces were affected, however, since a thin layer of different structure than the graphite body can be seen even where graphite cement is not present. Dr. Earl Feingold of our Materials Characterization Laboratory has pointed out that such thin layers of subtle difference from the substrate often lead to substantial changes in surface properties. This has clearly occurred here since it can be seen that the copper wet this surface layer. Tne graphite cement under other conditions

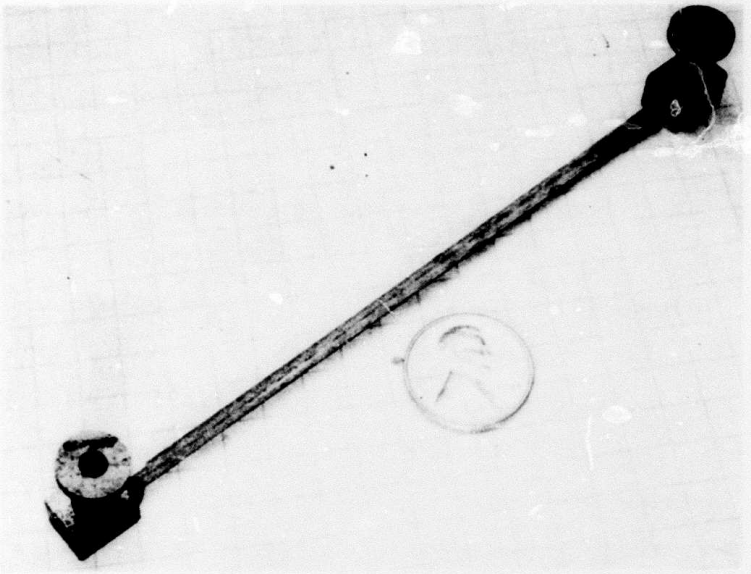

Figure A-1. One Millimeter Copper Vapor Generator

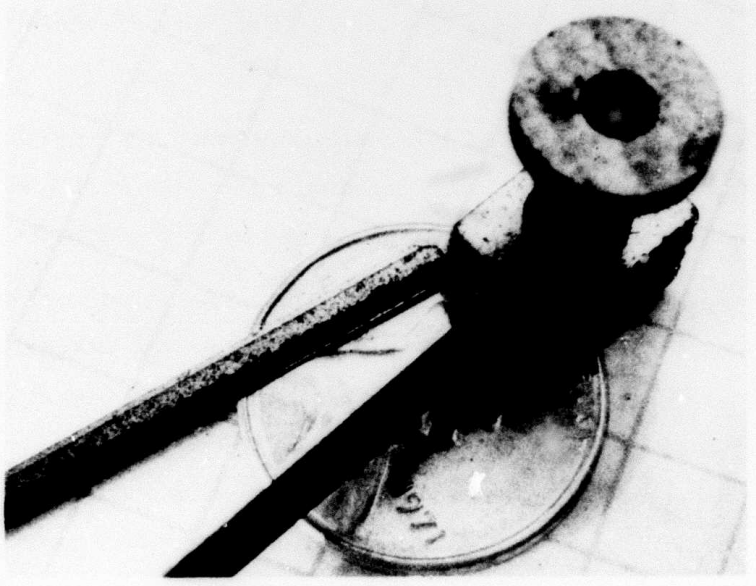

Figure A-2. Close Up of One End of One Millimeter Copper Vapor Generator. Lid has been removed.

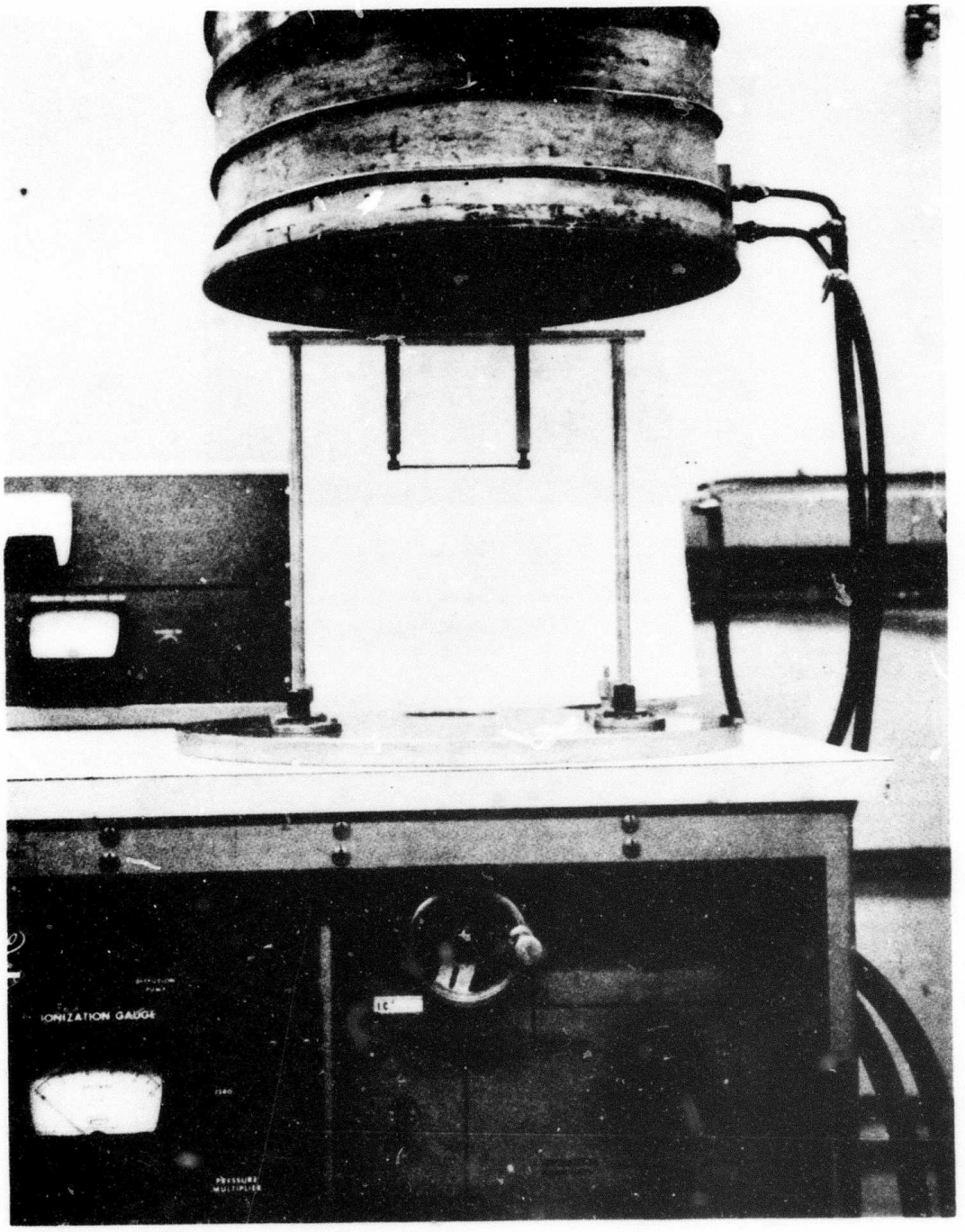

Figure A-3. One Millimeter Copper Vapor Generator Mounted in Zirconium Oxide Reservoir Tube and Suspended in Test Facility

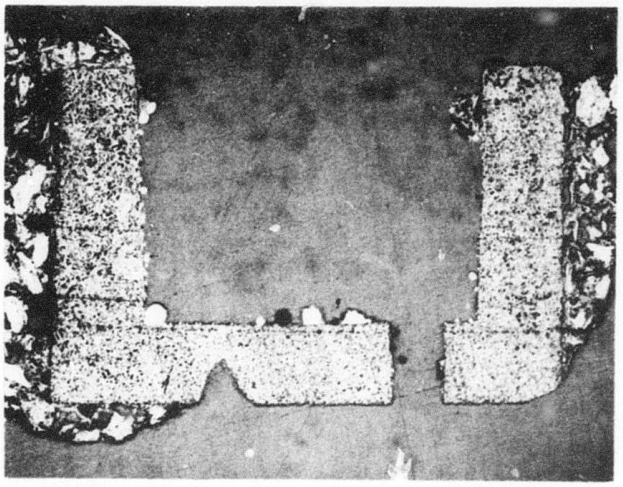

Figure A-4. One mm Wide Injector Channel
50X Magnification, Location 4

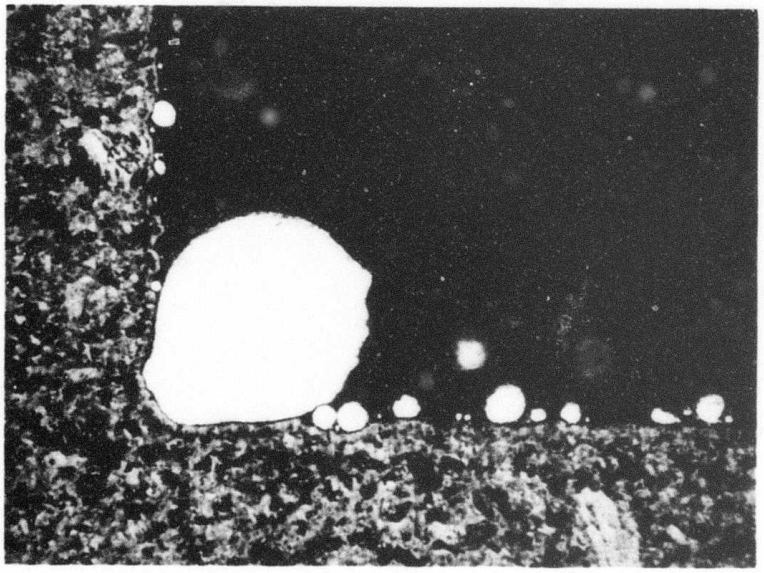

Figure A-5. One mm Wide Injector Channel
500X Magnification, Location 4

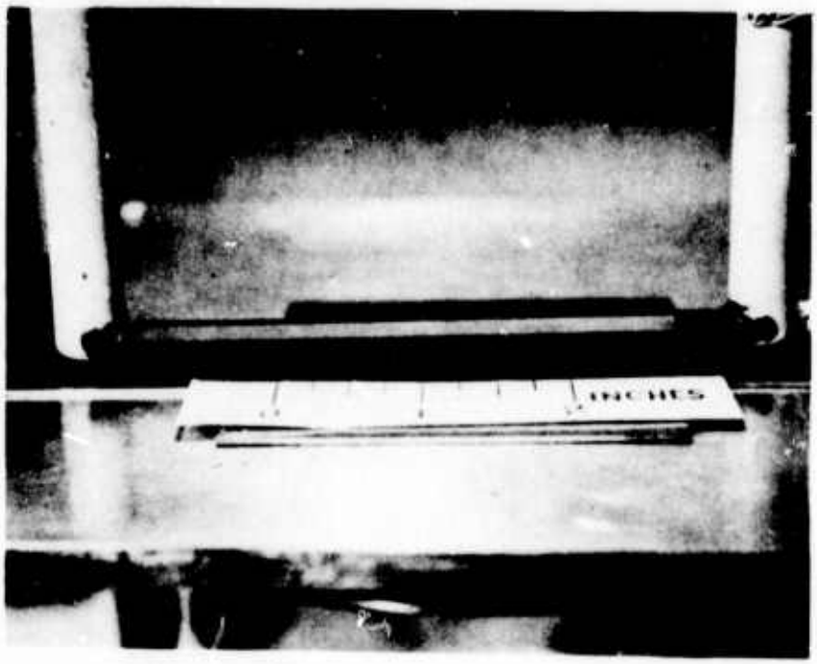

Figure A-6. One cm Copper Vapor Injector Strip. Zirconium oxide reservoir tubes can be seen on each end. Two sapphire discs for film analysis lie under the injector.

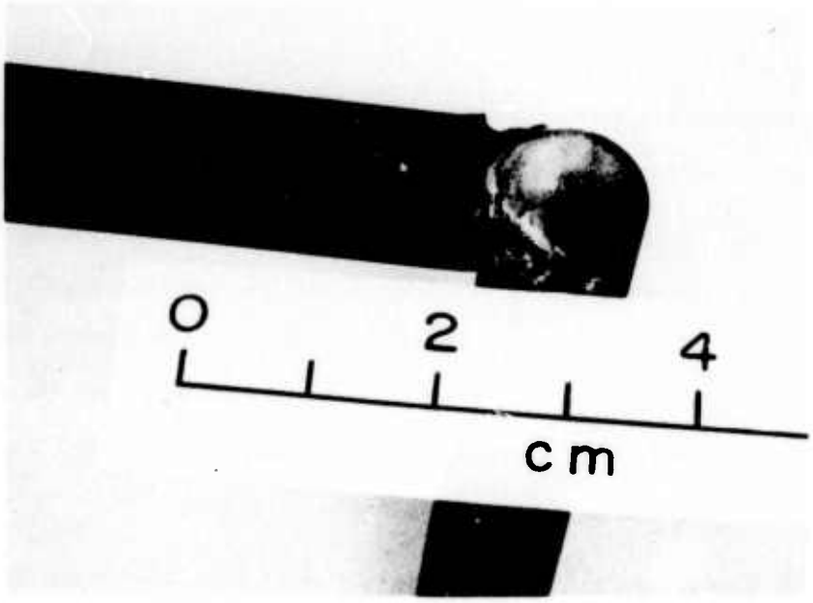

Figure A-7. Results of Molybdenum-Graphite High Temperature Interaction. View of damaged reservior tube.

allowed no such wetting. Dr. Feingold has suggested that the binder in the cement was driven off during operation and affected the pure graphite in this way.

Evidently the presence of graphite cement, though convenient, led to uncontrollable surface effects. Its use was therefore curtailed in future tests.

B. ONE CM WIDE INJECTOR - INJECTOR A

Construction of the one millimeter device was time consuming and the coarse structure of the graphite used was unsuitable for the fine machining required. In addition the copper vapor injected by a one mm wide strip cannot provide a uniform fill in a wide laser cavity. As a result, a much wider injector of different design was developed. This injector was described as injector A in Section 5.0. A fine grain graphite was used so that up to 50 percent open area could be obtained on the injector face while retaining structural integrity. The elbows of the previous design were also abandoned as being unnecessarily complicated and each end of the injector assembly was inserted in a slot in a zirconium oxide reservoir tube and cemented in place with graphite cement. Figure A-6 shows the assembled generator.

Here too the graphite cement used for bonding, the zirconium oxide tubes used for the reservoir, and the molybdenum rods used for electrical contact ultimately proved to be of questionable value. This was found to be true despite the well known compatibility and inertness of these materials.

The cement always provided an excellent bond between graphite and graphite. Unexpectedly, it also provides a satisfactory bond between zirconium oxide and graphite. With proper preparation the graphite vehicle infiltrated the zirconium oxide pores and adhered. Even during sudden cooling from 2000 ^{o}C the joint remained intact. This is an interesting result since the materials suppliers were unaware of any effective means for bonding zirconium oxide and graphite.

Unfortunately, the long term compatibility of the cement with the zirconium oxide was not as satisfactory. At sufficiently high temperature (>1100 ^{o}C) the cement ultimately reduces the zirconium oxide to zirconium metal in exothermic reaction that removes material, breaks the bond, and causes an opening in the electrical

circuit. Figure A-7 shows the result of one such reaction. Similarly, the presence of the molybdenum rod used to bring in power has proven undesirable in proximity to the zirconium oxide.

The compatibility of the copper-zirconium oxide, copper-molybdenum, and molybdenum-zirconium oxide systems is well known. However, when all three are present at temperatures above 1100 ^{o}C a violent exothermic reaction takes place. The zirconium oxide wall is penetrated and gouts of material ejected. The reasons for this reaction are not clear.

Since it was not the purpose of this program to investigate complex reactions, the above materials were abandoned. In their place the all graphite design described in Section V was used.

APPENDIX II

WETTING TESTS

A series of tests were performed to determine the proper design for drawing the liquid copper from the reservoir into the injector. Before the program began the use of wetting forces in some form was decided upon[2]. This implied that a substance wet by the liquid must run from the reservoirs through the injector cavity. The tests allowed determination of the proper form of this material, its composition, and its application.

The configurations considered ran from wires and foils placed within the injector to making the interior injector surfaces out of the wetting material. This latter technique proved by far the best of the three since wires did not provide adequate wetting area and foils tended to block the injector cavity with small wrinkles.

A large number of tests were conducted using lids (see Figure 7) made entirely of materials wet by liquid copper. The materials used were tantalum and molybdenum. In both cases the liquid wet very well and flowed into the injector easily. However, at high temperatures these metals would lose their strength and sag, closing off the injector cavity. Equally serious, the solubility of these metals in copper, small as they are[15], was sufficient to allow wetting at the holes in the base (see Figure 7) so that liquid could leak through them. Experiments have been reported in the literature[16] that support this observation.

The use of carbide films sputtered on the interior surfaces of both the lid and base proved more satisfactory. The strength of graphite holds up at high temperatures and carbide films proved quite insoluble in copper. Pure carbide may be usable but simplicity dictated machining of graphite and then its coating with the carbide film.

Several carbides were investigated to determine the optimum material. These studies included sessile drop tests to determine wetting angles as a function of temperature and injector runs to verify liquid copper flow. Tungsten carbide, tan-

talum carbide, and vanadium carbide all proved to be sufficiently refractory, wet by copper and insoluble (in that a one micron film would not dissolve in a period of hours when left in contact with liquid copper). The higher temperature capability of the tungsten and tantalum carbide films allows them to survive longer at high temperature and so they were chosen for use. Their characteristics are described in Section V, and Appendix III.

A series of films of various thicknesses and proportions of the two carbides were also studied. It was found that films much thinner than about one micron were not durable enough and those much thicker took too long to form. In addition, tungsten carbide was chosen for its adherence properties (see Appendix III) as the base film. Top layer films of tantalum carbide proved to wet best. A top film of tungsten carbide could be satisfactory but ultimately a two layer film of tungsten-tantalum carbide, one micron thick, was chosen.

This choice was found to provide adequate wetting for copper flow into the injector at temperatures just above copper melting. Almost indefinite survivability of the film was also found at temperatures up to 2200 ^{o}K. Even above that temperature wetting and solubility seem to be adequate. Adherence of the film to the substrate may be a problem however.

APPENDIX III

THE ADHERENCE OF CARBIDE FILMS

Early investigations with a pure tantalum carbide film showed that injector failure could occur from poor film adherence to the graphite substrate. The primary mechanism for this damage involves the strong wetting forces with copper. Unless there is equally strong adherence between the film and its graphite substrate the liquid copper will separate them.

This can be seen on Figure A-8. A photomicrograph of a long section of a .005 inch injector channel is shown in two pieces. The fine grain graphite structure appears as textured black to gray and the copper as the white zone. The light colored strip is the tantalum carbide film. The black areas inside of the channel are voids. It can be seen that once the film continuity was sufficiently disrupted copper continuity broke (see on the right where the injector channel enters the reservoir) and the copper flow stopped. The strength of the wetting forces can be gauged by the degree to which the film has been broken up.

To some degreee proper preheating can provide adequate adherence. Figure A-9 shows a photomicrograph of a section of an injector channel prepared in such a way. Film damage only resulted from repeated exposure to copper.

A more long term answer is the use of tungsten carbide at the graphite interface. Instead of a planar interaction, as with tantalum carbide and graphite, fingers of tungsten carbide have been found extending into its graphite substrate[19, 20]. One should consequently expect stronger adherence between the pair. Furthermore, the longer these materials are in contact at high temperature the deeper will be the diffusion and the stronger the bond.

Tungsten carbide films prepared with a tantalum carbide top layer were thus found to adhere adequately for the tests performed in this report. Operation at temperatures up to 2200 ^{o}K caused no damage, even when runs were long term and repeated. Only when higher temperatures were encountered did films begin to

break away from the substrate. This failure mode was not consistent and since run times at these high temperatures were fairly short, with the present generator design, verification must await longer run times with a new design. It is believed that curing of the injector components at higher temperatures for longer times will provide the stronger adherence needed.

Figure A-8 is a foldout and appears at the end of report.

Figure A-9. Copper Within Injector Channel.

Tantalum carbide film can be seen at interface between copper and graphite.

APPENDIX IV

THERMAL BALANCE OF COPPER VAPOR GENERATOR

The proper thermal balance is needed for the copper vapor generator if reliable, efficient, long term operation is desired. This includes low resistance, adequately cooled means for bringing the high current from the power supply to the injector, efficient means for maintaining the reservoir above the melting point of copper, and means for maintaining the injector at a uniform temperature.

With current designs the resistance of the feed throughs, molybdenum tubing, and interface connections to the copper vapor generator into the laser are the order of .012 ohms. This represents a serious limitation since currents above about 400 amps cause overheating. Substantial improvements are possible but only after a major design change. The considerable effort that evolved the design now in use cannot be improved upon easily.

The principal technique for improving the efficiency of heating the reservoirs has been the use of radiation shields surrounding them. A three concentric molybdenum tube shield construction is now being used. Radiation losses from the sides of the reservoirs are reduced to the range of ten to twenty watts. Losses from the unshielded bottom of the reservoir with one-fifth the area far exceed this (about 100 watts).

The importance of these shields cannot be overemphasized. Several earlier designs using non-optimum configurations and materials led to exceesive power requirements for reservoir heating and frequent failures.

Losses by radiation from the reservoir bottom and conduction through the molybdenum support tube can only be reduced through a fundamental design change. Any shield placed below the reservoir will interfere with laser operation. Reduction of the thermal conduction losses in the support tube will increase its resistance. While not a serious problem the 300-400 watts needed to initially melt the copper are largely lost in these two ways and should be considered carefully in any new system design.

Finally, the critical temperature uniformity of the injector, which reflects directly in uniform vapor flow, has been maintained by keeping the injector resistance per unit length uniform. Clips are designed to run from reservoir to reservoir as is the hole array. Particularly during high temperature operation, the slightest asymmetry can lead to overheating in one spot, a consequent increase in the resistance there, and further heating and burn out.

Slight bulging in the injector due to internal copper pressure does lead to some nonuniformity. This may explain the tendency of the injectors to fail where they enter the reservoir slot, since that is also where the injector is prevented from bulging.

APPENDIX V

ELECTRON GUN DISCHARGE INITIATION

The requirement for very low inductance discharge circuitry and the success of electron beam sustained carbon dioxide lasers led to an initial laser design (in part supported by IR&D funds) using such a concept. Figure A-10 shows an early photograph of the basic unit. An electron gun with two filaments is within the cavity toward the top of the picture. The screen electrode immediately above it is at wall potential and is placed so that the electron gun acts as the central conductor of a 50 ohm line. A short high voltage pulse can then be propagated from one end of the gun to the other, accelerating a similar pulse of electrons to and through the screen electrode. The electron pulse can then enter the region between the screen electrode and the lower electrode. Computer analyses were conducted to insure that the electron beam was uniform.

The volume between the screen and lower electrode forms the laser cavity. The copper vapor will be flowing through (from the subassembly which has been removed, as shown in Section X, so that the inside of the device can be seen, to the cooled catcher at the opposite end) and is coincident with the optical axis running through the Brewster angle windows at the ends of the box. The discharge that excites the inversion will take place parallel to the electron flow from the upper electrode to the screen electrode.

This main discharge comes from a series of coaxial cables connected to the transmission line protruding from the center flange at the top of the box. The electrical energy passes along this five ohm line to the upper electrode where it terminates directly in the discharge. The lack of a switch in this circuit minimizes inductance and discharge pulse time. The electron beam provides this switching with its ionization of the copper vapor and, since it is uniform, insures a uniform discharge. The beam in turn can be switched by a low energy pulser operating into a constant 50 ohms. This allows one nanosecond risetime pulses to be produced at high rates, something that could not be easily done if the main discharge had been switched directly. Figure A-11 shows a pulse used to actuate the electron gun.

One of the principal requirements of this concept is that the high voltage not break down the gap until triggered by the electron beam. However, in the presence of even small quantities of copper this proved to be impossible. Even when Pashen curves for the fill gas indicated breakdown voltages of several kilovolts, only a few hundred could be maintained. This implies that copper vapor-inert gas mixtures, in contradiction to expectations based upon the ionization potential of copper, have a broad Pashen minimum extending from 10 to 10^{-1} mm hg-cm.

Other shortcomings of the design included copper vapor deposited upon the transmission line and sparking between elements of the transmission line and the walls. These problems could be overcome, but the inability to hold off a high voltage is too fundamental. The use of a switch between the energy storage elements and the five ohm transmission line was suggested so that the high voltage could be applied just before the electron beam pulse. However, once a switch was inserted in the main circuit it was decided to allow it to control the whole discharge and eliminate the electron beam. The availability of fast spark gaps that could provide the switch function at high rates[14] made that choice particularly attractive.

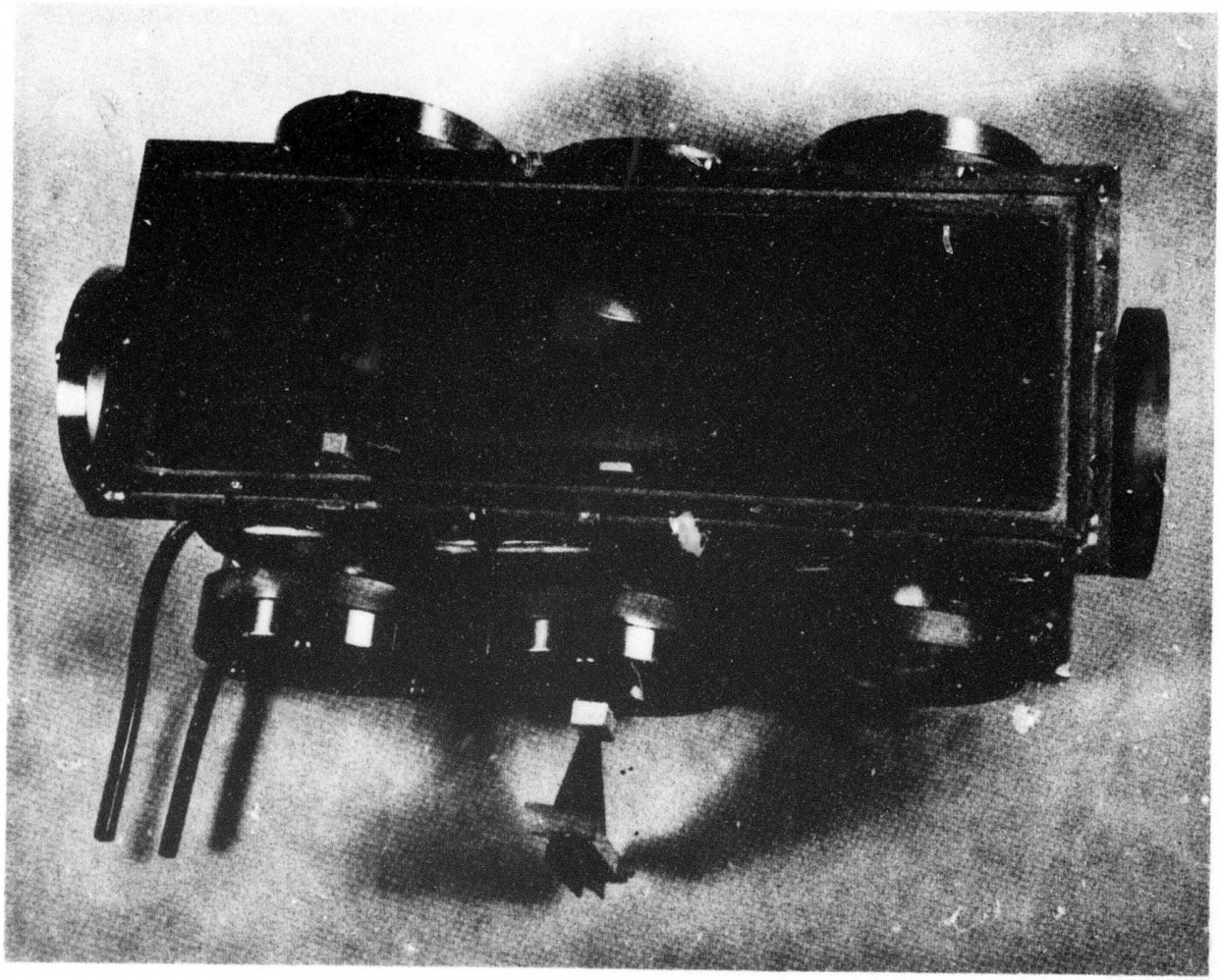

Figure A-10. Experimental Laser. Electron gun accelerates electrons through screen electrode where it ionizes metal vapor. Main discharge then occurs between third electrode and screen electrode.

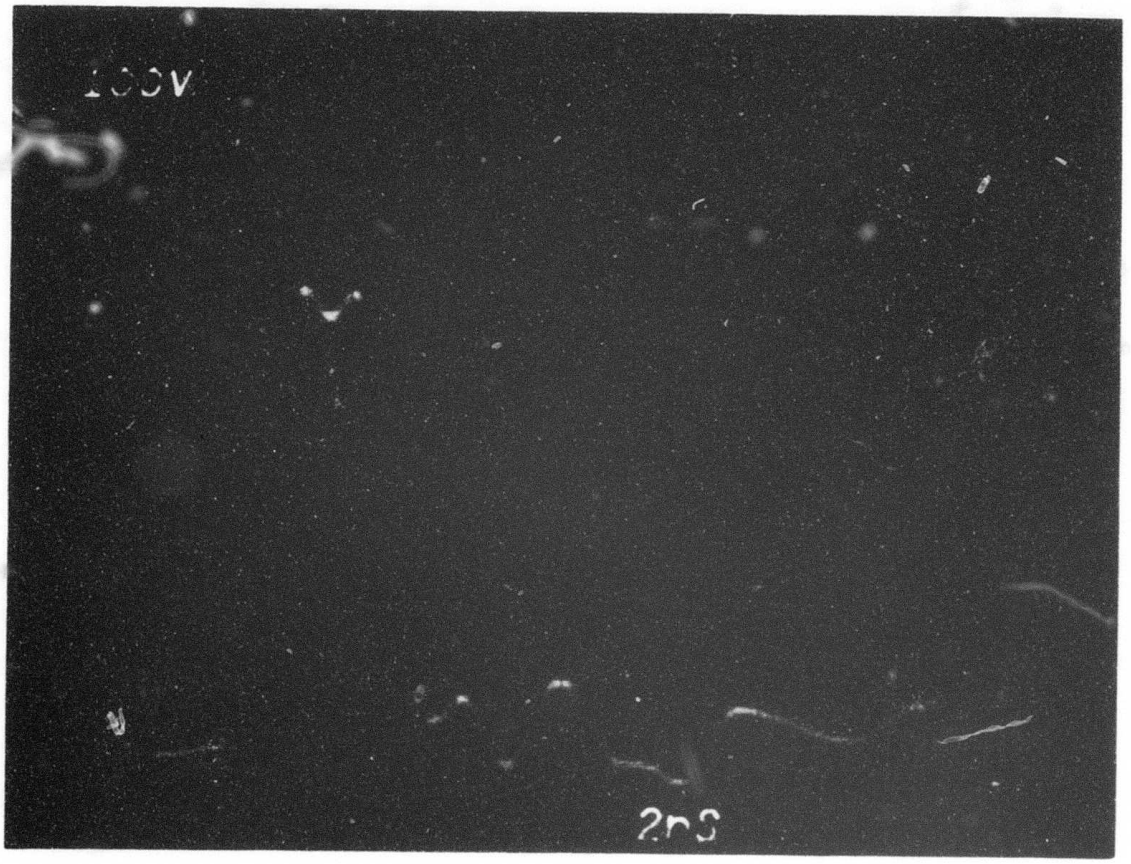

Figure A-11. Electron Gun Excitation Pulse Shape Entering Laser

APPENDIX VI

SUMMARY OF COPPER VAPOR GENERATOR TESTS

A. ONE MILLIMETER INJECTOR TESTS

Early tests were conducted with the one millimeter injector described in Appendix VI. A number of tests were conducted with this device before this program began. Results were uneven but successful demonstration of copper vapor injection was obtained.

An entirely successful run was obtained shortly after this effort was begun. A full set of measurements are summarized on Table VI-1.

B. INJECTOR A TESTS - ZIRCONIUM OXIDE RESERVOIR

An extensive series of tests were then conducted with an injector as described in Section V and Table 3. Zirconium oxide reservoirs were used as described in Appendix I. Runs 1 through 19 as listed on Table VI-2 tabulate these runs.

It was found that demonstration of injector feasibility could be obtained by using the zirconium oxide reaction as a heat source (run number 2) or by heating the injector rapidly. This way vapor injection could take place by means of electrical heating before the reaction destroyed the generator. Failures were most spectacular at these more elevated temperatures (run 18) causing final abandonment of the design after graphite reservoir generators had been built.

C. INJECTOR A TESTS - GRAPHITE RESERVOIRS

The clear success of the graphite reservoir copper vapor generators is tabulated on Table VI-2 beginning with run 19. Success was uneven, however, due to difficulties with the wetting film. Only by runs 34 and 42 was the design and character of the wetting film decided upon and only by run 50 was its full composition settled. Laser tests with the electron beam design were also begun during this period.

Table VI-1. One MM Injector Test

Characteristics	Value
Number of Holes	277
Area of Holes	.113 cm^2
Temperature Measured with Pyrometer	1933 ^oK
Expected Mass Flow Rate	1.4×10^{-2} gm/cm^2-sec
Run Time	600 sec
Expected Total Mass Vaporized	.95 grams
Measured Total Mass Vaporized	1.12 grams
Power Input	338 watts
Expected Total Mass Vaporized	1.28 grams
Vapor Density	2×10^{15} atoms/cc

Substantial success was obtained with this injector design through run 78. The tabulation gives the highest power at which the generator ran during the run in question. Its most successful operation may have been at lower levels, however, and the high power point the place where it failed. Nonetheless, the comment "good run" denotes successful vapor generation. Further characteristics of a few runs are also given to show ranges of those parameters. Successful laser testing began during run 72.

D. INJECTORS B AND C - GRAPHITE RESERVOIRS

Tests of injectors B and C and use of reservoir heaters[13] were begun during runs 79-97. It can be seen that after the development stage successful operation became the role again. Runs 98 through 103 represent this period when largely injector B was used.

A long period stretching from run 104 through 121 had few good runs due to the accidental substitution of titanium for tantalum. A few of the successful runs were high temperature short time tests. Once this error was discovered successful runs became common.

Most of these latter runs were conducted on another program in which copper vapor laser characteristics were being investigated as a model for the development of a bismuth vapor laser. They are included here to show the reliability of the device since copper generators were being exchanged for bismuth quite frequently.

Table VI-2. Tabulation of Generator Tests

Run	Date	Max. Power	Comment
1	May 8	120	No copper flow
2	May 8	665	Heat provided by reaction between $2rO_2$ and C
	Run time	100 sec	
	Flow density	8×10^{-4} gm/sec	
	Number density	10^{13} atoms/cc	
3-16			Failures due to reaction with zirconium oxide or poor flow
17	June 8	~1000	Current raised before reaction occurred
	Density	2×10^{12} atoms/cc	
18	June 9	1500	Dramatic failure leading to final abandonment of zirconium oxide reservoir
19	June 19	1440	Clearly successful run
	Mass injected	25 grams	
	Run Time	250 sec	

Run	Date	Max. Power	Comment
	Density		4×10^{15} atoms/cc
	Measured Temp.		2073 °K
20-21			Marginal failures
22	June 27	4400	Run with no carbide film. No flow.
23	July 3	2300	TaC film failure
24	July 3	4100	TaC film failure
25	July 12	1680	Good run
26	July 17	2350	Good run with radiation shields burned at 3,080 w.
27	July 27	2520	Good run but burn out at 3230
28	August 4		Failure
29	August 7		Failure using Ta foil
30-34	August 9-10		TaC film flow tests proving that sputtered films on base and lid and fully exposed in reservoir operate best.
35	August 10		VC flow tests
36	August 17	2240	Good run using vanadium carbide
37	August 18	3140	Good run using VC
38-42			Wetting film tests
43	Sept. 10	4250	Good run using well cured TaC
44	Sept. 21	2870	Good run using well cured TaC
	Temperature		2150 °
	Mass		2 grams

Run	Date	Max. Power	Comment
45	Sept. 25	3570	Good run well cured TaC
	Mass	1.7 grams	
	Copper Film Thickness Deviation	2.6% (11 measurements)	
46	Sept. 27	1740	No flow. Film not exposed.
47	Sept. 28	2910	Good run
48	Sept. 29	2250	Good run
49	Oct. 25	2200	Film comes off
50	Oct. 31	2000	Tungsten-tantalum Tungsten carbide film
	First runs with uniform fill along full length of injector		Good run
51	Nov. 1	1600	WC-TaC-WC good run
	Thickness Deviation	2.26%	
52	Nov. 6		Burn out, bad contact
53	Nov. 7		Burn out, bad contact
54		4210	Good run
55	Dec. 6	1500	Good run
56		2040	Good run
57	Dec. 7	2210	Good run
58	Dec. 8		Bad contact
59	Dec. 11	1460	Good run
60	Dec. 14	1950	Good run

Run	Date	Max. Power	Comment
61	Dec. 19	1620	Good run
62	Dec. 20		Burn up
63	Dec. 21	2225	Good run
	Temperature		2100 °K
	Density		2×10^{15} atoms/cc
	Mass Vaporized		11 grams
64	Dec. 22		Did not flow
65	Dec. 26	1055	Good run
66	Dec. 27	2440	Good run
67	Dec. 29	2580	Good run
68	Jan. 1	2220	Did not flow
69-70	Jan. 4-5		Failure, cracks, etc.
71	Jan. 6-7	1100	Good run
72	Jan. 9	2115	Good run
	Mass		6.65 grams
	Density		2×10^{15}
73	Jan. 9	2460	Good run
	Jan. 10	2580	Good run
	Mass		3.2 grams
74	Jan. 11	3780	Good run
	Density		4×10^{15}
	Mass		18 grams
	Run Time		150 sec.

Run	Date	Max. Power	Comment
	Mass	4 grams	
106?	March 20	3740	#4 - Good run
	Time	38 sec	
	Mass	11 grams	
122	May 9		Failure
123	May 10	2050	Good run
124-126	May 14	See Table 6	Good run
127	May 19?		Good run
	Time	7 sec.	
	Mass	11 grams	
128	May 22	1560	Good run
	Run time	45 sec	
	Mass Flow	2.7 grams	
129	May 23	2332	Good run
	Run time	15 sec	
	Mass Flow	1.3 grams	
130	May 26	1100 w, 5 min 1200 w, 8 min 1315 w, 3.5 min.	Good run
	Mass Flow	3 grams	
131-132	May 29	1775 w, 10.5 min 1923 w, 2 min	Good run

Run	Date	Max. Power	Comment
75	Jan. 15	2310	Good run
76	Jan. 16	2870	Good run
77	Jan. 17	1250	Good run
78	Jan. 18	2340	Good run
79-97	March 6		About 20% good runs. Development of #3 and #4 CVG.
98	March 7	See table 6	#3 - Good run
99	March 7	750	#3 - Good run
100	March 12	6320	#3 - Good run
	Time	20 sec	
	Mass	15.2 grams	
101	March 12	1510	#3 - Good run
102	March 13	1180 w, 12.75 min. 720 w, 50 min.	#3 - Good run
	Mass Flow	6 grams	
103	March 13	4500	#3 - Good run until burn out
	Time	10 sec	
	Mass Flow	3.5 grams	
	Density	10^{16}	
104-121?	3 - 4		Runs largely failures due to accidental use of titanium wetting film
110	March 23?	3600	#4 - Power may have been higher
	Time	5 sec.	

Run	Date	Max. Power	Comment
133-134	May 30	2440 w, 5 min 2700 w, 1 min	Good run
	Mass Flow	11 grams	
	May 31	2560 w	Good run
	Mass Flow	6.3 grams	
135	May 31*	2208	Good run
136	May 31	2560	
137	June 1	4000	Good run
138	June 1	3020	Failed
139	June 4	2205	Good run
140	June 4	2300	Good run
141	June 5	2305	Good run
142	June 5	2500	Good run
143	June 5	2720	Good run
144	June 7	2140	Failed
145	June 11		Failed
146	June 12	1803	Good run
147	June 12	2580	Good run
148	June 13	2500	Good run
149	June 15		Failed
150	June 18	1920	Good run
151	June 18	3440	Good run

*Beyond this date tests were conducted for another program but are included here to show reliability.

REFERENCES

1. W. T. Walter, N. Solimene, M. Piltch, and G. Gould, IEEE J.Q.E. 2, 474 (1966).

2. T. W. Karras, and C. E. Anderson, "Copper Vapor Generator," GE N11262 (1971).

3. W. H. McMahan, Optical Spectra (December 1971).

4. G. R. Russell, N. M. Nerheim, and T. J. Pivirott, Applied Physics Letters 21, 565 (1972).

5. D. Leonard, Final Report Contract DAHC-60-70-C-0030 (1970). IEEE J.Q.E. 3, 380 (1967).

6. J. F. Asmus and N. K. Moncur, Applied Physics Letters 13, 384 (1968).

7. A. A. Isaev, JETP Letter 16, 27 (1972).

8. G. G. Petrash, Sov. Phy. Uspekhi 14, 747 (1972).

9. S. J. Robertson and D. R. Willis, AIAA J. 9, 291 (1971).

10. L. Holland, Vacuum Deposition of Thin Films, Wiley (1961).

11. T. W. Karras, "ELM: Valveless Propellant Injection," Technical Report AFAPL-TR-67-77 (1967).

12. T. W. Karras, "Continuous and Quasi-Continuous Flow Metal Vapor Generators," General Electric Co., Space Sciences Laboratory PIR 2A40-RK2-052 (1971).

13. T. W. Karras, R. S. Anderson, and B. G. Bricks, "Pulsed Metal Vapor Generator," Phase I Final Report to contract N62269-72-C-0921 (1973).

14. T. W. Karras, and W. E. Austin, "High Repetition Rate Metal Vapor Lasers," Final Report to Contract N00014-73-C-0042.

15. M. Hansen, Constitution of Binary Alloys, McGraw Hill (1958).

16. D. A. Mortimer and M. Nicholas, J. of Mat. Sci. 5, 149 (1970).

17. D. T. Livey and P. Murray in Warmfeste und korrosionsbestundige Sinterwerkstoffe 2. Plansee Seminar "De Re Metallics" Springer-Verlag Wien (1956).

18. S. K. Rhee, J. Am. Cer. Soc. 55, No. 3 (1972); J. Am. Cer. Soc. 54, No. 7 (1971).

19. E. K. Storms, The Refractory Carbides, Academic Press (1967).

20. L. E. Toth, Transition Metal Carbides and Nitrides, Academic Press (1967).

21. S. Dushman, Scientific Foundations of Vacuum Technique, Wiley (1966).

22. S. J. Robertson and D. R. Willis, AIAA Journal 9, 291 (1971).

23. J. H. Keenan and J. Kage, Gas Tables, Wiley and Sons (1948).

24. L. Holland, Vacuum Deposition of Thin Films, Wiley (1961).

25. P. N. Shankar and F. E. Marble, Phy. of Flu. 14, 510 (1971).

26. P. P. Wegener et al, Phys. of Fluids 15, 1869 (1972).

27. A. N. Nesmeyanov, Vapour Pressure of the Elements, Academic Press (1963).

28. E. Mayer et al, "Condensation of Rarefied Supersonic Flow Incident on a Cold Flat Plate," Rarefied Gas Dynamics Fourth Symposium, VII Academic Press (1966).

29. J. P. Hirth and G. M. Pound, Condensation and Evaporation--Nucleation and Growth Kinetics, Macmillan (1963).

30. R. A. Aziz and G. D. Scott, Can. J. Phys. 34, 731 (1956).

31. T. E. Ernst, AFWL, Private Communication.

32. C. R. Corliss and W. R. Bozman, Experimental Transition Probabilities for Spectral Lines of Seventy Elements, NBS Monograph 53, 1962.

33. Airco Temescal Data Sheet 1972-73 Catalog.

34. G. Brewer, "Ion Propulsion," Bordon and Breach (1970).

35. R. Stair, W. E. Schneider, and J. K. Jackson, App. Optics 2, 1151 (1963).

36. Contract N00014-73-C-0042, Metal Vapor Laser (1973).

DISTRIBUTION

No. of Copies	
1	Hq USAF, AFTAC/TAP, Patrick AFB, FL 32925
	AFSC, Andrews AFB, Washington, DC 20334
1	(DLSP)
	USAF Academy, CO 80840
1	(FJSRL, CC)
	AFML, Wright-Patterson AFB, OH 45433
1	(Tech Lib)
	AFSWC, Kirtland AFB, NM 87117
1	(HO)
	AFWL, Kirtland AFB, NM 87117
5	(SUL)
5	(LRT)
	Dir, DNA, Washington, DC 20305
2	(APTL)
2	(SPSS)
2	(STAP)
	DDR&E, Washington, DC 20301
1	(Asst Dir, Strat Wpns)
	Dir, DIA, Washington, DC 20305
1	(DIAAP-8B)
1	(DIAST-3)
1	Dir, OSD, ARPA (NMR), 1400 Wilson Blvd, Arlington, VA 22209
1	Comdr, FC DNA (FCSD-A2), Kirtland AFB, NM 87115
1	Dir, Wpn Sys Eval Gp (Doc Cont), Washington, DC 20305
1	JSTPS (JLTW), Offutt AFB, NE 68113
12	DDC (TCA), Cameron Sta, Alexandria, VA 22314
5	General Electric Space Sciences Div., PO Box 8555, Philadelphia PA 19101
1	AUL (LDE), Maxwell AFB, AL 36112
1	Official Record Copy to Capt Rhodes/LRT

A

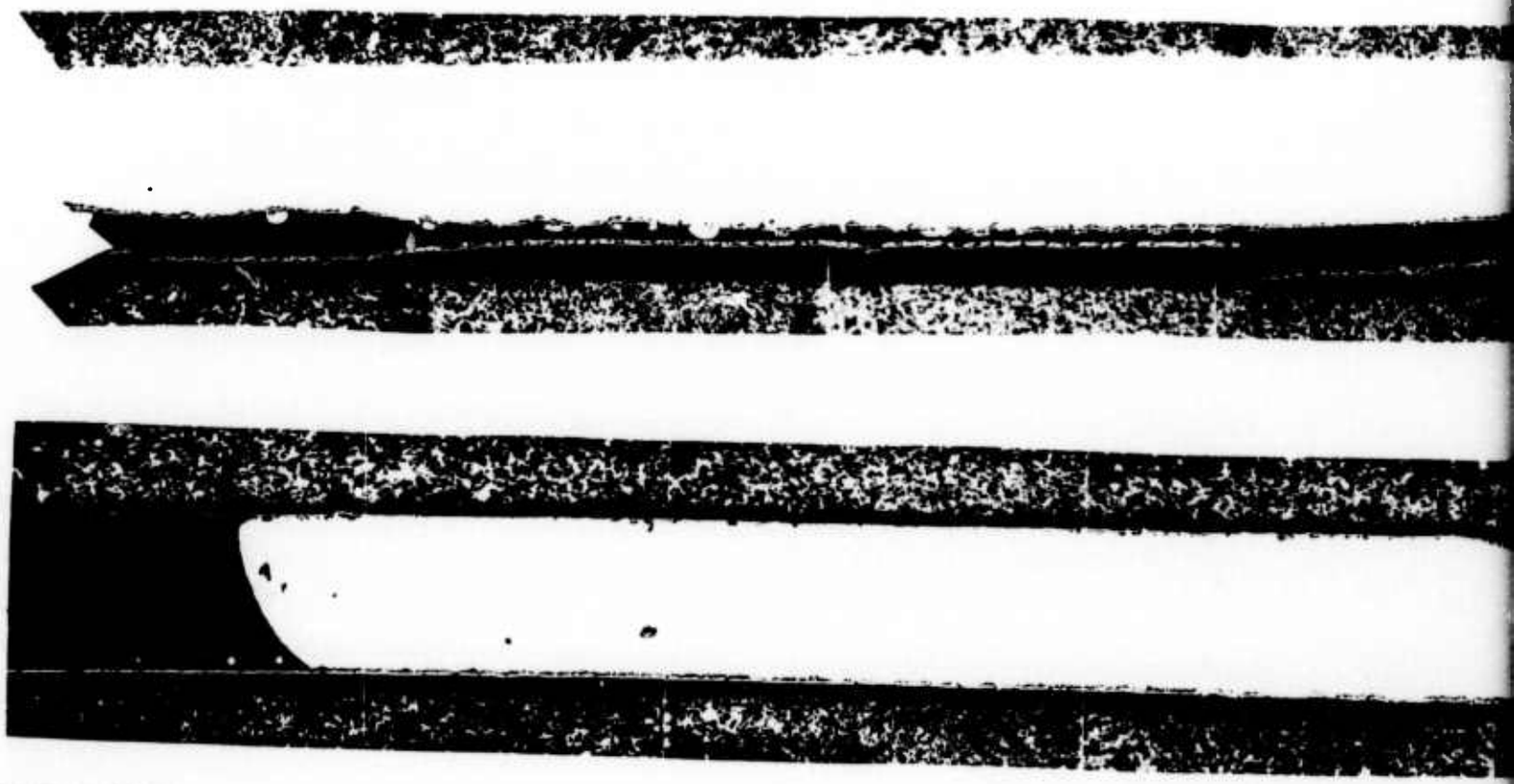

EMPTY CHANNEL

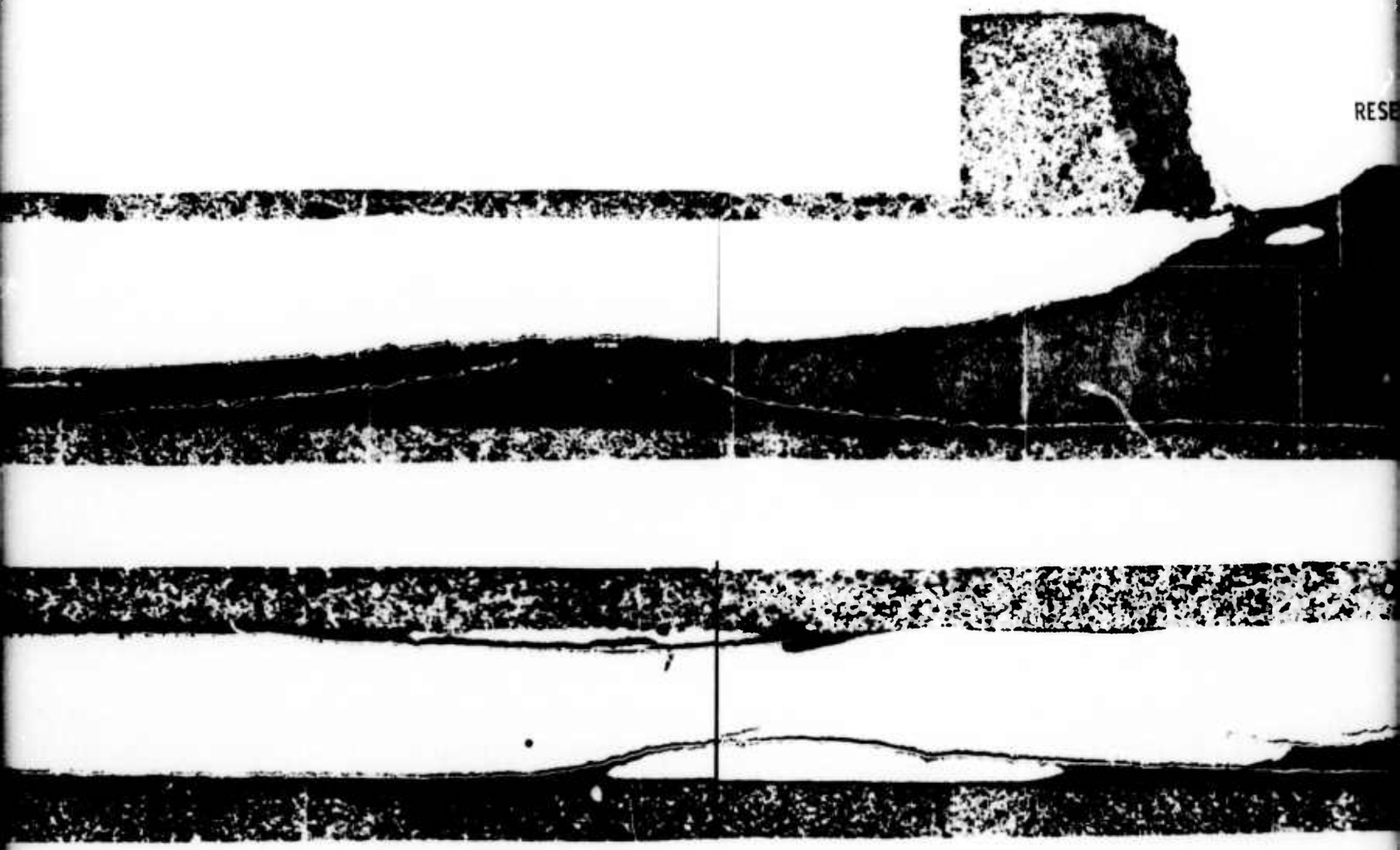

TANTALUM CARBIDE FILM STRIPPED
FROM SUBSTRATE BY LIQUID COPPER

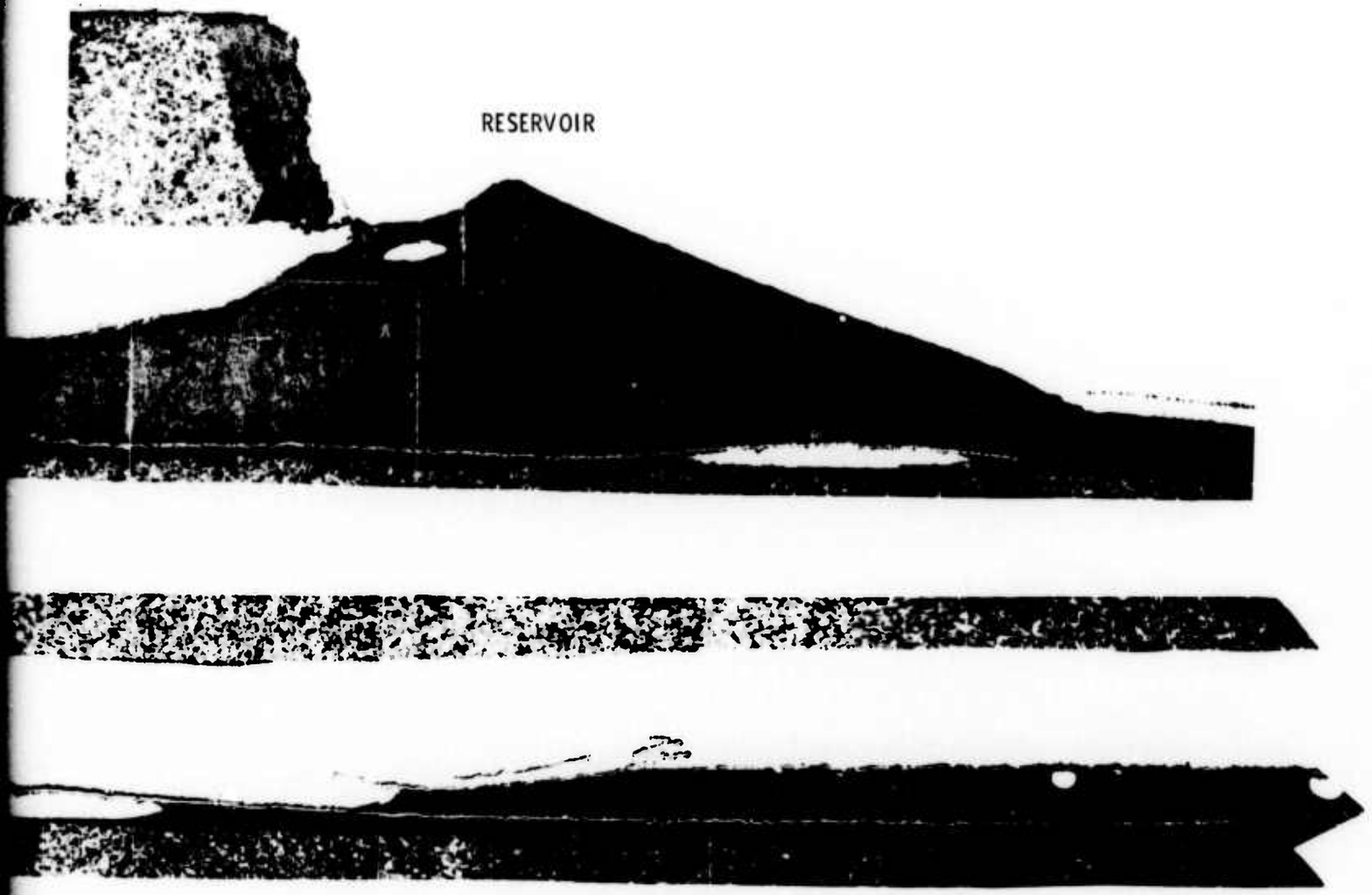

Figure A-8. Photomicrograph of Injector Channel